MONASH University

Hydrological cycle and tree water use in remnant urban reserves

Valentina Marchionni

MSc in Civil Engineering, University of Perugia, Italy (2009)

A thesis submitted for the degree of Doctor of Philosophy at
Monash University in 2019
Faculty of Engineering

Abstract

Natural habitats and biodiversity are increasingly removed to accommodate the rapid expansion of cities and metropolitan regions. What remains of the natural habitats is often fragmented into small and isolated patches of natural vegetation, which maintain high level of urban biodiversity and provide a collection of ecosystem services essential to the quality of life of urban dwellers. These areas are often surrounded by artificial surfaces and embedded in a highly disturbed environment, thus being subjected to biophysical and ecological conditions different from those prior to urbanization. Combining field measurements and ecohydrological modeling, this project provides a unique and comprehensive analysis of the water dynamics and tree water use in small urban reserves hosting native vegetation within the Melbourne metropolitan area in southeast Australia. Over the past 165 years, Melbourne has grown from a small village to a city of more than 4 million people, with substantial consequences for native plants. Large areas of native vegetation have been replaced by urban and suburban landscapes, with less than 4% vegetation cover remaining within the urban growth boundary. Moreover, the recent Millennium Drought between 2001 and 2009 have resulted in below median rainfall (since at least 1900), regional declines in water table depths, and reductions in vegetation biomass. In this context, this project provides novel insights on mechanisms of tree water use in urban areas. The data collected between July 2016 and June 2018 in three small urban reserves showed that native vegetation had enough water to sustain its transpiration rates despite the urban surrounding. Specifically, shallow groundwater (with water table between 3 and 5 m below the ground surface in two of the three study sites) played an essential role by helping trees sustain transpiration especially during the driest periods of the year, contributing to about 30-40% of the total transpiration, and during nights with temperatures above 25°C, helping trees to maintain night-time water use from 3 to 16% of the daily water use. To further investigate the ecosystems response to groundwater availability, an ecohydrological model was used to carry out long-term simulations (July 1999 - June 2018) under both present and variable climate. Results from the numerical simulations confirmed that these ecosystems strongly depend on groundwater, with the presence of a reference value for water table depth, below which vegetation is more susceptible to water stress. In particular, woody plants were found to transpire more than 40% when the water table was maintained within the reach of the plant roots. Finally, groundwater (or its capillary fringe) appear to strongly help these ecosystems buffering changes in environmental variables, such as increased air temperature and atmospheric CO_2 concentrations as well as rainfall reduction. Model results also suggest that groundwater might control trees-shrubs-grass coexistence and competition for resources, with soil properties playing a crucial role in amplify and dampen these dynamics. These results emphasize the importance of understanding the water regime of each urban reserve in order to support government authorities in evaluating appropriate management practices. For this reason, the potential impact of irrigation and revegetation strategies on hydrological fluxes and vegetation productivity was also investigated using an ecohydrological model.

Declaration

This thesis is an original work of my research and contains no material which has been accepted for the award of any other degree or diploma at any university or equivalent institution and that, to the best of my knowledge and belief, this thesis contains no material previously published or written by another person, except where due reference is made in the text of the thesis.

Signature: .....

Print Name: Valentina Marchionni

Date: 11/11/2019

Publications during enrollment

- **Marchionni V.**, Revelli R., and Daly E. (2019), "Ecohydrology of urban ecosystems". In *Dryland Ecohydrology*, pages 533?571. Springer.
- **Marchionni V.**, Guyot A., Tapper N., Walker J.P., and Daly, E. (2019), "Water balance and tree water use dynamics in remnant urban reserves", *Journal of Hydrology, 575, 343-353.* (I.F. 3.727, Q1 in Water Science and Technology)
- **Marchionni V.**, Daly E., Manoli G., Tapper N., Walker J.P., and Fatichi S., "Groundwater buffers drought effects and climate variability in urban reserves", *revised and resubmitted to Water Resources Research.* (I.F. 4.36, Q1, in Water Science and Technology)

Acknowledgements

The first words of appreciation are devoted to my main supervisor, A./Prof. Edoardo Daly, who has been a truly great person from whom to learn, to work with, and to learn with. I am especially grateful for his constant encouragement, guidance, and support. I am also very grateful to my co-supervisors, Prof. Jeffrey P. Walker and Prof. Nigel Tapper, for their helpful comments. I am also very grateful to my Ph.D. panel committee, A./Prof. Stephen Livesley, A./Prof. Valentijn Pauwels, and Dr. Christoph Rudiger, for their important feedback.

Many friends and colleagues have been very important in my doctoral process. I would like to thank first Kiri Mason for her continuous support during field works but even more for the enjoyable time we spent collecting data. I wish to thanks also Dr. Adrien Guyot, A./Prof. Matteo Camporese, A/Prof. Melodie McGeoch and Dr. Gillis Horner, as well as the staff from Mooney Valley City Council (Michelle Gooding) and Great Dandenong City Councils (Bertrand Salmi, Alexandra Moodie, Maree Keenan) for their support throughout the development of this project. I would also like to thank Filomena Innella, Sabah Sabaghy, Andrea Massetti, Marcela de Freitas Silva, Jayaram Pudashine, Juri Jung, Stefania Grimaldi, and Ali Azarnivand for being great colleagues and good friends throughout my postgraduate career. A special thank goes to Dr. Simone Fatichi and all the other people I met during my visiting experience at the ETH Zurich.

In the very first turn, this thesis is devoted to my parents for letting me grow so freely and for guiding me in the times of need. I am very grateful to my brother, Edoardo, for his pragmatism and support.

Lastly, and to the greatest extent, I would like to thank my partner, Francesco. His commitment and tenacity in carrying out his research drove me to start my postgraduate career. He is a truly inspiration to me and I owe him a huge debt of gratitude for the encouragement and support during the many moments of despair. I am so grateful to have him in my life and I can't wait to start our new adventure with our little boy.

This research was supported by the Australian Research Council, and the City of Greater Dandenong and Mooney Valley City councils through the Linkage project LP150100901.

Contents

List of Figures

List of Tables

Chapter 1

Introduction

Urbanization and the associated land transformations generate a fragmented and heterogeneous landscape where patches of vegetation, often remnants of natural habitats, are embedded in a highly disturbed environment (McKinney, 2002). Remaining pockets of vegetation within the built environment are recognized as important areas for biodiversity conservation (Elmqvist et al., 2015; Lepczyk et al., 2017; Tulloch et al., 2016), mitigating the urban heat island (UHI) effect (Bowler et al., 2010; Gill et al., 2007; Declet-Barreto et al., 2016), restoring hydrological and biogeochemical processes closer to natural conditions (Yang et al., 2015; Livesley et al., 2016a; Berland et al., 2017), and positively influencing human health and psychological well-being (Chiesura, 2004; Pataki et al., 2011b).

Urban expansion, in addition to reducing the extent of the vegetation cover, may be exerting negative impacts on the remaining vegetation by imposing changes in the radiation and energy budget, the hydrologic regime, and ecosystem composition and structure (Roberts, 1977; Sieghardt et al., 2005a). The increase of impervious surfaces and the introduction of drainage infrastructure reduce the volume of water that infiltrates the soil, decreasing the water available to sustain vegetation growth and health (Xiao et al., 2007; Barron et al., 2013; Shields and Tague, 2015). Increased temperatures and lower air humidity due to the UHI often expose the trees embedded in the urban landscape to high atmospheric evaporative demand. This can lead to higher transpiration rates, in particular when soil moisture is not a limiting factor (Litvak et al., 2011;Chen et al., 2011; Litvak and Pataki, 2016; Zipper et al., 2017a; Litvak et al., 2017; Asawa et al., 2017). In addition, increasing drought (Van Loon et al., 2016a) and extreme heat events amplify the water stress of urban trees, resulting in the decline of their health conditions.

What remains of natural habitats within the urban boundaries can also undergo changes in vegetation structure with the introduction of non-native species, thus creating unique

biotic communities with different water needs and more complex patterns of evapotranspiration, interception, and infiltration (Pataki et al., 2011a;Endter-Wada et al., 2008; McCarthy and Pataki, 2010). In the Melbourne metropolitan area in southeast Australia, for instance, large areas of native vegetation have been replaced by urban and suburban landscapes over the past decades (DELWP, 2016). As a result, less than 4% cover of native vegetation remains within the urban boundaries (Bradshaw, 2012; Hahs and McDonnell, 2014). This remaining native vegetation is severely fragmented into small reserves, which become isolated and sometimes degraded. Moreover, a further decline in vegetation health have been documented during the Millennium Drought that occurred approximately between 2001 and 2009 (van Dijk et al., 2013).

In this context, maximizing the effectiveness of remnant native vegetation conservation through active management is important to avoid further losses of vegetation associated with urbanization. Therefore, there is an increasing need for empirical evidence of the role that water availability and the built landscape play in the physiological response of vegetation to urban conditions (Livesley et al., 2016a). More information is also needed to understand the water requirements of these green spaces, enabling better design management guidelines for the preservation of these ecosystems. This involves the identification of the water resources that are most important to maintain key ecosystem features and processes, including the degree of the ecosystem groundwater dependency (Eamus and Froend, 2006; O'Grady et al., 2006).

This project is motivated by the need for evidence related to interactions and feedback between water resources and vegetation health in small reserves hosting remnant native vegetation embedded in the urban environment and their specific management to deliver positive impacts (Livesley et al., 2016a). The focus of most studies so far was on large bio-diverse ecosystems often in natural environments or mildly affected by human activities. Conversely, the links between the water balance and vegetation health in urban ecosystems has received considerable less attention. This study aims to fill this gap, understanding the environmental water requirements and the response to climate variability of small natural reserves embedded in urban environment.

Chapter 2 of this thesis contains an extensive literature review on the ecohydrology of urban ecosystems followed by the specific questions that this project addresses. The literature review refers to all urban green spaces, including street trees, lawns and parks, urban forests, cultivated land, and green corridors, as well as green roofs and green walls technologies, and the essential ecosystem services they can provide. In addition, this section describes the links between urbanization and microclimate, water fluxes, and greenhouse gas emissions

from urban soils, taking also into account the role of urban vegetation in affecting the urban microclimate and restoring more natural hydrological and biogeochemical processes. An overview of the available models that have extended the analysis of hydro-biophysical processes from natural environments to urban areas is also presented. Different modeling scales are identified, such as (i) ecohydrological models that represent regional- to catchment-scale interactions between major biogeochemical cycles, water cycle, and vegetation dynamics, (ii) models that operate at the neighborhood scale to simulate soil-plant-atmosphere interactions, and (iii) models that simulate water and nutrient dynamics at the tree level. With regard to this project, the focus is on remnant urban reserves which can be defined as less managed areas compared to urban parks hosting mostly remnant native vegetation.

Chapter 3 gives an overview of the methods adopted in this project. These include an extensive description of the study sites followed by the specific experimental setup and modeling approach that were chosen for addressing the research questions. Specifically, three urban reserves located in the Melbourne metropolitan area in southeast Australia are considered: National Drive Reserve, Alex Wilkie Reserve, and Napier Park. These sites host predominantly remnant native plants, with some occasional introduced species, and differ for vegetation structure, soil characteristics, and management practices. Moreover, because of a strong spatial heterogeneity of rainfall within the Melbourne metropolitan area, the sites are also characterized by different rainfall regimes. A series of experimental measurements have been collected within the study sites between July 2016 and June 2018 to quantify the water balance and tree water use of the reserves, including continuous observations of micrometeorological data, soil water content and groundwater levels, sap flow measurements, and stem diameter variations. To explore the reserves ecosystem dynamics, the mechanistic ecohydrological model Tethys-Chloris is used, being well suited to represent the essential components of the hydrological and carbon cycles, resolving energy, water, and CO_2 fluxes at the land surface.

Chapter 4 outlines the results of a comprehensive analysis of the water balance and tree water use dynamics from the observations over a two-year period (July 2016 - June 2018) in the three study sites. This chapter provides insight about the variations in the water balance of the urban reserves under different water regimes, also highlighting the influence of micro-meteorological drivers and groundwater availability on tree water use. Warm nights following days with temperatures above 35°C are also taken into account in the analysis to understand the impact of heat stress on night-time tree water use.

Chapter 5 discusses a series of numerical experiments designed to investigate how different scenarios of groundwater availability control the water balance and vegetation productivity

in two of the three urban reserves: National Drive Reserve and Alex Wilkie Reserve. The mechanistic ecohydrological model Tethys-Chloris is used to run long term simulations supported by field observations to explore the ecosystem resilience to water availability in the present climate, including the Millennium Drought (2001-2009) and in response to perturbations in key environmental variables.

Chapter 6 focuses on the application of the ecohydrological model Tethys-Chloris to analyze the effects of different management scenarios on the hydrological fluxes and vegetation productivity at Napier Park. A series of irrigation and vegetation cover scenarios were taken into account, thus improving the understanding of how urban reserves can be effectively managed ensuring both vegetation health and water savings.

Chapter 7 summarizes this thesis. The chapter outlines the results of the study both in terms of experimental measurements and ecohydrological modeling, highlights the contributions of the research, and provides several topics for future research efforts.

Chapter 2

Literature Review and Scope of Research

This chapter contains the book chapter **"Ecohydrology of urban ecosystems"**[1], which is included in the second edition of the book *"Dryland Ecohydrology"* (Springer, 2019) edited by Prof. Paolo D'Odorico[2] and Prof. Amilcare Porporato[3]. The chapter was written in collaboration with A/Prof. Edoardo Daly[4] and Prof. Roberto Revelli[5,6]. The chapter was peer-reviewed by Prof. Paolo D'Odorico and Dr. Christiane Runyan[7].

The chapter includes an extensive literature review on ecohydrological aspects of urban ecosystems. In particular, it focuses on urban green spaces and their role in providing a collection of environmental, socio-cultural, and economic benefits essential to the quality of life of urban dwellers. The chapter also reviews the links between urbanization and micro-climate, water fluxes, and greenhouse gas emissions from urban soils, highlighting the role of urban green spaces in providing benefits at different scales. Finally, it gives an overview of models available in literature that have extended the analysis of hydro-biophysical processes from natural environments to urban areas from tree to regional scale.

[1] Marchionni et al. (2019b)
[2] Department of Environmental Science, Policy, & Management, UC Berkeley, Berkeley (CA)
[3] Department of Civil and Environmental Engineering, Princeton (NJ)
[4] Department of Civil Engineering, Monash University, Melbourne (Australia)
[5] Department of Environment, Land and Infrastructure Engineering, Politecnico di Torino (Italy)
[6] Pratt School of Engineering - DUKE University - Durham (NC - US)
[7] Johns Hopkins University (MD)

2.1 Introduction

More than half of the world population lives in urban areas with projections showing a population increase up to 66% by 2050 (UN, 2015). To accommodate the growing number of city dwellers, urban areas are expanding twice as fast as their population (e.g., Seto et al., 2012), raising concerns about sustainability and livability of cities. Given the increasing importance of urban areas in both driving and being impacted by global environmental changes, there is a rapidly growing interest in understanding their dynamics (Seto and Shepherd, 2009).

Urbanization drives significant environmental changes at multiple spatial and temporal scales. The most direct impact of urbanization is the removal of natural spaces and biodiversity to build structures and impervious surfaces, thus creating a complex mosaic of land uses and covers. In urban areas, artificial surfaces are often mixed with pervious green areas, such as parks, gardens, remnant forests, and green corridors. This heterogeneous patchwork results in complex interactions between local microclimate, and hydrological and biogeochemical cycles, which affect ecosystem properties and functions (Grimm et al., 2008; Seto et al., 2011).

Pervious soil and vegetation are important components of urban ecosystems and provide essential services, such as pollution mitigation, biogeochemical cycling, and community health and well-being (Livesley et al., 2016a). At the same time, vegetation and soils that persist in the urban landscape are increasingly under threat due to human disturbances and stress factors related to changes in temperatures, water availability, nutrient, and pollution levels. Within this context, an urban ecohydrology perspective allows us to place more emphasis on interactions and feedbacks among soil, plant, and atmosphere specifically related to cities (Jenerette and Alstad, 2010; Wagner and Breil, 2013).

In urban areas, as in natural environments, ecosystem dynamics and hydrological processes are strongly coupled. The conversion of natural and vegetated land to urban uses alters land surface properties, and hence the energy balance and water fluxes. Evident changes in local microclimate have been observed in terms of higher temperature in urban areas than in their rural surroundings, a phenomenon known as urban heat island (UHI) effect (Oke, 1982). The introduction of impervious surfaces and drainage infrastructure affects ecosystem hydrologic regimes. These changes reduce the volume of water infiltrating soils, and hence groundwater recharge, as well as the volume of soil water lost through evapotranspiration, thus increasing the volume of runoff (Xiao et al., 2007). Urban development may also lead to the coexistence of native plant with non-native species, creating unique biotic communities that may have high water demand, different patterns of evapotranspiration, interception,

and infiltration (Pataki et al., 2011a). Finally, urban areas strongly impact biogeochemical cycles, thus affecting urban ecosystem dynamics (Grimm et al., 2008). Cities are usually net sources of CO_2 and other greenhouse gases (GHGs) such as nitrous oxide (N_2O) and methane (CH_4), with anthropogenic activities controlling the diurnal and seasonal patterns of these fluxes (Kaye et al., 2005).

In arid and semiarid urban areas, where almost 22% of the world population lives (McDonald et al., 2011), limited natural resources magnify the importance of understanding the coupled relationship between ecosystems and hydrological processes. Urbanization drastically changes the structure and functions of arid and semiarid ecosystems; landscape plantings in an otherwise desert setting along with water and energy subsides have a great impact on both hydrologic regime and carbon stocks and fluxes.

This chapter reviews recent studies and advances in understanding and modeling links and feedback among soil, vegetation, and atmosphere in urban environments, with a particular focus on arid and semi-arid regions.

2.2 Urban ecosystem services

Urbanization is one of the most irreversible human impacts on the global biosphere, fragmentizing natural environments, introducing non-native species, increasing surface runoff and erosion, and degrading or altering ecosystem processes. The rapid expansion of urban areas raises the attention on preserving and restoring ecological processes and functions to reduce the ecological footprints of cities (Menz et al., 2013).

Vegetation and natural soils may play a crucial role in reducing the negative impacts of urbanization on the physical environment. In urban areas, most of the natural and semi-natural elements serve as green infrastructure. Green spaces - street trees, lawns and parks, urban forests, cultivated land, and green corridors, as well as green roofs and green walls technologies (Table 2.1) - provide a collection of environmental, socio-cultural, and economic benefits essential to the quality of life of urban dwellers (Dover, 2015a; Palmer et al., 2015). Green areas are widespread in the urban environment. For example, in the United States, urban lawns cover a land area three times larger than any other irrigated crop in the country (Milesi et al., 2005), while trees cover about 35% of the urban land (Nowak and Greenfield, 2012).

Numerous studies over recent years have documented the role of urban green spaces in promoting ecosystem health and resilience, contributing to biodiversity conservation, and enhancing urban ecosystem functionality through the provision of ecosystem services (Chiesura,

2004; Tyrväinen et al., 2005; Dobbs et al., 2014; Sander, 2016). Ecosystem services are defined as the indirect and direct benefits that urban populations derive from ecosystem functions on local and global scales, which enhance urban sustainability and climate change adaptation (Costanza et al., 1997; Costanza et al., 2014). Following this definition, the Millennium Ecosystem Assessment (Toth, 2003) and the Economics of Ecosystem Services and Biodiversity (TEEB, 2009) classified ecosystem services in four major categories (Figure 2.1) each relying on fundamental ecological processes (Pataki et al., 2011b): three of them (provisioning, regulating, cultural) with a direct and short-term impact on people, while supporting and habitat services show an indirect and long-term impact. As a consequence, the temporal scales of the provided ecosystem services assume a fundamental role in every decision-making process.

Urban green spaces provide direct and locally generated services, which are essential for both ecosystem and human health in urban areas. These include the potential to mitigate the UHI effect, limit GHG emissions, regulate the hydrological cycle, affect carbon c and nitrogen (N) biogeochemistry, and improve air and water quality by removing pollutants (Bolund and Hunhammar, 1999; Escobedo et al., 2011; Coutts et al., 2013b; Livesley et al., 2016c). Interactions with the natural environment also positively influence the physical and mental health of urban dwellers (Chiesura, 2004).

In addition to their ecological and socio-cultural values, ecosystem services have demonstrated economic value (Elmqvist et al., 2015; Pandeya et al., 2016). For example, the loss of urban vegetation can lead to increased energy costs for heating and cooling buildings, health care expenses related to respiratory diseases, and maintenance of expensive infrastructures to abate noise and pollution (Gómez-Baggethun and Barton, 2013). McPherson et al. (2005) examined the economic benefits associated with many services of urban trees (e.g., energy savings, air quality improvement, and stormwater runoff reduction among others) in five cities in the USA over a period of three years. They found annual benefits returns between \$1.37 and \$3.09 per tree. Specifically, in relation to tree shading and evaporative cooling, energy savings reached up to ∼\$550,000 a year in locations where trees were located in close proximity to buildings. Much lower savings (∼\$115,000) were reported in cities where trees were mainly planted along wide roads.

The urban ecosystem services framework, integrating biophysical and socio-economic concepts, is an essential component of the green infrastructure planning and preserving strategies, which aim to maximize well-being outcomes for city dwellers (Elmqvist et al., 2013; Sirakaya et al., 2017). On the contrary, there is a growing literature on ecosystem disservices (e.g., respiratory allergies to wind-pollinated plants, pathogens and pests, and

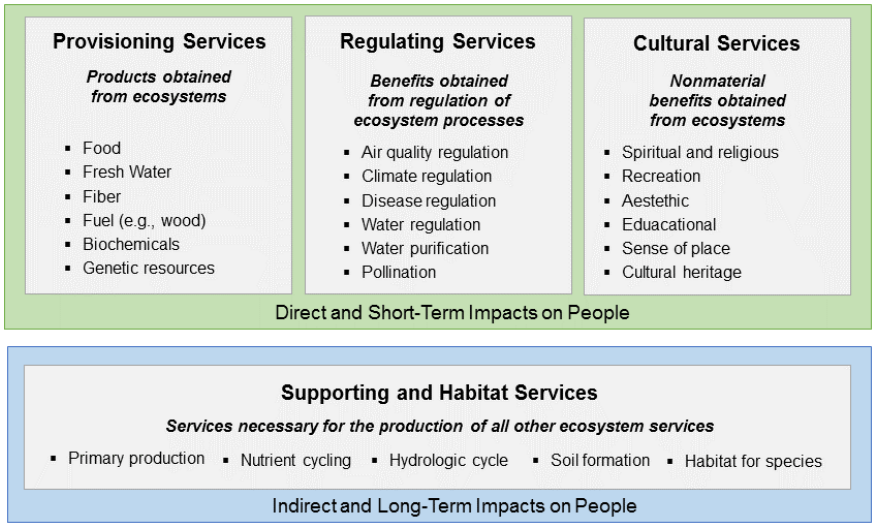

Figure 2.1: Ecosystem services classification based on the Millennium Ecosystem Assessment (Toth, 2003) and The Economics of Ecosystems and Biodiversity (TEEB, 2009) .

invasive or native species causing damage to property), which are also important to be taken into account in the planning of green infrastructure establishment and maintenance (e.g., Lyytimäki, 2014; von Döhren and Haase, 2015.

As green infrastructure is increasingly adopted to mitigate the impact of urbanization on the natural environment, there is a need to obtain empirical evidence on the magnitude of such impacts, both beneficial and adverse (e.g., Matthews et al., 2015). For example, green roofs are commonly reported as a key measure to mitigate heat in urban areas. However, their performance is highly dependent upon their design (e.g., soil depth), vegetation species, and climatic conditions, which might require irrigation to support evapotranspiration (Coutts et al., 2013a). Several factors thus need to be considered for their effective use and installation.

2.3 Green areas and climatic, hydrological, and biogeochemical processes

Urbanization strongly alters an ecosystems structure and functions, which has a profound impact on biophysical and ecological processes at multiple scales. Urban ecosystems play a crucial role in global climate change, being significant sources of GHGs, including 78% of total carbon emissions (Grimm et al., 2008). In addition, by altering energy, water, and momentum exchanges between the land surface and atmosphere, urban development can

Table 2.1: Types of Urban Green Spaces (*Photo Credits: Edoardo Daly*).

Types of Urban Green Spaces		**Description**
Street trees	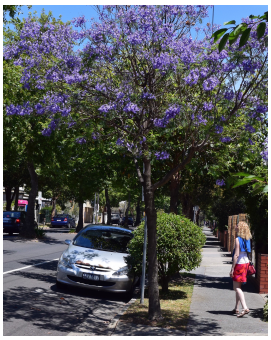	Stand-alone trees, often surrounded by paved ground.
Lawns Parks		Turf grass systems, with or without trees and other plants, created and maintained by humans for aesthetic and recreational purposes. Sports grounds and playgrounds may also be included in this group.
Urban reserves		Less managed areas with higher density of trees and shrubs compared to the urban parks. They can be remnant, regrowth, or newly created forests.
Cultivated land		Patches of land used for the local production of food products (e.g., community gardens, small scale urban farms).
Green corridors		Linear green spaces which connect natural habitats and wildlife populations. When located along waterways they are called riparian corridors.
Green roofs Green walls		Green roofs are building roofs partially or completely covered with vegetation. Green walls are vertical gardens on the side of a building.

significantly alter climate (Bonan, 1997). Land-use and land-cover transformations due to urbanization have significant impacts on hydrological processes and water quality dynamics (DeFries and Eshleman, 2004; Van Loon et al., 2016a; Van Loon et al., 2016b), as well as biogeochemical cycles (Pataki et al., 2011b).

This section separately reviews the links between urbanization and microclimate, water fluxes, and greenhouse gas emissions from urban soils, considering also the role of urban green spaces in providing benefits at different scales. The focus is on the role of urban vegetation in affecting urban microclimate and restoring more natural hydrological and biogeochemical processes, as well as the role that the built landscape plays in the physiological response of urban vegetation. Urban vegetation is generally subject to different biophysical and ecological conditions than rural and natural environments, in particular with respect to soil and climatic conditions. Therefore, in order to provide a positive effect, urban vegetation needs to remain healthy in spite of severe growing conditions and abiotic stress factors, e.g., high temperatures, low moisture conditions, light intensity, chemical stress, and air pollution (Roberts, 1977; Sieghardt et al., 2005a).

2.3.1 Microclimate

Emissions of greenhouse gases and anthropogenic land-cover and land-use changes associated with urbanization have significant impacts on the local microclimate (Kalnay and Cai, 2003; Georgescu et al., 2014). Evident changes have been observed in terms of properties of urban surfaces (e.g., thermal, radiative, and aerodynamic properties), which in turn modify atmospheric conditions such as temperature and precipitation patterns (e.g., Oke, 1982; Oke, 1987; Yow, 2007).

Urban areas have been known to be warmer than the surrounding rural areas due to the UHI effect (Chapman et al., 2017). The magnitude of such urban-rural temperature difference varies as a function of the geographic location, the corresponding climatic region, local topography as well as specific characteristics of the built environment (e.g., urban landscape geometry and intensity of human activities) (Grawe et al., 2013).

Reviewing two decades of urban climate research (i.e., 1980-2000), Arnfield (2003) pointed out some generalizations about the UHI effect. It has long been known that UHI strongly depends on weather conditions (i.e., cloud cover and wind speed) and shows a distinct diurnal and seasonal cycle. In particular, UHI is more intense during summer, especially at night, and under stable weather conditions with light winds and clear skies.

Land cover changes and the structure of urban canyons (defined as the space above the street and between the buildings) are relevant factors that alter the energy balance,

thus controlling the UHI development. The reduction of vegetation cover and the increase of artificial surfaces cause the reduction of latent heat exchange in urban canopies, which favors the UHI, except in arid areas where irrigation may increase the latent heat flux (Yow, 2007). Urban geometry and the thermal and radiative properties of building materials result in more energy absorbed and stored within urban canyons (Harman et al., 2004; Kusaka and Kimura, 2004). As a consequence, the release of stored heat is the dominant contributor to the urban warming at night, regardless of the climatic zone.

UHI intensity during daytime varies geographically because of the influence of local background climate. Zhao et al. (2014) found that UHI intensity increases in humid regions due to vegetation loss and the reduction in the convective heat transfer efficiency. Conversely, UHI intensity should decrease in arid zones where urban landscapes may have a better convection efficiency than the adjacent rural land dominated by low vegetation.

Simulations and observations in semi-arid and arid regions, however, show an urban-induced warming effect (e.g., Hedquist and Brazel, 2006; Georgescu et al., 2014) with a magnitude that can be more significant at midday during summer (Sofer and Potchter, 2006) or during night hours (Saaroni and Ziv, 2010). Compared to UHI patterns in more temperate climates, cities like Phoenix, Arizona (USA), may have cooler summer daytime temperatures due to the higher vegetation cover than the surrounding semi-desert areas (i.e. oasis effect) (Brazel et al., 2000; Stabler et al., 2005). Contrary to the oasis effect, Georgescu et al., 2011 suggests that modification of adjacent conditions, such as land cover and soil moisture, may affect the diurnal cycle of near-surface temperature, for example eliminating the daytime urban cooling.

The UHI effect is often associated with the growing number and increased intensity of heat waves in cities, which cause heat stress and health risks on urban residents (e.g., Lemonsu et al., 2015; Murari et al., 2015; Schatz and Kucharik, 2015; Zhao et al., 2018). Integrating green spaces into the urban landscape has the potential to effectively mitigate the intensity of heat islands and improve human thermal comfort during hot conditions (Oke et al., 1989). The creation of patchy green areas within the urbanized environment generates so-called cool islands, thus mitigating the adverse effects of UHI and extreme heat events (Spronken-Smith and Oke, 1998; Gill et al., 2007; Broadbent et al., 2018). Evidence of the role of urban green spaces in affecting the air temperature of urban areas and the human thermal comfort are reported in a growing number of studies (Table 2.2).

Vegetation affects the thermal energy balance in urban areas mostly through direct shading and evaporative cooling (Holmer et al., 2007;Bowler et al., 2010; Coutts et al., 2016; Sanusi et al., 2016; Gunawardena et al., 2017). Tree canopies intercept solar radiation and,

through direct shading, prevent the energy storage and heating of the local land surface and air; this also helps to reduce buildings energy use (Akbari, 2002; Armson et al., 2012). This shading effect creates local cool areas beneath tree canopies and protects people from the direct exposure to the sun (Dimoudi and Nikolopoulou, 2003). For example, Shahidan et al., 2010 found that for species with high leaf area index (LAI), dense foliage covers, and multiple layers of branches and twigs, the reduction of thermal radiation through absorption and reflection is about 93%, thus producing only 7% radiant heat underneath the canopy. Therefore, vegetation makes a substantial contribution to human thermal comfort (Shashua-Bar et al., 2011).

Table 2.2: Some results from recent literature on the cooling effect of green spaces.

Urban area/ Climate	**Period**	**Data**[a]	**Urban green space**	**Size (ha)**	**Cooling Effect Findings**	**Reference**
Vancouver (Canada) *Marine West Coast*	August 1992	T_a	- 10 parks[b]: - 1 grass (dry) - 2 grass (moist) - 2 grass (irrigated) - 2 grass TB - 1 multi-use - 1 garden - 1 savannah - 1 forest	3-53	Max PCI[d,e]: - 3.2°C d - 4.5°C d - 4.0°C (N) - 3.8°C d - 5.0°C (N) - 4.6°C (N) - 3.7°C (N) - 4.0°C d	Spronken-Smith and Oke (1998)
Sacramento (California) *Mediterranean with hot dry summer*	August 1993	T_a	- 10 parks[c]: - 2 grass (irrigated) - 2 golf course - 4 multi-use - 1 Savannah - 1 Forest	2-15	Max PCI[d,e]: - 4.1°C (N) - 5.1°C (N) - 3.8°C (N) - 5.4°C (N) - 5.3°C (N)	
Goteborg (Sweden) *Marine West Coast*	January 1994 to September 1995 Night-time	T_a	3 urban parks: - Gubberoparken - Vasaparke - Slottsskogen	2.4 3.6 156	Max PCI[d]: - 1.7°C - 2.0°C - 5.9°C Park size is important for the magnitude of PCI.	Upmanis et al. (1998)
Tel Aviv (Israel) *Subtropical with hot and humid summer*	June 2002	Ta	- Park A: grass and few low trees, mostly without shade - Park B: dense medium size trees, partially shaded (65%) - Park C: trees with high and wide canopy, well shaded (95%)	2.5 35 28	- D[e]: warmer up to 1°C - N[e]: cooler up to 1.5°C - D[e]: cooler up to 2°C - N[e]: cooler 0.5-0.7°C - D[e]: cooler up to 2.5°C - N[e]: cooler 0.5-1.2°C Cooling effect of trees is influenced by foliage density, trees height, and size/canopy volume. Grass parks can be warmer during daytime.	Potchter et al. (2006)
Taipei (China) *Humid subtropical*	August to September 2003 December 2003 to February 2004	Ta	61 parks out of the 490 municipal parks: - 30 - 14 - 17	<1 0.5-1 >1	Average PCI[d]: - Summer noon: 0.81°C - Summer night: 0.29°C - Winter noon: 0.57°C - Winter night: 0.16°C Parks as local heat islands: - Summer noon: 0.42°C, (14 parks out of 61) - Summer night: 0.39°C (8 parks out of 61) - Winter noon: 0.59°C (16 parks out of 61) - Winter night: 0.45°C (12 parks out of 61)	Chang et al. (2007)

Continued on next page

Table 2.2 – *Continued from previous page*

Urban area/ Climate	Period	Data[a]	Urban green space	Size (ha)	Cooling Effect Findings	Reference
Lisbon (Portugal) *Mediterranean*	Summer 2007	Ta	Garden in a residential setting with a dense plant community	0.6	Max PCI[d]: 6.9°C	Oliveira et al. (2011)
Phoenix (Arizona) *Tropical and Subtropical Desert*	October 2007 Early morning	- Ta - RH	Small park with irrigated lawn and xeric surfaces within an university campus	∼3	Mean (maximum) PCI[d] intensities ∼3.5°C (∼6°C). Surface type affects PCI intensities with larger PCI over the irrigated lawn.	Chow et al. (2011)
Shenzen (China) *Humid subtropical*	November 2010 to October 2011	- Ta - RH	Plant community within 3 parks: - Multilayer - Palm mixed - Trees-grass - Bamboo grove	29-66	Temperature reduction - Humidity increase - 4.7°C - 7.7% - 3.2°C - 6.7% - 3.6°C - 7.0% - 2.7°C - 6.2%	Zhang et al. (2013)
Melbourne (Australia) *Marine West Coast*	May 2011 to May 2012 October 2011 to June 2013	- Ta - RH - Ws	Street trees in: - Deep urban canyon - Shallow urban canyon with very little tree canopy cover - Shallow urban canyon with dense tree canopy cover		- Street trees support daytime cooling during heat events in the shallow canyon by around 0.2 to 0.6°C and up to 0.9°C between 9-10 AM. - Maximum daytime cooling in shallow canyon is 1.5°C. - In the deep canyon, the shading effect of the tall buildings mask the influence of trees.	Coutts et al. (2016)
Gothenburg (Sweden) *Marine West Coast*	Daytime and Night-time on warmer days of 2012-2013	- g_s - T - PAR - Ta - RH	- 7 of the most common street tree species in Gothenburg; - 1 plot for each specie containing 3 to 6 similar trees		- Midday energy loss due to tree transpiration: 206 Wm^{-2} (about 30% of incoming solar radiation converted in latent heat flux). - Night-time energy loss due to tree transpiration: 24 Wm^{-2}. - Sunlit leaves transpire 3 times more than shade leaves.	Konarska et al. (2016)
Adelaide (Australia) *Mediterranean*	February 2011	- Ta - RH - Ws	Suburb of Mawson Lakes: - pervious (including trees, grass, low vegetation, and bare soil) - open water - impervious	374 (54%) 42 (6%) 260 (40%)	- Irrigation can significantly reduce microscale air temperature during heatwave conditions. - Average air temperature reduction during daytime ∼2.3°C.	Broadbent et al. (2017)

[a] Ta: Air Temperature; RH: Relative Humidity; Ws: Wind Speed; g_s: Stomatal Conductance; T: Transpiration Rate; PAR: Photosynthetic Active Radiation.
[b] Grass: open grass surface; grass TB: grass with tree border; multi-use: park with many different components (grass playing fields; garden: cultivated park with a mixture of grass, trees, and shrubs; savannah: grass surface with trees interspersed throughout).
[c] Golf course: open grass fairways lined by trees; forest: park that has a continuous tree canopy coverage.
[d] PCI, park cooling island: maximum urban temperature (Tu) - minimum park temperature (Tp).
[e] N: night-time cooling; D: day-time cooling.

Increasing interest is directed to evaporative cooling. Through transpiration, more radiant energy is used to increase latent heat rather than sensible heat, allowing the loss of water from plants and wet surfaces as vapor into the atmosphere (Oke, 1987). The achieved cooling potential is influenced by vegetation species (i.e., C3 and C4 photosynthetic metabolism) as well as plant characteristics (e.g., crown area, foliage density, and stomatal resistance) and soil water availability (Caird et al., 2007; Doick et al., 2014).

Several aspects can influence the thermal effect of urban green areas including their characteristics (e.g., size, vegetation composition, and irrigation practices), the nature of the surrounding landscape, and the climate (Spronken-Smith and Oke, 1998; Upmanis et al., 1998; Shiflett et al., 2017). The size of vegetated areas as well as their plant density and composition may affect the magnitude of the temperature difference with their urban surrounding (Cheng et al., 2014). For example, Potchter et al., 2006 found that an urban park covered by grass and a few low trees was warmer (up to 1° C) during the day compared to the surrounding built landscape, whereas a park containing a greater number of trees with a wide canopy reached a cooling effect of 3.5°C. Multilayer plant communities have the most significant effect on temperature reduction (∼4.7°C) and relative humidity increase (∼7.7%) (Zhang et al., 2013), as well as plants with higher foliage density (Yu and Hien, 2006).

Long-term analysis on diurnal and seasonal variations of climatic conditions in urban green spaces show a much higher cooling effect in summer than in winter and during the day than at night (Cohen et al., 2012). Several studies suggest that the cooling effect of vegetation also exists at night (Chow et al., 2011; Konarska et al., 2016). Vegetated areas may have an increase in outgoing long-wave radiations due to higher sky view factor (i.e., the proportion of visible sky above a certain observation point) compared to built-up areas; this helps the night-time cooling effect (Holmer et al., 2013). In addition, tree transpiration may increase the cooling rate around and shortly after sunset, in particular in warm climates and during heat waves (Konarska et al., 2016).

Local climate change within urban areas may affect biophysical and ecological conditions of urban vegetation. Increases in temperature associated with UHI affect the growing season length, with existing observations showing longer growing season lengths in urban environments than surrounding rural areas (Zipper et al., 2016). There are thus complex relationships between the effect of urban green spaces on local climate and how the local climate in turn affects urban vegetation (Zhou et al., 2016).

Beside atmospheric temperatures, precipitation patterns are also affected by urbanization. Early investigations in the 1970s (i.e. METROMEX project, see Changnon, 1981) found evidence of increased precipitation during summer months. Since then, assessing the role of urbanization on rainfall variability has become a topic of active research (Smith et al., 2012). Shepherd (2005) reviewed observational and modeling studies on urban-induced precipitation variability. It is generally recognized that urbanization can affect precipitation mainly through [a] enhanced convergence due to increased surface roughness, [b] destabilization of the boundary layers due to UHI, [c] increases in aerosols associated with land use influencing cloud condensation nuclei (CCN) sources, and [e] changes in the urban canopy (Yu and Liu,

2015).

In most cases, studies report increases in the precipitation amount during summer months (Collier, 2006), even though such estimates can have a high degree of uncertainty (Salvadore et al., 2015). A radar-based analysis using 91 thunderstorm cases in Indianapolis, Indiana (USA), found a strong urban impact on the intensity and structure of approaching thunderstorms (Niyogi et al., 2011). Burian and Shepherd, 2005 found an increase in the average warm-season rainfall amount registered in the Houston, Texas (USA), metropolitan area due to urbanization, especially during afternoons. Other studies conducted in arid cities, such as Phoenix, found increases in mean precipitation of 12-14% from a pre-urban to post-urban period (Shepherd, 2006) and more-frequent late-afternoon storms (Balling and Brazel, 1987).

Modeling studies and satellite-based observations (Miao et al., 2011; Shem and Shepherd, 2009) confirm the crucial role of urban areas in determining storm movement and rainfall amount as a function of the degree of urbanization, the UHI effect, and air pollution. Rosenfeld (2000) pointed out new insights into the negative impact of air pollution on rain-forming processes in clouds. In fact, elevated concentrations of CCN in polluted clouds might lead to many small droplets that cannot easily grow in size to produce precipitation. However, the effects of urban areas on precipitation may depend on the climate regime and the geographical locations of cities. For this reason, in some regions rainfall patterns may decrease in response to urbanization (Zhang et al., 2014b). In Beijing, China, for instance, less evaporation, higher surface temperatures, and larger sensible heat fluxes lead to a decrease in precipitation. In such a scenario, increasing vegetation cover could help to produce more rainfall (Zhang et al., 2009).

2.3.2 The urban water cycle and the role of vegetation

Following Lerner (1990) it is possible to identify two interconnected networks of hydrological pathways in the urban environment, namely a modified natural set of pathways and water supply-sewerage pathways (Figure 2.2). The pathways of the natural network include precipitation, evapotranspiration, runoff, infiltration, and groundwater recharge, which are often affected by the urban microclimate and land cover changes. The water supply-sewerage network includes groundwater extraction through boreholes, flow in water mains and stormwater flow in the sewage system, irrigation, and leakage from pipes, to mention the most relevant.

In the face of increasing urbanization, there is a growing need to restore the water cycle and water quality to a regime closer to that preceding the establishment of urban developments (Fletcher et al., 2013). This is aligned to the natural flow paradigm (Poff, 1997),

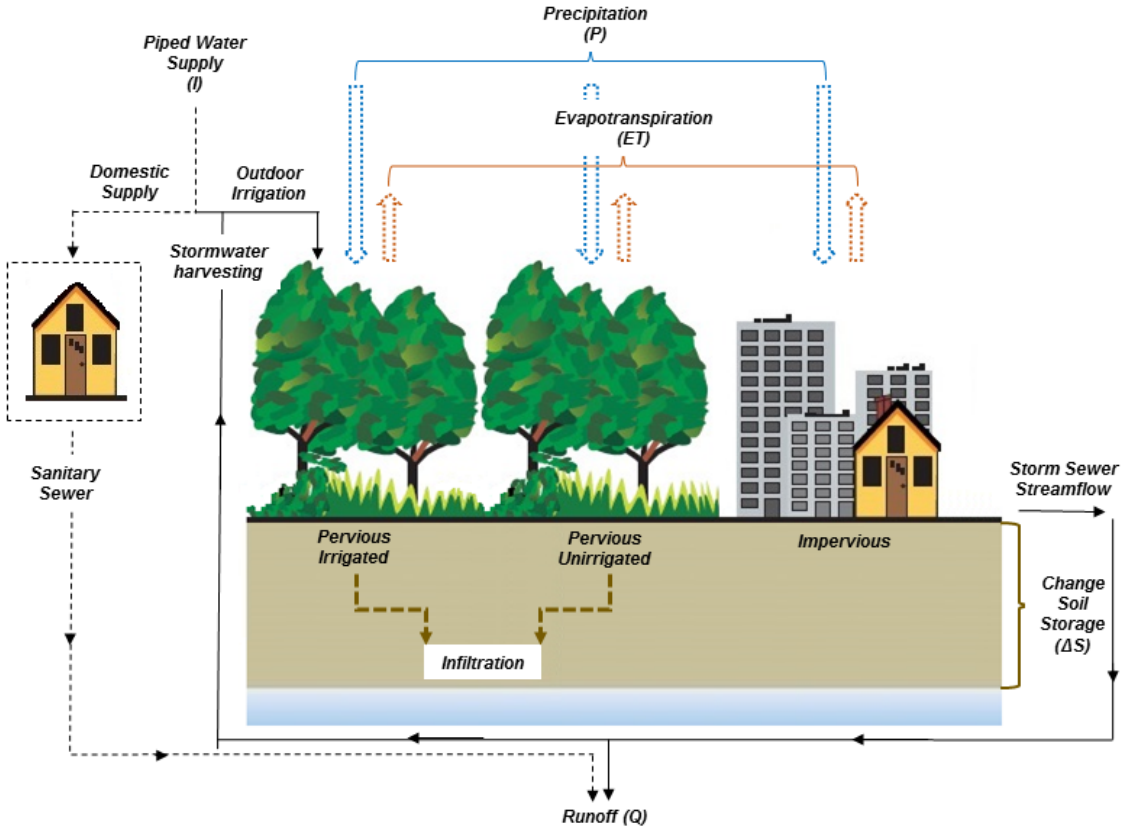

Figure 2.2: Urban water balance (i.e., $P+I=Q+ET+\Delta S$) (Grimmond et al., 1986).

which prescribes the maintenance of streams close to their natural regime (Bonneau et al., 2017).

The aim of this section is to give an overview of the pathways underlying the urban water cycle and the role that urban vegetation plays in influencing such dynamics. Moreover, it provides a review of the current status of the literature about the physiological response of urban vegetation to the altered environmental conditions caused by urbanization. We did not include a review of green technologies for stormwater harvesting, i.e., low impact development (LID), water sensitive urban design (WSUD), and sustainable urban drainage systems (SUDS). Interested readers are referred to Wong and Brown (2009), Fletcher et al. (2015), Bonneau et al. (2017), and Golden and Hoghooghi (2018), just to name a few.

The rates and volumes of surface runoff from urbanized watersheds are expected to be greater due to soil compaction, vegetation removal, and impervious surfaces (e.g., Leopold, 1968; Endreny, 2005; Xiao et al., 2007). In a study conducted in North Carolina, USA, for example, Boggs and Sun (2011) found that the mean annual discharge ratio (discharge/precipitation) was 75% higher in urban precincts compared to a forested watershed. The amount of im-

pervious areas and their degree of connectivity with the drainage network are key factors in determining the increase of peak flows and surface runoff (Boyd et al., 1993; Shields and Tague, 2015). At the same time, it is generally accepted that the increase of urban impervious surfaces leads to a reduction in catchment evaporative losses (e.g., Dow and DeWalle, 2000; Barron et al., 2013), even though evapotranspiration (ET) in urban areas has complex patterns associated with landscape heterogeneity and changes in the urban microclimate (e.g., Salvadore et al., 2015; Owuor et al., 2016; Litvak et al., 2017).

Several parameters were found to influence the interactions between urbanization and subsurface processes, including natural catchment characteristics, e.g., topography, vegetation, as well as anthropogenic factors, e.g., catchment imperviousness, spatial distribution of impervious surfaces, anthropogenic water inputs and outputs (Hamel et al., 2013).It is also well known that the introduction of impervious surfaces and drainage infrastructure decrease infiltration and groundwater recharge (e.g., Shuster et al., 2005; Hibbs, 2016). However, several authors suggest that external anthropogenic water inputs, such as leakage from water supply systems, sewers, and stormwater drainage networks, as well as irrigation, may offset subsurface water losses (e.g., Lerner, 2002; Price, 2011; Locatelli et al., 2017). In particular, irrigation may play an essential role in groundwater recharge, being a conspicuous portion (i.e., 40-75%) of residential water use, especially in arid and semi-arid regions (Balling et al., 2008; Hilaire et al., 2008). In Austin, Texas (USA), for example, an estimated 8% of water that flows through city mains becomes groundwater recharge (Garcia-Fresca and Sharp Jr, 2005); this water and irrigation results in flows that represent at least 5% of total annual discharge (Passarello et al., 2012).

Urban vegetation has been identified as an effective measure to decrease runoff by increasing rainfall interception, soil permeability, and thus evapotranspiration (Yang et al., 2015; Berland et al., 2017). However, rainfall-runoff-infiltration processes associated with urban pervious green spaces are quite uncertain, being affected by the combined effect of soil compaction, vegetation type, topsoil removal as well as increased soil hydrophobicity and deposition of pollutants (e.g., Fletcher et al., 2013; Redfern et al., 2016).

The potential of urban trees to retain and store rainfall on leaves and branches is recognized to be extremely effective in reducing stormwater runoff because a large fraction of the water temporarily retained within the canopy is lost to the atmosphere by evaporation, a process known as canopy interception (Xiao et al., 1998; Kermavnar and Vilhar, 2017). For example, Livesley et al. (2014) estimated that eucalypt tree species can reduce rainfall reaching the ground by up to 45% in an urban street setting in Melbourne (Australia). However, canopy interception is strongly influenced by tree structure (e.g., leaf and stem surface areas,

foliation period, species dimensions) and meteorological factors (e.g., amount, duration, intensity of rain events, evaporation rates) (Xiao et al., 2000; Holder and Gibbes, 2017). Xiao and McPherson (2002) found variations in the rainfall interception both depending on tree species (i.e., small canopy trees are much less effective in intercepting rainfall) and season (i.e., 14.8% of rainfall interception during a winter storm and 79.5% during a similar storm in summer for a large deciduous tree).

The ability of urban trees to be effective in mitigating the impacts of urbanization is strongly linked to the their health, stability, and longevity, which in turn depend on the ability of the root systems to grow in urban soil conditions to then acquire water and nutrients (Day et al., 2010a; Bijoor et al., 2012). Root growth and development in urban settings are often impaired by impenetrable or inhospitable soil layers, little suitable soil volume, and underground infrastructure, as well as by chemical contamination and excessive heat, thus influencing tree growth (Day et al., 2010b). In turn, tree roots alter the belowground environment through their impact on biological, physical, and chemical soil properties, thus affecting nutrient and carbon cycling, soil structure and infiltration processes. In particular, root systems increase the capacity and rate of soils to infiltrate rainfall along root channels, thus improving groundwater recharge (Bartens et al., 2008). Biological factors such as tree size, rooting depth, and LAI also have a great impact on tree transpiration. Trees planted in urban landscapes are often exposed to high atmospheric evaporative demand because of the UHI, which results in increased temperatures and lower air humidity; this can raise tree transpiration rates, where sufficient soil moisture can sustain higher transpiration levels (Zipper et al., 2017a). At the same time, limited rooting space, soil compaction, and water stress strongly affect stomatal regulation, and thus transpiration rates (Cregg, 1995a; Cregg and Dix, 2001a; Litvak et al., 2011; Chen et al., 2011; Asawa et al., 2017).

Vegetation response to urban conditions also strongly depends on the plant species and composition. For example, Peters et al. (2010), measuring sap flux in several dominant tree species in a suburban neighborhood in Minnesota (USA), found that evergreen needle leaf trees have higher total annual transpiration than deciduous broadleaf trees.

The coexistence of remaining native vegetation and introduced non-native species in urban green spaces may create unique biotic communities with potentially higher water demand, and different and more complex patterns of ET (Pataki et al., 2011a). In irrigated urban landscapes, soil moisture may be non-limiting, and vegetation can show higher transpiration rates largely controlled by stomatal responses to environmental conditions (e.g., Litvak and Pataki, 2016; Litvak et al., 2017). In southern California, for example, the combination of moist, irrigated soils and dry air often leads to higher urban ET than the

surrounding natural ecosystem (Litvak et al., 2011). In the Los Angeles metropolitan area, where trees are often irrigated, their stomatal behavior can be consistent with the general relationship between transpiration and stomatal sensitivity in natural environments, as shown by Litvak et al. (2012).

In arid and semi-arid urban landscapes, plant-available soil moisture is the major driver for the viability of vegetation species, in particular for high water use, non-native plants (McCarthy and Pataki, 2010). For this reason, water-conserving landscape designs are encouraged as well as appropriate irrigation-scheduling depending on plant water demands (Pataki et al., 2011c; Breyer et al., 2018). Landscape design strategies include the conversion of more traditional mesic landscapes with xerophytic vegetation, which requires less water and it is recognized to be more water conservative (e.g., Martin and Stabler, 2002; Holder and Gibbes, 2017). In this context, McCarthy et al. (2011) suggested the water-use efficiency (WUE) (i.e., the ratio of water used in plant metabolism to water lost by the plant through transpiration) as a measurable indicator of the trade-off between the water use and the ecosystem services related to the growth rate to help in maximizing the growth while conserving water.

2.3.3 Greenhouse gas emissions from urban soils

The environmental changes associated with urbanization, combined with human disturbances and landscape management, make urban areas hotspots for biogeochemical cycling and production of greenhouse gases (GHGs) (Kaye et al., 2006; Pouyat et al., 2007; Hutyra et al., 2014; Decina et al., 2016; Livesley et al., 2016b).

Cities are commonly sources of CO_2, N_2O, and CH_4 as shown by eddy covariance observations above urbanized areas (Grimmond et al., 2004; Famulari et al., 2010; Crawford et al., 2011; Pawlak and Fortuniak, 2016). Human activities are mostly responsible for greenhouse gas emissions from urban areas, mainly from burning fossil fuels for electricity, heat, and transportation (Kennedy et al., 2009; IPCC, 2015). For example, Idso et al. (2001) found a strong but variable urban CO_2 dome in the Phoenix metropolitan area with a maximum peak in CO_2 concentration in the center of the city 75% greater than that of the surrounding rural area. Vegetated areas also have the potential to offset these anthropogenic emissions by reducing the level of atmospheric CO_2 as a result of their CO_2 uptake through photosynthesis (Kordowski and Kuttler, 2010; Nordbo et al., 2012).

Urban soils represent a major source of GHGs with the magnitude of emissions greatly influenced by urban environmental factors. Urbanization strongly affects soil carbon c and nitrogen (N) cycling and related GHG emissions (Pouyat et al., 2002; Lorenz and Lal, 2009).

The exchange of CO_2, N_2O, and CH_4 between urban soils and the atmosphere strongly depends on factors that are greatly modified by urbanization, such as soil moisture and temperature, soil structure and texture, nutrient inputs and substrate availability (van Delden et al., 2016).

In urban environments, soils are often disturbed through removal and compaction, and the introduction of impervious surfaces, having strong influences on the soil structure and texture, C pools, and microbial community structure and function. Additionally, land management practices, such as fertilization and irrigation, have the potential to increase soil organic C accumulation and N inputs, which might result in increased GHG emissions, including N_2O and CH_4 (e.g., Kaye et al., 2004; Livesley et al., 2010). For example, in northern Colorado, urban lawns account for 30% of the soil N_2O emissions from that region, just occupying 6.4% of the land area (Kaye et al., 2004).

The impact of all these anthropogenic drivers on C and N cycles takes place through complex interactions at various levels, making it difficult to identify the contribution of individual factors. This section focuses on the exchange of the three major GHGs (i.e., CO_2, N_2O, and CH_4) between soil and atmosphere, and does not provide a complete review of the soil C and N cycles (Lal and Stewart (2017) for more details).

Several studies in the last two decades have been conducted to assess the magnitude of GHG fluxes from urban vegetated soils and the related effects of urban environmental changes. Some of these results are shown in Tables 3, 4, and 5 for CO_2, N_2O, and CH_4 respectively.

Variations in soil CO_2 emission rates across urban, rural, and natural environments are shown in (Table 2.3). Long-term data collected within the Baltimore Ecosystem Study (Groffman et al., 2006; Groffman and Pouyat, 2009) showed marked seasonal patterns in the CO_2 fluxes with highest rates during warmer seasons. Lawns often have the highest CO_2 fluxes, especially when highly managed (i.e., watered and fertilized regularly) (e.g., Pouyat et al., 2002; Kaye et al., 2005; Golubiewski, 2006; Koerner and Klopatek, 2010). In arid and semiarid regions, such as the Phoenix metropolitan area, urbanization drastically changed the biologic structure of the ecosystem mainly due to water and energy subsidies, which in turn impact carbon stock and fluxes (Koerner and Klopatek, 2002; Pouyat et al., 2002; Koerner and Klopatek, 2010). In such ecosystems, soil respiration rates significantly increase compared to desert remnant areas because soil moisture is recognized to be the main factor controlling soil CO_2 efflux.

Table 2.3: CO_2 soil emission rates in g_{CO_2-C} m^{-2} h^{-1} for different cover types and climatic regions. Ranges have been often extrapolated from figures and then rounded for clarity (see original literature for more details).

Region/Climate	Land type	Rate	Comments	Findings	Reference
Phoenix (Arizona) *Tropical and Subtropical Desert*	- Native desert - Abandoned agricultural - Xeric landscape - Mesic landscape [a] - Agricultural land - Golf courses - Landfills	0.02 0.04 0.04 0.30 0.25 0.33 0.59	Means June 2000 - May 2001	Lowest CO_2 emissions in the desert area, abandoned agricultural and xeric land. Highest rates of CO_2 in the landfills. CO_2 fluxes increase with increasing soil moisture.	Koerner and Klopatek (2002)
Fort Collins (Colorado) *Tropical and Subtropical Steppe*	- Urban lawns [b] - Dryland wheat-fallow - Irrigated corn - Native shortgrass	0.31 0.05 0.12 0.10	Annual means January - December 2001	Seasonal and annual variability in CO_2 fluxes. Higher CO_2 emissions and C allocation in urban lawns due to fertilization and irrigation inputs.	Kaye et al. (2005)
Baltimore [c] (Maryland) *Humid Subtropical*	- Urban forest - Rural forest	0.09 0.07	Means Fall 1998 - Fall 2002	CO_2 fluxes are strongly influenced by exposure to the urban land use and atmosphere.	Groffman et al. (2006)
Baltimore [c] (Maryland) *Humid Subtropical*	- Urban forest - Rural forest - Urban grassland	0.12 0.08 0.11	Means June 2001 - May 2004	High CO_2 fluxes in the grass plots driven by high productivity and high temperatures in the grass plots (lack of tree canopy).	Groffman et al. (2009)
Melbourne (Australia) *Marine West Coast*	- Urban lawn[d] : - Rain only - Rain+Fertilizer - Irrigated - Irrigated+Fertilizer - Rain reduced - Mulch+Irrigated	0.39 0.41 0.42 0.47 0.37 0.38	Means August-November 2007	No significant difference in CO_2 emissions among the lawn and mulched treatments.	Livesley et al. (2010)
Melbourne (Australia) *Marine West Coast*	Biofilter[e] : - Cell I - Cell III	0.10 0.10	Means March-May 2011 January-February 2012	Small values of CO_2 fluxes due to low levels of soil C in the biofilter (new sand dominated system).	Grover et al. (2013)
Singapore *Tropical Rainforest*	- Bare soil NC [f] - Bare soil WC - Turf soil NC - Turf soil WC,	0.10 0.14 0.36 0.30	Means July - December 2012	Influence of management practices on CO_2 fluxes in urban tropical grassland. Bare soils: lowest mean CO_2 efflux rates. Turf with no grass clipping: highest mean CO_2 efflux rates.	Ng et al. (2015)
Boston (Massachusetts) *Hot Summer Continental*	- Urban forest - Rural forest - Urban lawn - Urban landscaped	0.11 0.19 0.29 0.13	Growing season means May - November 2014	Similar values between urban and rural forest soils considering growing season mean soil CO_2 efflux rates.	Decina et al. (2016)

[a] Grass lawns
[b] Well-managed with irrigation, mowing, and fertilization.
[c] Baltimore ecosystem Study Long-term Study Plots.
[d] Five different lawn treatments with different water and nutrient management and 1 mulched and drip irrigated garden bed.
[e] Biofilter that treats stormwater from a multistory carpark; no fertilization. It is divided in three cells, but experiments were conducted in cell I (sandy loam) and cell III (80% sandy loam, 10% compost, and 10% hardwood mulch).
[f] NC: no grass clipping; WC: whit grass clipping.

In terms of N_2O fluxes (Table 2.4), the climatic region plays a crucial role in the magnitude of such emissions. In humid areas, such as Baltimore, although urban grasslands can be heavily fertilized and irrigated, N_2O fluxes are not higher than those from urban forest plots; moreover, lower fluxes were found in the more heavily fertilized grass sites compared to less fertilized sites (Groffman and Pouyat, 2009). In dry regions, such as Colorado and Arizona, on the contrary, urban lawns exhibit higher N_2O fluxes compared to the native

landscapes due to the combination of fertilizer and water inputs (Kaye et al., 2004; Hall et al., 2008).

The use of fertilizer may not have an immediate effect on N_2O and CO_2 fluxes. For example, Raciti et al. (2011) found a significant increase in N_2O fluxes several days after fertilization. Livesley et al. (2010) obtained similar results by measuring N_2O emissions in lawn plots in Melbourne (Australia). In this specific case study the application of fertilizer caused a peak in N_2O emissions six days after its application. However, they found that irrigation and soil moisture content, rather than fertilizer, determine the long-term mean differences in N_2O emissions.

Table 2.4: N_2O soil emission rates in μg_{N_2O-C} m^{-2} h^{-1} for different cover types and climatic regions. Ranges have been often extrapolated from figures and then rounded for clarity (see original literature for more details).

Region/Climate	Land type	Rate	Comments	Findings	Reference
Fort Collins (Colorado) *Tropical and Subtropical Steppe*	- Urban lawns[a] - Dryland wheat-fallow - Irrigated corn - Native shortgrass	2.20 1.80 23.20 27.60	Annual fluxes November 2000 to November 2001	N_2O fluxes from urban grassland are about 10 times larger than emissions from native grassland.	Kaye et al. (2004)
Baltimore[b] (Maryland) *Humid Subtropical*	- Urban forest - Rural forest	14.30 7.00	Means Fall 1998 - Fall 2002	Finest textured soils lead to higher N_2O fluxes. Species change (plant or soil community) is a powerful driver of N cycling along urban to rural gradients.	Groffman et al. (2006)
Baltimore[b] (Maryland) *Humid Subtropical*	- Urban forest - Rural forest - Urban grassland	40.54 6.22 25.14	Means June 2001 - May 2004	Although urban grasslands can be heavily fertilized and irrigated, N_2O fluxes are lower than urban forest plots. Water could be the key driver of N_2O emissions in urban landscapes. Highest N_2O fluxes rates during wetter months.	Groffman et al. (2009)
Phoenix (Arizona) *Tropical and Subtropical Desert*	- Urban lawns - Managed Xeriscapes - Remnant desert sites[c]	36.11 11.11 5.78	Means taking into account measurements before and after watering March 2001 May/June 2006	Higher N_2O emissions in urban lawns. Alternative urban landscaping practices (xeriscape) can reduce N_2O emissions and promote water conservation. Increased N_2O emissions in urbanized areas compared to the native landscaped due to the expansion of irrigated and fertilized lawns.	Hall et al. (2008)
Irvine (California) *Mediterranean*	Urban lawns (ornamental lawns and athletic fields)	11.52-34.25	Annual means depending on fertilization rate	Great impact of fertilization on N_2O emissions.	Townsend-Small and Czimczik (2010)
Melbourne (Australia) *Marine West Coast*	- Urban lawn[d]: - Rain only - Rain+Fertilizer - Irrigated - Irrigated+Fertilizer - Rain reduced - Mulch+Irrigated	 18.00 15.67 28.67 28.00 9.00 14.13	Means August-November 2007	Irrigation and soil moisture content, rather that fertilizer and N status, influence long-term mean differences in N_2O emissions among treatments	Livesley et al.(2010)
Melbourne (Australia) *Marine West Coast*	Biofilter[e]: - Cell I - Cell III	 13.70 65.60	Means March-May 2011 January-February 2012	Higher N_2O in cell III may be attributed to denitrification occurring within the saturated zone and the wet pockets within the unsaturated filter media.	Grover et al. (2013)

[a] Grass lawns
[b] Well-managed with irrigation, mowing, and fertilization.
[c] Baltimore ecosystem Study Long-term Study Plots.
[d] Five different lawn treatments with different water and nutrient management and 1 mulched and drip irrigated garden bed.
[e] Biofilter that treats stormwater from a multistory carpark; no fertilization. It is divided in three cells, but experiments were conducted in cell I (sandy loam) and cell III (80% sandy loam, 10% compost, and 10% hardwood mulch).

The net flux of CH_4 (Table 2.5) from soils is the results of anaerobic production and aerobic consumption of CH_4 (Wachinger et al., 2000). Soils in natural ecosystems, such as temperate forest, grassland, and desert, are normally CH_4 sinks; soils in urban ecosystems instead have low rates of CH_4 uptake (Costa and Groffman, 2013). Reduced CH_4 uptake were recorded in the urban forest sites within the Baltimore Ecosystem Study compared to the rural forest sites, while almost negligible fluxes were found in lawns (Groffman and Pouyat, 2009). Rural sites show higher CH_4 consumption compared to urban forest sites also in Guangzhou City metropolitan area (South China) (Zhang et al., 2014a).

Table 2.5: CH_4 soil emission rates in μg_{CH_4C-C} m^{-2} h^{-1} for different cover types and climatic regions. Ranges have been often extrapolated from figures and then rounded for clarity (see original literature for more details).

Region/Climate	**Land type**	**Rate**	**Comments**	**Findings**	**Reference**
Fort Collins (Colorado) *Tropical and Subtropical Steppe*	- Native shortgrass - Dryland wheat-fallow - Irrigated corn - Urban lawns[a]	20.43 34.85 11.42 16.82	Annual fluxes November 2000 to November 2001	Highest CH_4 uptake in the native grasslands. Lowest mean CH_4 uptake rates in corn and urban lawns. CH_4 from urban soils is half of the flux from native grasslands.	Kaye et al. (2004)
Baltimore [b] (Maryland) *Humid Subtropical*	- Urban forest - Rural forest	42.19 79.17	Means Fall 1998 - Fall 2002	Significant differences in CH_4 uptake between urban and rural land. CH_4 strongly influenced by soil texture and moisture. Coarse-textured dry soils have the highest rates of uptake due to enhanced diffusion of atmospheric CH_4 into the soil.	Groffman et al. (2006)
Baltimore [b] (Maryland) *Humid Subtropical*	- Urban forest - Rural forest - Urban grassland	33.75 70.68 1.06	Means June 2001 - May 2004	Highest consumption in rural forest sites. Negligible fluxes from urban lawns due to the inhibitory effect of N additions on CH_4 uptake ("lawn effect"). CH_4 is strongly affected by soil moisture with an effect on diffusion (essential for the movement of CH_4 from the atmosphere to the microorganisms that oxidize in the soil).	Groffman et al. (2009)
Melbourne (Australia) *Marine West Coast*	- Urban lawn[c]: - Rain only - Rain+Fertilizer - Irrigated - Irrigated+Fertilizer - Rain reduced - Mulch+Irrigated	6.67 4.17 5.00 5.00 3.33 31.25	Means August-November 2007	No significant difference between the long-term mean soil CH_4 exchange rates in any of the lawn treatments.	Livesley et al. (2010)
Melbourne (Australia) *Marine West Coast*	Biofilter[d]: - Cell I - Cell III	18.30 3.80	Means March-May 2011 January-February 2012	CH_4 sink strength of the cell with the saturated zone (cell III) is lower than cell I. CH_4 uptake rates similar to other urban lawn systems. Biofilter cells have occasional large CH_4 emissions following inflow events.	Grover et al. (2013)

[a] Well-managed with irrigation, mowing, and fertilization.
[b] Baltimore ecosystem Study Long-term Study Plots.
[c] Five different lawn treatments with different water and nutrient management and 1 mulched and drip irrigated garden bed.
[d] Biofilter that treats stormwater from a multistory carpark; no fertilization. It is divided in three cells, but experiments were conducted in cell I (sandy loam) and cell III (80% sandy loam, 10% compost, and 10% hardwood mulch).

CH_4 uptake is affected by urbanization through environmental changes in chemistry, climate, and land transformation (Costa and Groffman, 2013). In particular CH_4 uptake can be influenced by soil texture and moisture, mainly because of the rate of diffusion of atmospheric CH_4 into the soil. For example, coarse-textured and dry soils have higher rates of uptake due to enhanced diffusion rates. CH_4 uptake is also strongly affected by high levels of atmospheric CO_2 and N additions (i.e. N deposition), which exert an inhibitory effect. Finally, differences in the population of CH_4 oxidizing organisms may play an important role in the CH_4 dynamics.

2.4 Modeling urban ecosystems

Hydrologic modeling of urban environments is very complex because of the range of natural and anthropogenic processes involved. Although the nature and objectives of urban models cover a wide range (Masson, 2006), a large part of the hydrologic modeling in urban areas has focused on simulating storm water quantity and quality, often with lumped and semi-distributed models (Zoppou, 2001; Fletcher et al., 2013; Mejía et al., 2014; Petrucci and Bonhomme, 2014; Salvadore et al., 2015). Ecohydrological models, describing the water dynamics across the soil-plant-atmosphere continuum through coupling hydrologic and biophysical processes, have been mainly used to study natural and rural environments (e.g., Fatichi et al., 2014; Fatichi et al., 2016). However, the need to quantify impacts and reveal tradeoffs associated with the conversion of natural to urban landscapes has led to a growing interest in applying ecohydrological models to urbanized areas (Salamanca et al., 2018).

The objective of this section is to give an overview of available models in literature that have extended the analysis of hydro-biophysical processes from natural environments to urban areas at different scales. Three main scales are identified: (i) ecohydrological models that represent regional- to catchment-scale interactions between major biogeochemical cycles, water cycle, and vegetation dynamics, (ii) models that operate at the neighborhood scale to simulate soil-plant-atmosphere interactions, and (iii) models that simulate water and nutrient dynamics at the tree level.

We do not explicitly discuss urban storm water models, such as MIKE URBAN[8], Storm Water Management Model (SWMM; Huber et al., 1988), Models of Urban Storm-water Improvement Conceptualization (MUSIC; Wong et al., 2002), Urban Runoff Branching Structure (URBS; Rodriguez et al., 2005), MOdel for Urban SEwers (MOUSE; Lindberg et al., 1989), and CANOE (Lhomme et al., 2004), which are frequently used for the integrated

[8] *www.dhisoftware.com/mikeurban*

management of urban runoff (Fletcher et al., 2013). Some of these models are also useful to predict water flow effects of LID, WSUD, and SUDS (Elliott and Trowsdale, 2007) as well as the water treatment performance of such systems (e.g., Vezzaro et al., 2011; Daly et al., 2012; Vezzaro et al., 2012; Randelovic et al., 2016; Hertwig et al., 2017a; Locatelli et al., 2017;).

2.4.1 Regional to catchment scale

Applications of catchment scale ecohydrological models in urbanized environments are still rare, and few examples are reported here.

To investigate water fluxes at the regional scale over a long period where dramatic environmental changes in climate and land use happened, Liu et al. (2013) applied the dynamic land ecosystem model (DLEM) to the drainage basin of the Gulf of Mexico during the period 1901-2008. Coupling major biogeochemical cycles, water cycle, and vegetation dynamics, DLEM allowed for the investigation of spatial and temporal variations in evapotranspiration (ET) and runoff (R) due to climate and land use changes. The study shows that climate change is the dominant factor controlling the inter-annual variations of ET and runoff, with precipitation playing the major role in the variations of annual water fluxes over the whole region. Both changes in land use and climate led to a general reduction in ET during the study period with high spatial heterogeneity due to different microclimate conditions across the region.

Shields and Tague (2015) have applied the Regional Hydro-Ecological Simulation System (RHESSys) to an urbanized catchment in Santa Barbara, California (USA), to study the impact of impervious area connectivity on water and carbon fluxes in a heterogeneous urban precinct. Results show that the amount of impervious surfaces with a direct hydrologic connection to the drainage network (i.e., effective impervious area, EIA) has a significant impact on transpiration (T) and net primary productivity (NPP). In particular, by reducing the EIA fraction, the reductions in T and NPP associated with increased impervious areas and vegetation loss are significantly lower.

To simulate the effects of changes of urban tree cover and impervious surfaces on urban hydrology at the catchment scale, the U.S. Department of Agriculture (USDA) Forest Service developed UFORE-Hydro, now called i-Tree Hydro, a semi-distributed urban soil-vegetation-atmosphere transfer scheme (Wang et al., 2008). The model represents the watershed surface as impervious or pervious surfaces both with a certain percentage of canopy cover. The model was firstly applied to an urban catchment of about 15 km2 in Baltimore to examine the tree interception under different vegetative and meteorological conditions as well as the

tree effects on runoff generation. Results showed how trees significantly reduce runoff, in particular for low intensity and short duration rainfall events. i-Tree Hydro is part of the i-Tree software suite for urban forest analysis and benefit assessment. Within i-Tree, entire urban forests and street trees can be studied with i-Tree Eco and i-Tree Streets respectively, to estimate vegetation structure (e.g., urban tree growth) and ecosystem services (McPherson and Peper, 2012; Pace et al., 2018).

2.4.2 Neighborhood scale

At smaller spatial scales, a more extensive literature exists on modeling the interactions between urban surfaces, vegetation, and the atmosphere.

Common urban canopy models available in the literature are radiative models centered on the energy balance of urban canyons or precincts. A review of the features of these models can be found in Grimmond et al. (2010) and references therein. A recognized limitation of these models is the description of latent heat fluxes associated with the presence of vegetation in the urban landscape. These fluxes are often not included (Krayenhoff and Voogt, 2007) or their description is simplified (Lee and Park, 2008; Krayenhoff et al., 2014).

Recently, urban trees have been embedded in some urban canopy energy balance models, linking these models to the soil water balance (e.g., Ryu et al., 2016). For example, Niu et al. (2014) modified the Temperature and Urban Facets in 3D (TUF-3D; Krayenhoff and Voogt, 2007) to create Vegetated Temperatures of Urban Facets in 3D (VTUF-3D). TUF-3D is a microscale energy balance model for urban environments, where energy fluxes are described via radiation, convection and conduction. VTUF-3D was developed by coupling TUF-3D to the MAESPA tree process model (Duursma et al., 2012), which couples canopy processes, such as radiative transfer, transpiration and carbon assimilation, to the soil water and energy balances. Once embedded into TUF-3D, MAESPA can account for the effect of trees due to shading of buildings as well as the role of urban trees in affecting soil and air temperatures via root water uptake, interception, and transpiration.

These energy balance models keep a certain level of simplicity and are mostly centered on the simulation of surface temperatures of buildings and paved areas, using a simplified description of atmospheric wind speed and temperatures. Computational fluid dynamics models (CFD), such as Large Eddy Simulation (LES) (e.g., Bou-Zeid et al., 2009; Kanda et al., 2013; Giometto et al., 2016; Girard et al., 2017; Hertwig et al., 2017b; Toparlar et al., 2017), can provide detailed descriptions of wind speed and temperatures within the urban atmospheric boundary layer. Differently from radiative models, CFD models are computationally demanding and present challenges with the representation of geometrical

features of the urban landscape. Nonetheless, recent studies with LES were able to include the geometry of street trees identifying their role in reducing pressure loads on buildings (Giometto et al., 2016; Giometto et al., 2017).

A well-established CFD model for urban precincts is ENVI-met (Bruse and Fleer, 1998), which couples the incompressible Reynolds Averaged Navier-Stokes equations to advection-diffusion equations for specific humidity and temperature and includes spatially variable sources due to tree canopies. ENVI-met is largely used in microclimatic analysis that involve the study of urban vegetation and its potential to mitigate human heat stress (e.g., Lee et al., 2016; Morakinyo et al., 2017; Simon et al., 2018).

2.4.3 Tree scale

Very few studies exist in the literature focused on modeling the water dynamics in soil-plant systems in urban environments at the local tree scale, despite the importance of urban trees and their ecosystem services.

Several authors suggest the application of a stochastic model of the soil water balance, previously applied to natural and agricultural environments (e.g., Laio et al., 2001; Vico and Porporato, 2011; Daly et al., 2004), to urban areas. Specific applications include the study of water dynamics in isolated and in-row trees (Vico et al., 2014) and irrigated and non-irrigated experimental landscaping treatments (Volo et al., 2014). These models, explicitly including rainfall unpredictability within a probabilistic framework, quantify the statistics of tree transpiration and water stress from the statistics of soil moisture, which depend on tree characteristics (i.e., species, size), planting design, root zone features, and precipitation and irrigation frequencies and amounts.

Having a model to explore planting design and irrigation scenarios on plant water stress can be particularly useful in desert urban landscapes, where plant-available soil moisture is a major driver for vegetation health, in particular for non-native plants (McCarthy and Pataki, 2010). For example, Volo et al. (2014)applied the model to the Phoenix metropolitan area to explore the effects of irrigation in terms of soil moisture dynamics, water balance partitioning, and plant water stress taking into account xeric (i.e., low water use vegetation) and mesic (i.e., turf grass and high water use trees) landscape design.

The model used by Vico et al. (2014) for assessing street tree water balance was recently coupled with the nutrient dynamics model proposed by Porporato et al., 2003 to explore the feedbacks between water and nutrient dynamics in the context of urban street trees (Vico et al., 2014; Revelli and Porporato, 2018). Model results (i.e., soil water and N concentration, water and N fluxes in and out of the system) can be used to quantify some

ecosystem services provided by street trees, such as cooling effect, soil carbon sequestration, and storm-water management. In particular, the authors found that urban design (e.g., design of the soil compartment around the tress) and irrigation schedules must be optimized to enhance ecosystem services and minimize plant water stress.

2.5 Summary

Given the speed at which cities are expanding and becoming densely populated, there is a growing need to support sustainable uses of soil, vegetation, and water resources in urban areas. This chapter reviews literature on ecohydrological studies and approaches which are focused urban areas. It is well known that urbanization drives significant environmental changes at multiple spatial and temporal scales. Evidence of the influence of urbanization on local and regional climate are extensively documented, in particular in relation to the UHI effect and human thermal comfort. The impacts of urban development on hydrological and biogeochemical cycles have been quite well studied in the last two decades. Recently, more attention has been paid to the components of the urban water balance that are still highly uncertain (e.g., ET) and quite difficult to determine due to the complex heterogeneity of the urban landscape. Modeling tools are also available to assess the interactions between surfaces, vegetation, and the atmosphere in urban areas in particular from a climatic perspective.

2.6 Scope of research

Focusing on urban reserves which host remnant native plants (Table 2.1), this project aims to improve the understanding of interactions and feedback between water resources and vegetation health, providing also important knowledge for their specific management. In collaboration with two councils, the *City of Greater Dandenong* and *Moonee Valley City*, that manage a number of remnant urban reserves across the Melbourne metropolitan area, this project addresses basic scientific problems and provides practical guidelines to support reserves and parks management. Specifically, the research addresses the following questions:

a) *What is the water balance of urban reserves experiencing different rainfall and irrigation regimes?*

   The scientific purpose of this question is two-fold. First, understanding the reserves water balance, this project delivers insights on how hydrological conditions affected

by the urban environment may impact on the water regime and, as a result, on the health of the remnant vegetation. Second, quantifying tree water use informs about tree response to water restrictions, heat stress, and drought. These results complement the research effort currently dedicated to understanding and quantifying the tree water use in urban settings.

Practically, a better understanding of the reserve hydrology can assist government authorities in the management of urban trees and landscape. The remnant urban reserves involved in this project are endangered and extremely valuable in terms of cultural heritage and social well-being, as highlighted by government authorities and people living around them. The major issue is the declining health of the native vegetation, as some trees are dying within the reserves. Therefore, understanding the water requirements of these reserves can help the councils in developing irrigation management plans for their preservation.

b) *How do different scenarios of water availability control the ecosystem response under both present and variable climate?*

This question explores how the presence of a shallow water table or its capillary fringe within the reach of the plant roots might support urban reserves during inter-annual water stress periods due to rainfall shortage. Using a mechanistic modeling approach to simulate the coupled dynamics of energy-water-vegetation, this question provides quantitative answers considering both present climate (including the recent Millennium Drought from 2001 to 2009) and future climatic stressors (such as increased air temperature and atmospheric CO_2 concentrations as well as rainfall shortage), thus overcoming the time constraints of experimental studies.

There is also a practical interest in highlighting the role of groundwater in supporting urban reserves functioning during prolonged droughts. Robust predictions of vegetation response to groundwater depletion and climate variability are essential to highlight the need for extensive groundwater monitoring networks, especially in urbanized areas, and appropriate management practices in terms of vegetation and groundwater resources both at local and catchment scale.

c) *How might an ecohydrological model support the management of urban reserves?*

Using an ecohydrological model, this project provides a direct link between the alteration in the hydrologic regime (e.g., through irrigation) and biophysical structure of vegetation (e.g., through revegetation) and energy, water, and carbon fluxes in order

to integrate the knowledge derived from empirical studies.

In practical terms, government authorities managing remnant urban reserves, and more in general urban green spaces, will be able to use the results from the model to predict the impact of different management practices, such as different irrigation and vegetation cover scenarios, on the overall status of the vegetation.

Chapter 3

Methods

This chapter contains an overview of the methods adopted in the project. This includes a comprehensive description of the study sites, followed by the specific experimental setup and the ecohydrological modeling approach that were chosen to address the three research questions, whose results are shown in *Chapter 4*, *Chapter 5*, and *Chapter 6*.

3.1 Study sites

This project focused on three urban reserves located in the Melbourne metropolitan area in southeast Australia: National Drive Reserve and Alex Wilkie Reserve are embedded in the south-eastern suburbs, while Napier Park is located about 9 km north-west of the Melbourne Central Business District (CBD) (Figure 3.1). The climate of the area is Mediterranean (Cfa in the Köppen classification) with a strong spatial heterogeneity of rainfall within the metropolitan area, decreasing from southeast to northwest. The sites host predominantly remnant native plants, with some occasional introduced species, and differ for vegetation structure, soil characteristics, and management practices.

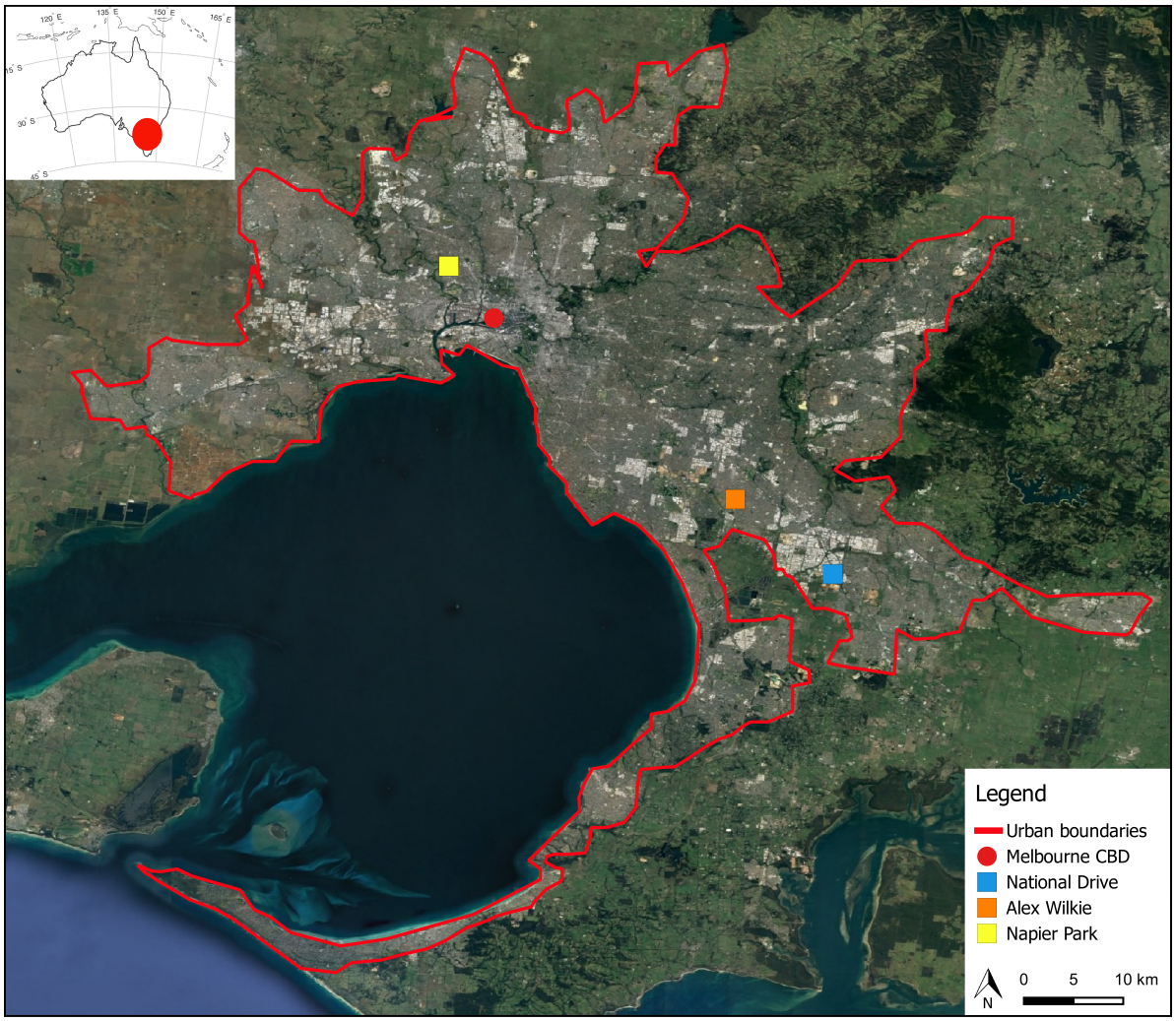

Figure 3.1: Location map of the study sites in the Melbourne metropolitan area (Australia).

3.1.1 National Drive Reserve

National Drive Reserve (Figure 3.2) is a 14 ha grassy woodland and is located about 40 km from the Melbourne CBD. The area consists of a large stand of *Eucalyptus Camaldulensis* (River Red Gum) woodland with the understory dominated by pasture grasses. The majority of land surrounding National Drive has been developed for industrial purposes, with large warehouses and yards. The soil is predominantly silty clay in the first 40 cm followed by clay, with a shallow water table (i.e., between 3 and 4 m below the ground surface) within the reach of the plants root zone (*E. Camaldulensis* has a deep taproot system reaching depths greater than 10 m; Doody et al., 2015), potentially making vegetation dependent on groundwater. Long-term average annual rainfall is 757 ± 148 mm (mean ± SD), mean daily minimum temperature is 10.0°C and mean daily maximum temperature is 19.8°C (1968-2018, Bureau of Meteorology (BOM), Dandenong station, no. 086224; Moorabbin Airport station, no. 086077, located at about 10 km from National Drive was also used to fill extensive data gaps in daily temperature series).

Figure 3.2: National Drive Reserve

3.1.2 Alex Wilkie Reserve

Alex Wilkie Reserve (Figure 3.3) is a sandy plain woodland of about 1.8 ha located 10 km to the northwest of National Drive Reserve. The reserve is populated mostly with *E. Viminalis* (Coast Manna Gum) and *E. Cephalocarpa* (Silver-leafed Stringybark), with other natural and planted lower trees (e.g., *Allocasuarina Littoralis* (Black Sheoke), *Banksia Marginata* (Silver Banksia)) and shrubs. The soil consists of loamy sand, which becomes sandy clay to about 3 m below ground level and then silty sand at about 7 m below ground level. As

for National Drive, the water table is quite shallow, ranging between 3 and 5 m below the ground surface. Long-term average annual rainfall is 684 ± 132 mm, mean daily minimum temperature is 10.2°C, and mean daily maximum temperature is 19.8°C (1968-2018; BOM, Moorabbin Airport station, no. 086077).

Figure 3.3: Alex Wilkie Reserve

3.1.3 Napier Park

Napier Park (Figure 3.4) covers an area of about 4.1 ha and is located about 9 km northwest of the Melbourne CBD. The site is home to a valuable population of *E. Camaldulensis* with a number of significant *E. Melliodora* (Yellow Box). Texture-contrast soils (duplex) cover the entire area of the reserve, with the soil profile consisting of a sandy silt followed by a sandy silty clay (up to depths between 0.3 and 0.6 m), overlaying a heavy clay (up to about 1.8 m) followed by sandy silt again. Groundwater depth is about 20 m below the ground surface. Long-term average annual rainfall is 557 ± 119 mm, mean daily minimum temperature is 10.0°C, and mean daily maximum temperature is 20.4°C (1968-2018; BOM, Essendon Airport station, no. 086038). Napier Park is also equipped with an extensive irrigation system covering about 85% of the park that uses stormwater harvesting from an upstream drainage catchment of about 16.3 ha to recharge the soil stores throughout the site. Based on the specific requirements of the remnant population of *E. Camaldulensis*, which needs to be intermittently flooded, the irrigation strategy was designed to increase the volume and the length (by up to 3 hours) of each rainfall event. Irrigation started irregularly in January 2016, becoming more consistent towards the end of the same year.

Figure 3.4: Napier Park

3.2 Data description

A series of experimental measurements have been collected over the two-year period from July 2016 to June 2018 to quantify the water balance and tree water use of the reserves. All experimental activities were conducted in each reserve within several 50 m x 50 m plots (Figure 3.5), thus covering an exhaustive range of vegetation and environmental conditions.

Figure 3.5: Location map of the experimental plots (yellow dashed line) within the boundaries of the study sites (red line): (a) National Drive Reserve, (b) Alex Wilkie Reserve, and (c) Napier Park.

3.2.1 Stand characteristics

For each plot, stand density (stems ha^{-1}) was calculated from tree count and area, taking into account both live and dead trees. Total basal area (BA, m^2ha^{-1}) was estimated by

measuring diameter at breast height (DBH, at 1.3 m from the ground) of all trees (alive and dead) with stems larger than 10 cm in diameter, including multi-stemmed trees. Percentage of live basal area (%LBA) was then calculated as the proportion of the total basal area contributed by live trees.

3.2.2 Micrometeorology

Micrometeorological data, including rainfall (P), air temperature (T_a), relative humidity (RH), and incoming shortwave solar radiation (R_s) were measured every 15 minutes using automatic weather stations (AWS) (Campbell Scientific) (Figure 3.6 and Figure 3.7a). Daily vapor pressure deficit (VPD) was calculated from T_a and RH. Measurements were conducted in appropriate open grassy areas within National Drive and Alex Wilkie reserves for the entire period of the study; at Napier Park, a weather station was placed within a private garden adjacent to the park between November 2016 to February 2017.

The data collected from the site specific weather stations were combined with the daily data from the closest Bureau of Meteorology (BOM) weather stations (i.e., Dandenong, no. 086224, for National Drive, Moorabbin Airport, no. 086077, for Alex Wilkie, and Essendon Airport, no. 086038, for Napier Park) to estimate long-term (1968-2018) average annual rainfall and daily temperature for all sites, to fill data gaps in the daily rainfall time series recorded at National Drive (between July to December 2016) and Alex Wilkie (in March and July 2017 as well as from September 2017 to June 2018), and to integrate the limited time series of micrometeorological data available from the AWS installed at Napier Park (i.e., from November 2016 to February 2017).

Comparing the BOM data with the data recorded at National Drive, Alex Wilkie, and Napier Park using AWS, a good agreement was found in terms of monthly rainfall for National Drive (R^2 0.84), and in terms of weekly and monthly rainfall for Alex Wilkie (R^2 0.86 and 0.94, respectively) and Napier Park (R^2 0.74 and 0.81, respectively); therefore, BOM data were used to fill gaps in the data collected from the site specific weather stations.

Long-term (July 1999 - June 2018) hourly meteorological data, including rainfall, temperature, relative humidity, wind speed, and solar radiation, were also available at Melbourne Airport (BOM station no. 086282) and Moorabbin Airport (BOM station no. 086077) to use as meteorological forcing for the modeling tasks.

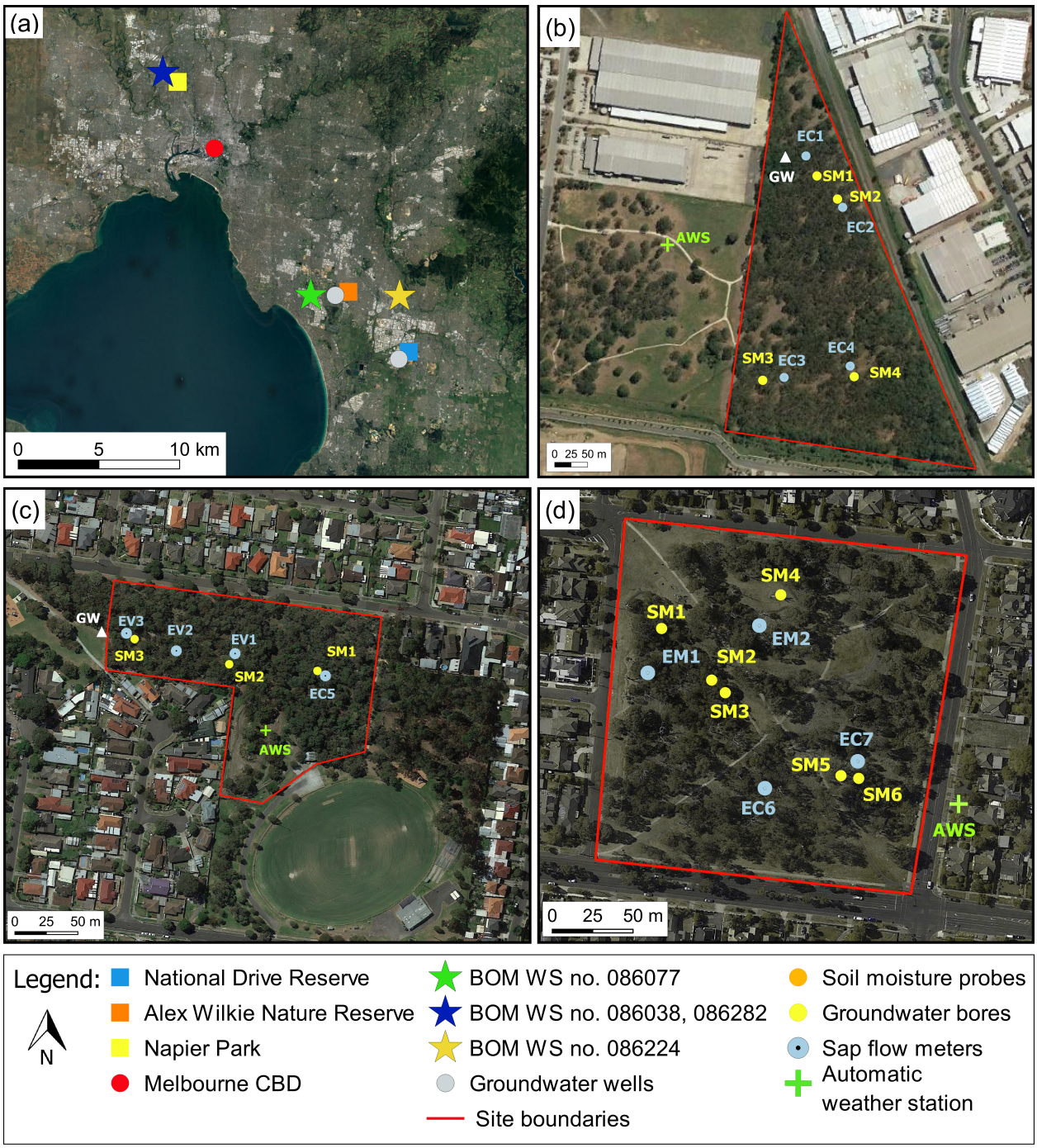

Figure 3.6: (a) Location map of the study sites, long-term groundwater wells, and Bureau of Meteorology weather stations (BOM WS) for Moorabbin Airport (no. 086077; 37.98° S, 145.24° E), Dandenong (no. 086224; 37.98° S, 145.22° E), Essendon Airport (no. 086038; 37.73° S, 144.91° E), and Melbourne Airport (no. 086282; 37.67° S, 144.83° E). Monitoring network at (b) National Drive Reserve, (c) Alex Wilkie Nature Reserve, and (d) Napier Park.

Table 3.1: Plot characteristics at the three study sites.

Plot[a] Code	DBH[b] (m)	Stand density (stems ha^{-1})	BA[b] (m^2 ha^{-1})	N. Trees Alive (LBA[b], %)	Monitored Trees[c] (DBH, m)
ND1	0.31 ± 0.12	632	41.2	109 (91)	EC1[d] (0.36)
ND2	0.32 ± 0.14	404	33.2	84 (95)	EC2 (0.33)
ND3	0.40 ± 0.13	248	27.6	47 (95)	EC3[d] (0.29)
ND4	0.24 ± 0.13	704	38.9	157 (96)	EC4[d] (0.29)
AW1	0.19 ± 0.09	600	23.8	116 (66)	EV3[d] (0.21), EV4 (0.21)
AW2	0.22 ± 0.10	428	18.4	93 (91)	EV1[d] (0.31), EC5 (0.46)
NP1	0.16 ± 0.09	336	18.0	62 (35)	EM1 (0.28)
NP2	0.24 ± 0.24	148	19.8	32 (58)	EC6 (0.22)
NP3	0.24 ± 0.19	128	19.8	29 (76)	EC7[d] (0.22)
NP4	0.19 ± 0.16	256	18.7	37 (38)	EM2 (0.19)

[a] ND: National Drive Reserve, AW: Alex Wilkie Reserve, NP: Napier Park.
[b] DBH: Diameter at Breast Height; BA: Basal Area; LBA: Live Basal Area
[c] Identification of the trees equipped with sap flow sensors in each plot (Figure 3.5); EC: *Eucalyptus Camaldulensis*, EV: *Eucalyptus Viminalis* EM: *Eucalyptus Melliodora*.
[d] Trees equipped with band dendrometers.

3.2.3 Soil water and groundwater

Soil volumetric water content (θ) and soil temperature were measured every 15 minutes using fully encapsulated soil water capacitance probes (Drill & Drop, Sentek) (Figure 3.6 and Figure 3.7b). These probes measure the volumetric water content through sensors fixed at 10 cm increments from the surface to a depth of 120 cm. Five probes were installed at National Drive, three at Alex Wilkie, and six at Napier Park. Measurements were validated using the gravimetric method with oven drying (O'Kelly, 2004), which involves the collection, using a sampling ring, of soil samples around the probes at different measuring depths. In our specific case, soil samples were collected at 5 cm and 15 cm depths, as deeper soil layers could not be reached due to the nature of the soils at all sites. The samples were then used to estimate dry mass and bulk density (i.e., dry mass of the soil in the given sampling volume), the latter showing variations with depth ($\rho_{bulk,5cm}$=1.1 ± 0.2 g/cm^3; $\rho_{bulk,15cm}$=1.4 ± 0.1 g/cm^3). Good agreement was found between θ measured with the Drill & Drop sensors and that estimated from the volumetric soil sample analysis in the first 20 cm of soil.

Water table depth (relative to the ground surface) was measured at 15-min intervals in monitoring bores at National Drive (11.1 m depth) and Alex Wilkie (9 m depth). Each bore was equipped with a water level datalogger (3001 LT Levelogger Edge, Solinist) and a barometric datalogger (3001 LT Barologger Edge, Solinist) to enable specific barometric compensation. Manual water level measurements were conducted on a regular basis using a dip meter (dipper-T, Heron Instrument Inc.) to validate the water level measurements.

(a) (b) (c)

Figure 3.7: (a) Automatic weather station (Campbell Scientific). (b) Drill&Drop soil moisture probe. (c) Sapflow meter (SFM1, ICT International, Australia) and band dendrometer (DBL60, ICT International, Australia).

Long-term water-table depth observations were also available within 7 km radius from the study sites from 1 July 1999 to 30 June 2016 (*https://www.vvg.org.au*).

Uncertainties related to the measurements of θ in the top 1.2 m of soil (i.e., $\pm$ 0.03%) and water-table depths (i.e., $\pm$ 0.05%) were not considered in the water balance, as annual changes in θ and water-table depths were small compared to the other components of the water balance.

3.2.4 Sap flow measurements and stand transpiration

Water use of individual trees was determined using commercially available sap flow sensors (SFM1, ICT International, Australia), which use the heat pulse velocity (HPV) technique to measure high, low, and reverse rates of sap flow from the velocity of a short pulse of heat moving along the xylem tissue (Figure 3.6 and Figure 3.7c). HPV was recorded at half-hourly intervals in several trees within the reserves and corrected for wounding effects following Burgess et al. (2001); wound widths were obtained from data in the literature collected for similar trees. Sensors were placed approximately at breast height (1.30 m from the ground) on a total of twelve trees, four at each site (Table 3.1). Because the reserves are open to the public, the number of trees selected could not be larger and remain inconspicuous. Measurements were converted to sap flux density (SFD, $cm^3cm^{-2}h^{-1}$), based on wood core measurements of dry wood density, gravimetric sapwood moisture content, and sapwood area

(calculated from stem diameter and thickness of sapwood and bark).

During warm summer nights with temperatures above 25°C (and consequent high VPD; Forster, 2014), the magnitude of night-time SFD (SFD_n) was estimated as a proportion of the 24-h sap flow, considering SFD_n from 23:00 to 05:00, following the method proposed by Zeppel et al. (2010).

Plot-level transpiration (T_{plot}) was calculated from the water use of individual trees using the linear relationship (R^2=0.86, p<0.05) between DBH (cm) and sapwood area ($A_{sapwood}$, cm^2) established based on the twelve selected trees across the three study sites (Figure 3.8). Estimates of T_{plot}(mm h^{-1}) were thus calculated as:

$$T_{plot} = \frac{SFD_{avg} A_T}{A_{plot} \cdot 10^4}, \tag{3.1}$$

$$A_T = \sum_{i=1}^{N} (10.02 \cdot DBH_i - 91.90), \tag{3.2}$$

where A_T is the total sapwood area in a plot (cm^2), SFD_{avg} is the average area-weighted SFD (mm h^{-1}) of the measured trees in the plot, and N is the number of trees within the 50 m x 50 m plot area A_{plot} (m^2). The transpiration at the scale of the reserve (T) was estimated by averaging T_{plot} for all measurement plots within each study site.

Potential errors in the measurements of SFD using HPV sensors might lead to an underestimation of the actual SFD of up to 35% after wound correction. These errors increase with SFD and are mainly caused by heterogeneity of the sapwood (Steppe et al., 2010). Additional errors may occur during the scaling of measurements from a single point to the whole tree due to the radial and circumferential variability in sap flux density; the magnitude of this error mainly depends on the width of the sapwood area (Nadezhdina et al., 2002). The HPV technique is recognized to be the most accurate when compared to the thermal dissipation (Peters et al., 2018a) and heat field deformation methods. Estimates of transpiration from stem sap flow data should also include a lag coefficient to account for the withdrawal of water from internal storage. Several studies demonstrated that 10 to 15% of daily transpiration may be provided by stem water stores (e.g., Meinzer et al., 2004; Matheny et al., 2015). However, because the dynamics of stored water affect mainly the patterns of intra-daily transpiration (Matheny et al., 2015), they have not been taken into account in this study.

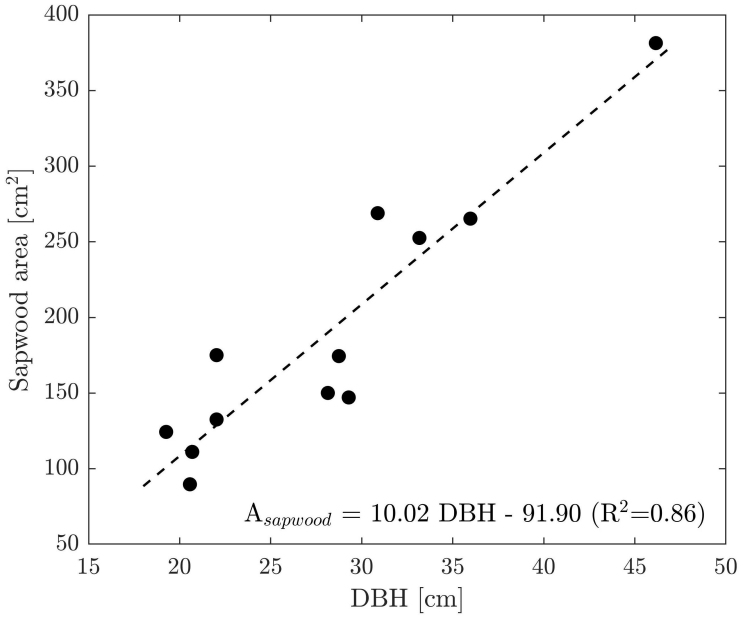

Figure 3.8: Relationship between tree diameter at breast height (DBH) and sapwood area ($A_{sapwood}$).

3.2.5 Stem diameter variation measurements

A total of six trees among the ones monitored with sap flow sensors were also equipped with band dendrometers (DBL60, ICT International, Australia), to measure tree diameters over time (Table 3.1). The DBL60 sensors were fixed to the tree trunk with a 12 mm wide stainless steel tape at about 1.3 m height on the southern side of the tree. A portion of the outermost bark was removed prior to installation to provide an undisturbed point of contact for the tape. Stem diameter variation (SDV) and temperature were recorded every 5 minutes; SDV signals were then corrected for sensor temperature sensitivity, applying an average thermal expansion coefficient of $1.17 \cdot 10^{-6} \mu$m (μm°C)$^{-1}$ according to Vandegehuchte et al. (2014).

3.2.6 Water balance

An estimation of the water balance of each reserve was conducted out for 2 years (July 2016 to June 2017, referred to as 2017 water year, and July 2017 to June 2018, referred to as 2018 water year) using:

$$P - T - \Delta S = Q + ET + \epsilon, \tag{3.3}$$

where P is rainfall, T is tree transpiration ($T = T_{sw} + T_{gw}$), T_{sw} and T_{gw} are the transpiration components depleting the unsaturated and saturated zones, respectively, ΔS is total water storage change ($\Delta S = \Delta S_{sw,s} + \Delta S_{sw,d} + \Delta S_{gw}$), accounting for unsaturated soil water change in the first 1.2 m of monitored soil ($\Delta S_{sw,s}$), unsaturated deep soil water change (below 1.2 m) ($\Delta S_{sw,d}$), and unconfined groundwater storage change (ΔS_{gw}), Q is runoff, ET is evapotranspiration ($ET = ET_{floor} + E_i$), accounting for floor evapotranspiration (ET_{floor}), including grass, ferns, and small shrubs, and canopy interception (E_i), and ϵ is the water balance errors including systematic errors in the estimates of the water budget variables. All terms of equation (3.3) are expressed in equivalent water depths per unit of ground area (mm). The equation was used to estimate $ET + \Delta S_{sw,d} + \epsilon$ for each site on a water year basis, Q being negligible in all study sites.

The change in soil water storage ($\Delta S_{sw,s}$) was calculated as the average change in volumetric water content in the soil profile at each measurement point (i.e., the average water content for the 12 sensors over the length of the probe). The change in groundwater storage (ΔS_{gw}) was calculated only for National Drive and Alex Wilkie reserves as the change in water table depth between consecutive years multiplied by the specific yield. The specific yield was estimated as a function of the sediment texture, as recommended for depths to the water table greater than 1 m (Loheide et al., 2005); in particular, the specific yield at National Drive was estimated as 2% and 7% at Alex Wilkie, as in Johnson (1963).

Deeper roots also extend below the depth to which soil water probes were installed, reaching the water table or its capillary fringe. To quantify the groundwater uptake (T_{gw}) by trees in the sites where plants have access to groundwater, the method developed by White (1932), and later refined by Loheide et al. (2005), was used. Accordingly,

$$T_{gw} = S_y(24r \pm s), \tag{3.4}$$

where S_y (-) is the specific yield, r (mm h^{-1}) is the rate of water table rise from midnight to 4 a.m., and s (mm) is the rise or fall of the groundwater level over a 24 h period (i.e., from midnight to midnight). The method was applied during rain-free periods of few days, for which water levels in the bores during the night can be reasonably assumed to be due to a net recovery flux toward the bore (Orellana et al., 2012).

3.3 Ecohydrological modeling: Tethys-Chloris

Model simulations were carried out using the mechanistic ecohydrological model Tethys-Chloris (T&C), which simulates essential components of the hydrological and carbon cycles, resolving energy, water, and carbon fluxes at the land surface at hourly time step (Fatichi et al., 2014; Manoli et al., 2018b). The T&C model was selected for this project because of its capability to represent ecosystem dynamics at the small scale of the study sites. For a detailed description of the mathematical formulation of the model components, specifically, energy and water fluxes, unsaturated-saturated zone interactions, subsurface-surface flows, and the processes affecting the carbon balance of vegetation, the reader is referred to Fatichi et al., 2012

The T&C model represents the principal components of the hydrological cycle (i.e., precipitation, interception, transpiration, ground evaporation, infiltration, and surface and subsurface water fluxes) (Figure 3.9). It resolves the mass and energy budgets over complex topography, explicitly considering the spatial variability of meteorological fields, soil properties, vegetation, and the topography effect on the distribution of incoming radiation (Mastrotheodoros et al., 2019). T&C further accounts for biophysical and biochemical vegetation attributes coupled with modules to simulate plant-related processes, such as photosynthesis, phenology, carbon pool dynamics, and tissue turnover (Fatichi et al., 2014; Fatichi and Pappas, 2017; Manoli et al., 2018a) (Figure 3.10).

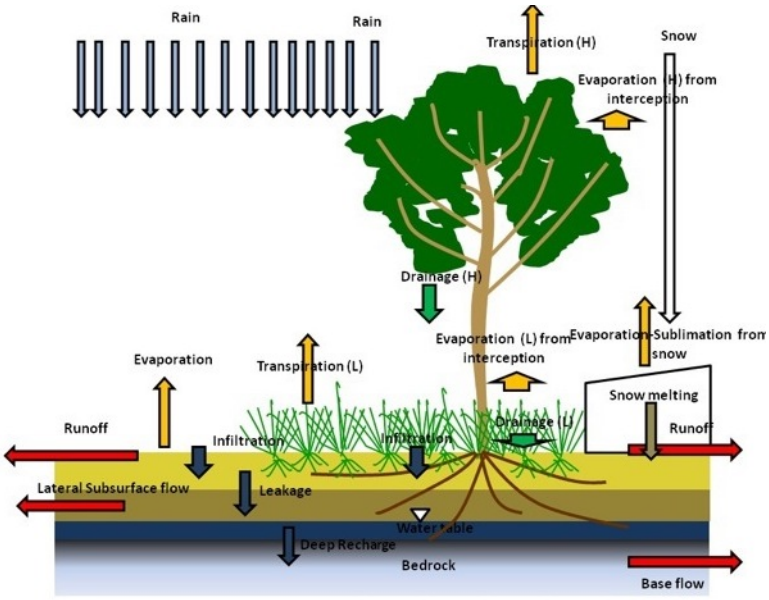

Figure 3.9: Components included in the hydrological and energy balance models (sourced from Fatichi et al., 2012).

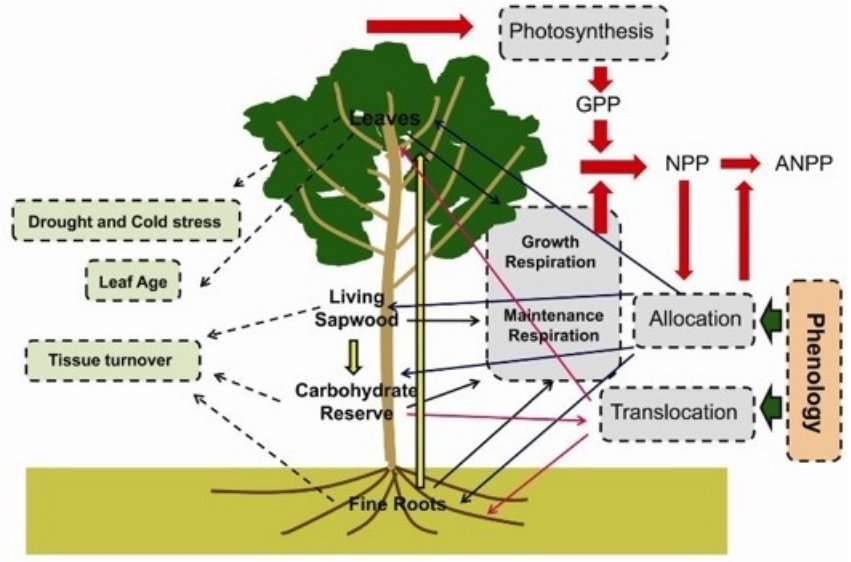

Figure 3.10: Conceptual diagram of carbon fluxes and the processes simulated by the model (sourced from Fatichi et al., 2012).

Vegetation species diversity can be explicitly represented at the species level or more often aggregating species that share the same file form and structural attributes described as Plant Functional Types (PFTs). In this project, two or three PFTs to account for the coexistence of trees, shrubs, and grass were used. The model can consider both horizontal and vertical composition of the vegetation patches; in particular, the horizontal land cover composition accounts for the area occupied by each vegetation type. Eventually, non-vegetated surfaces (i.e., bare soil) can be also taken into account. Incoming shortwave and longwave radiation is explicitly transferred through the vegetation (Ivanov et al., 2008).

T&C simulates a number of ecohydrological variables including transpiration, soil evaporation, evaporation from interception, leakage at the soil bottom (or groundwater recharge), runoff, and profiles of soil moisture. It further simulates vegetation gross and net primary production, plant water stress and Leaf Area Index (LAI). Plant water stress is indicated with a factor, β, that expresses how the root integrated water potentials departs from plant physiological thresholds. A reduction of β from 1 (unstressed conditions) affects plant photosynthesis and allocation as well as leaf shedding.

Meteorological inputs forcing T&C include rainfall, air temperature, relative humidity, wind speed, solar radiation, atmospheric pressure, cloud cover or longwave radiation, and CO_2 concentration. Soil moisture dynamics are described by the one-dimensional Richards equation for the vertical flow, with the soil column subdivided into $i = 1, .., n_s$ layers with thickness $d_{z,i}$ [mm]. Saturated and unsaturated parts of the soil column are explicitly identified. Runoff is generated either by saturation excess or by infiltration excess mechanisms

and depends on lateral moisture fluxes in the unsaturated and saturated zones and on the overland flow (Loague et al., 2010). Being this study focused on point-scale dynamics, lateral subsurface flow, surface overland, and channel flow are not taken into account.

In order to evaluate the soil moisture contents θ_i [m^3m^{-3}], the Richards equation (3.5) is simplified to a system of ordinary differential equations in the following general form:

$$d_{z,i}\frac{\mathrm{d}\theta_i}{\mathrm{d}t} = q_{i-1} - q_i - T_v r_{v,i} - E_g - E_{bare} + Q_{l,in,i} - Q_{l,out,i} \tag{3.5}$$

where q_i [mm h^{-1}] is the vertical outflow from a layer i, T_v [mm h^{-1}] is the transpiration from vegetation layers, E_g [mm h^{-1}] is the evaporation from the soil under the canopy, and E_{bare} [mm h^{-1}] is the evaporation from bare soil; the flux T_v is assumed to have access to moisture at the soil surface and in the root zone (with $r_{v,i}$ the fraction of root biomass in a given soil layer), whereas the fluxes E_g and E_{bare} are assumed to have access to moisture only in the first soil layer. The terms $Q_{l,out,i}$ and $Q_{l,in,i}$ [mm h^{-1}] are the lateral outflows and inflows. Evaporation and transpiration fluxes are obtained by explicitly solving the energy budget (3.6) and computing the latent heat flux.

The prognostic radiative temperature, T_s, is required in the estimation of heat fluxes to close the energy balance:

$$R_n(T_s) - H(T_s) - \lambda E(T_s) - G(T_s) + Q_v(T_s) = 0 \tag{3.6}$$

where incoming heat with precipitation, Q_v, net radiation, R_n, sensible heat, H, latent heat, λE, and ground heat, G, are all calculated based on T_s. A single T_s is adopted in T&C, representing a homogeneous radiative temperature of the surface assigned to all land cover types (Fatichi et al., 2012).

Photosynthesis is simulated with the biochemical model by Farquhar et al. (1980) (see also Collatz et al., 1991; Collatz et al., 1992) modified by Bonan et al. (2011). Net assimilation and stomatal resistance are computed separately for sunlit and shaded leaves, following the two big-leaves approach (Dai et al., 2004). Photosynthetic capacity decays exponentially through the canopy (Ivanov et al., 2008; Bonan et al., 2011). Stomatal resistance is parameterized as a function of assimilation rate and environmental conditions (Leuning, 1990; Tuzet et al., 2003). The dynamics of five carbon pools are explicitly simulated in the model, i.e., green aboveground biomass, living sapwood (woody plants only), fine roots, carbohydrate reserve (non-structural carbohydrates), and standing dead biomass.

The carbon assimilated through photosynthesis is used for growth and reproduction, and is lost in the process of maintenance and growth respiration and tissue turnover. Carbon

allocation is a dynamic process that accounts for resource availability (light and water) and allometric constraints (Kozlowski and Pallardy, 1996; Friend et al., 1997; Friedlingstein et al., 1999; Bonan et al., 2003; Krinner et al., 2005). Carbon from reserves can be translocated to favour leaf expansion at the beginning of the growing season or after a severe disturbance (Chapin III et al., 1990; Gough et al., 2009; Gough et al., 2010; Fatichi et al., 2012). Organic matter turnover of the different carbon pools is a function of tissue longevity and environmental stresses, i.e., drought and low temperatures (Bonan et al., 2003; Sitch et al., 2003; Arora and Boer, 2005; (Ivanov et al., 2008); Fatichi et al., 2012).

Four different phenological states control plant allocation (Arora and Boer, 2005): dormancy, maximum growth, normal growth, and senescence (Fatichi et al., 2012). Temperature, soil moisture and photoperiod define the beginning of the growing season. Nutrient dynamics and forest stand growth are neglected.

Chapter 4

Water Balance and Tree Water Use Dynamics

This chapter contains large parts of the article **"Water balance and tree water use dynamics in remnant urban reserves"** published in the *Journal of Hydrology*[1].

The chapter presents an estimation of the water balance over two hydrologic years (2017-2018) in the three small urban reserves (National Drive Reserve, Alex Wilkie Reserve, and Napier Park) for the purpose of understanding tree water use. Measurements of micrometeorological variables, soil moisture content profiles, water-table levels, sap flow velocities, and stem diameter variations were used to quantify the water sources of tree transpiration in these reserves. Results revealed that, despite the urban surroundings and the climate variations, these reserves have enough water to sustain tree transpiration. In two of the three reserves, groundwater was pivotal in sustaining transpiration rates; specifically, groundwater was estimated to contribute about 30-40% of the total transpiration amount during the driest periods of the year. Groundwater also played an essential role during nights with temperatures above 25°C, helping trees to maintain night-time water use from 3 to 16% of the daily water use. In the third reserve, the presence of a shallow layer of heavy clay supplied water to the trees, which were able to maintain relatively constant transpiration rates throughout the year. These results demonstrate the importance of understanding the water regime of each urban reserve in order to support government authorities in preserving these ecosystems.

[1]https://doi.org/10.1016/j.jhydrol.2019.05.022

4.1 Introduction

The rapid expansion of urban areas to accommodate the growing number of city dwellers represents one of the most irreversible human impacts on the global biosphere and poses unique challenges for ecosystems (Seto et al., 2012). Changes in land cover associated with urbanization generate a fragmented and heterogeneous landscape where patches of vegetation, often remnants of natural habitats, are embedded in a highly disturbed environment (McKinney, 2002). Remaining pockets of vegetation within the built environment are recognized as important areas for biodiversity conservation (Elmqvist et al., 2015; Tulloch et al., 2016; Melaas et al., 2016; Lepczyk et al., 2017), mitigating the urban heat island (UHI) effect (e.g., Bowler et al., 2010; Gill et al., 2007; Declet-Barreto et al., 2016), and restoring hydrological and biogeochemical processes closer to natural conditions (e.g., Yang et al., 2015; Livesley et al., 2016a; Berland et al., 2017).

Considering its importance, there are concerns that the urban surrounds may be exerting negative impacts on the remaining vegetation, by imposing changes in the radiation and energy budget, the hydrologic regime, and ecosystem composition and structure (Roberts, 1977; Sieghardt et al., 2005b). Specifically, increased temperatures and lower air humidity due to the UHI often expose the trees embedded in the urban landscape to high atmospheric evaporative demand. This can lead to higher transpiration rates, in particular when soil moisture is not a limiting factor (Litvak et al., 2011;Chen et al., 2011; Litvak and Pataki, 2016; Zipper et al., 2017a; Litvak et al., 2017; Asawa et al., 2017).

The increase of impervious surfaces and the introduction of drainage infrastructure lead to greater rates and volumes of surface runoff, and reduce the volume of water which infiltrates the soils, decreasing the water available to sustain vegetation growth and health (Xiao et al., 2007; Barron et al., 2013; Shields and Tague, 2015). In addition, increasing drought (Van Loon et al., 2016a) and extreme heat events amplify the water stress of urban trees, resulting in the decline of their health conditions. During heat events, being photosynthesis and stomatal conductance strongly coupled, net rates of leaf photosynthesis and transpiration are expected to decline toward zero due to the high temperatures and vapor pressure deficit (VPD). Recent studies, however, found that cooling of leaves by transpiration might be an important component to plant response to extreme temperatures, leading to substantial rates of transpiration (Drake et al., 2018).

What remains of natural habitats within urban areas can also undergo changes in vegetation structure with the introduction of non-native species, thus creating unique biotic communities with different water needs and more complex patterns of evapotranspiration,

interception, and infiltration (Endter-Wada et al., 2008; McCarthy and Pataki, 2010; Pataki et al., 2011a). In the Melbourne metropolitan area (Australia), for instance, large areas of native vegetation have been replaced by urban and suburban landscapes over the past decades (DELWP, 2016). The consequences for the native plants are substantial, with less than 4% cover of native vegetation remaining within the urban growth boundary (Bradshaw, 2012; Hahs and McDonnell, 2014). This remaining native vegetation is severely fragmented into small reserves, which become isolated and sometimes degraded. Moreover, a further decline in vegetation health have been documented during the Millennium Drought that occurred approximately between 2001 and 2009 (van Dijk et al., 2013)).

In this context, maximizing the effectiveness of remnant native vegetation conservation through active management is important to avoid further losses of vegetation associated with urbanization. Therefore, there is an increasing need for empirical evidence of the role that water availability and the built landscape play in the physiological response of vegetation to urban conditions (Livesley et al., 2016a). More information is also needed to understand the water requirements of these green spaces, enabling better design management guidelines for the preservation of these ecosystems. This involves the identification of the water resources that are most important to maintain key ecosystem features and processes, including the degree of the ecosystem groundwater dependency (Eamus and Froend, 2006; O'Grady et al., 2006).

This chapter aims to gain a better understanding of the interactions and feedback between water resources and vegetation health in the three small urban reserves that are part of this project, namely National Drive, Alex Wilkie, and Napier Park. The main research objectives are to: (a) determine variations in the water balance of urban reserves under different water regimes, (b) analyze the influence of micro-meteorological drivers and groundwater availability on tree water use, and (c) understand the impact of heat stress on night-time tree water use.

4.2 Results

4.2.1 Stand characteristics

Stand characteristics differed significantly across reserves, as well as between plots within the same reserve (Table 3.1). National Drive was overall the more dense site (248-704 stems ha^{-1}) with a woodland structure that varied from east to west across the reserve. Higher basal area was found in plots ND1 (ca. 41 m^2 ha^{-1}) and ND4 (39 m^2 ha^{-1}) in the north-east

and south-east parts of the site, respectively. In all plots, living trees accounted for more than 90% of the total basal area with a size about 2.2 times larger than dead trees. The woodland structure at Alex Wilkie varied from west to east with a higher stand density in the AW1 plot (600 stems ha^{-1}) compared to the AW2 plot (428 stems ha^{-1}); AW1 plot is also characterized by the highest abundance of large trees (16 trees ha^{-1}) within the reserve. However, in both plots living and dead trees had similar DBH distributions. At Napier Park, dead trees were on average 1.5 times larger than live trees and the mean basal area for the four plots was 19 $\pm$ 0.9 m^2/ha^{-1} (mean $\pm$ SD). The live tree distribution at Napier Park was dominated by trees with a DBH of 0.15 $\pm$ 0.17 m with few very large trees (DBH $>$ 0.6 m).

4.2.2 Water balance

Seasonal patterns of T_a, R_s, and VPD were similar across all study sites during the two year study period (Figure 4.1). Compared to the alternate year, mean temperatures were higher during November 2017 and January and February 2018 with the last two months characterized by a large number of very warm nights having temperatures over 25°C. The environmental factors (R_s and VPD) influencing tree transpiration strengthened from winter to summer, with R_s characterized by monthly means ranging between 4 and 25 MJ m^{-2} and monthly means of VPD varying from 1 to 2.5 kPa. The maximum recorded hourly mean R_s was 1200 W m^{-2} in summer and 520 W m^{-2} during winter for Alex Wilkie and Napier Park, and 910 W m^{-2} in summer to 415 W m^{-2} in winter for National Drive. The average maximum recorded VPD in an hour ranged from 7.4 kPa (National Drive), 6.1 (Alex Wilkie), and 5.95 (Napier Park) during summer 2018 to 1.8 kPa (for all sites) during winter 2018; lower values were recorded during summer and winter 2017.

Rainfall (P) did not display a marked seasonal variation, but varied significantly among the study sites for both the 2017 and 2018 water years, decreasing as expected from west to east (Figure 4.2a). During the 2017 water year, rainfall was close to the 50-year average with winter and spring above average; the 2018 water year was drier than average, despite the wetter months of December and January (Figure 4.2a; Figure 4.1).

Observed transpiration (T) at reserve scale (Figure 4.1) displayed a distinct seasonal pattern, particularly at National Drive where higher tree density overall led to higher transpiration rates. Transpiration ranged from 11.5 mm $month^{-1}$ in June 2017 to 40.8 mm $month^{-1}$ in January 2018, with an average of 26.2 mm $month^{-1}$. Lower transpiration rates were measured in Alex Wilkie where DBH are much lower than National Drive. Transpiration at Alex Wilkie ranged from 12.2 mm $month^{-1}$ in June 2017 to 22.4 mm $month^{-1}$ in

January 2018, with an average of 17.6 mm month^{-1}. Transpiration rates in different months at Napier Park were similar in the two years, with an average transpiration of about 7.5 mm month^{-1}.

Temporal averaged θ (calculated as the mean of all the measurements over the study period in each site) shows different soil moisture profiles in the sites (Figure 4.2b). Shallow layers of soil remained relatively dry at Alex Wilkie (θ<0.05 m^{3}m^{-3}) with a more pronounced response to rainfall events at depths of about 1 m, particularly for the wetter year 2017. Conversely, at National Drive and Napier Park, θ in shallow layers varied more compared to deeper layers. Three distinct soil zones could be identified at NP: very dry topsoil, increasingly wet layers between 0.3 to 0.6 m, and near-saturated layers below. These profiles clearly reflect the profile of soil texture at the three sites.

Water table depth (Figure 4.3) at Alex Wilkie had a visible seasonal cycle with recharge from rainfall occurring between September and December. At National Drive, groundwater appeared to be less sensitive to rainfall, but conversely the effects of prolonged rain-free periods were more pronounced. In particular, an increase of 0.35 m in the depth to groundwater table was recorded during the 20 days without rain between February and March 2017, and an increase of 0.18 m was measured during the 14-day rain free period in March 2018.

The data of P, T, θ, and water table levels were used to estimate the water balance of the reserves (Table 4.1), with considerable inter-annual and inter-site variability in the water balance components during the two years (2017-2018). National Drive received about 789 mm of rain, while for the irrigated site (i.e., Napier Park) the total amount of incoming water including both the annual precipitation and the irrigation water was 100 mm. Despite more rainfall during 2017 than during 2018, the site-averaged transpiration was quite similar for the two years of study. Of this rainfall, about 297-332 mm (42-45% of the annual rainfall) was returned to the atmosphere through tree transpiration at National Drive, 205-210 mm (31-35%) at Alex Wilkie, and only 85-91 mm (14-18%) at Napier Park, accounting for the high dependency of plot-level transpiration on the number of live trees (Table 3.1).

Among the three study sites, Alex Wilkie experienced in 2017 a strong soil water depletion in the first 1.2 m of monitored soil (-60 mm) with a pronounced recharge to groundwater (+16 mm). The opposite behavior was recorded in 2018 when a considerable decline of ΔS_{gw} (-31 mm) occurred, while the water content of the unsaturated zone increased. $\Delta S_{sw,s}$ increased overall at National Drive (+15 mm in 2017 and + 9 mm in 2018), whereas small variations were observed with respect to ΔS_{gw}. Taking into account only $\Delta S_{sw,s}$, Napier Park showed a response similar to Alex Wilkie, with a decline in 2017 and an increase in 2018.

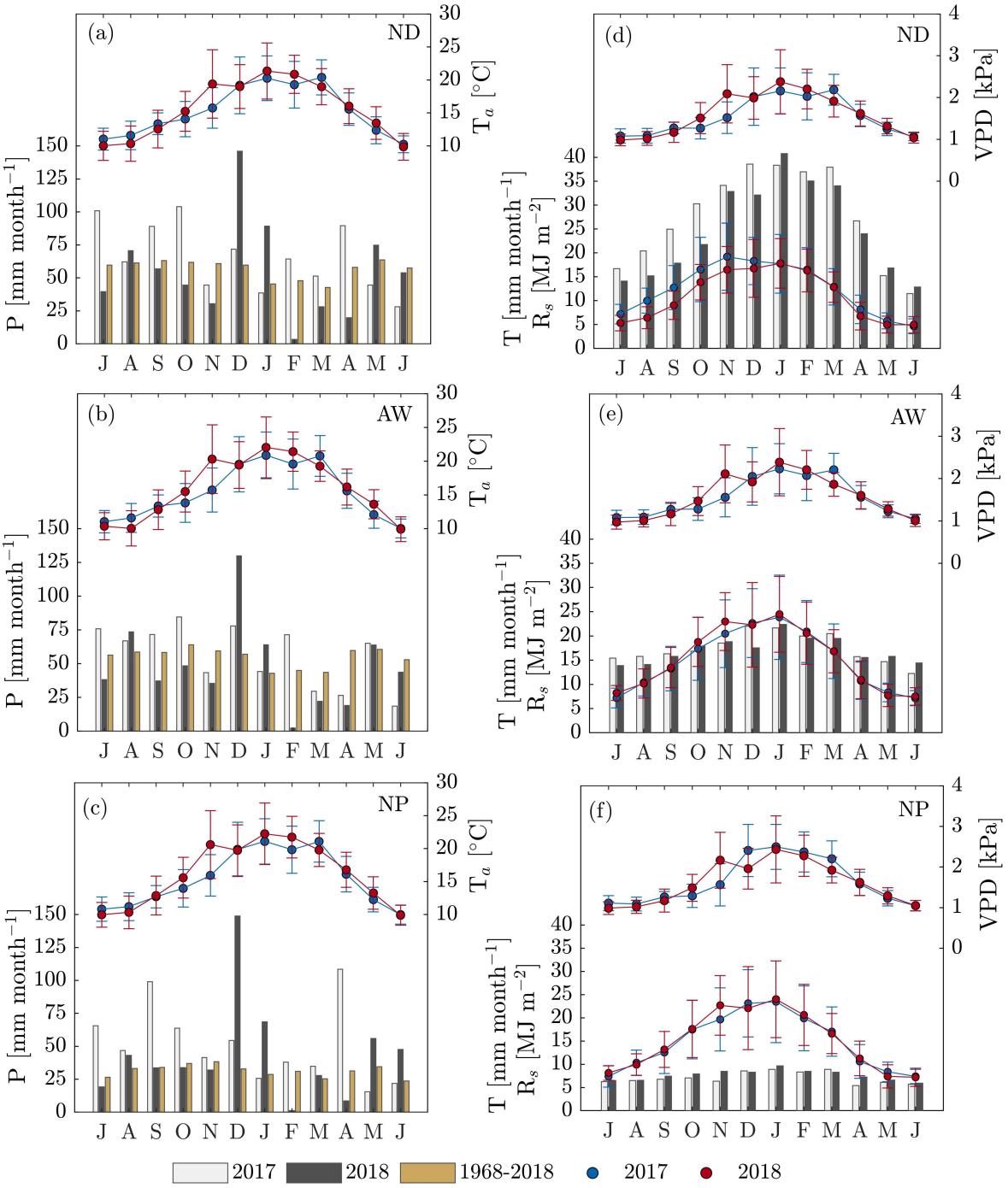

Figure 4.1: (a-c) Monthly rainfall (P) (bars) and monthly mean (± SD) of air temperature (T_a) for National Drive (ND), Alex Wilkie (AW), and Napier Park (NP). (d-f) Monthly transpiration (T) losses (bars) and monthly mean (± SD) of solar radiation (R_s) and vapor pressure deficit (VPD) for National Drive (ND), Alex Wilkie (AW), and Napier Park (NP).

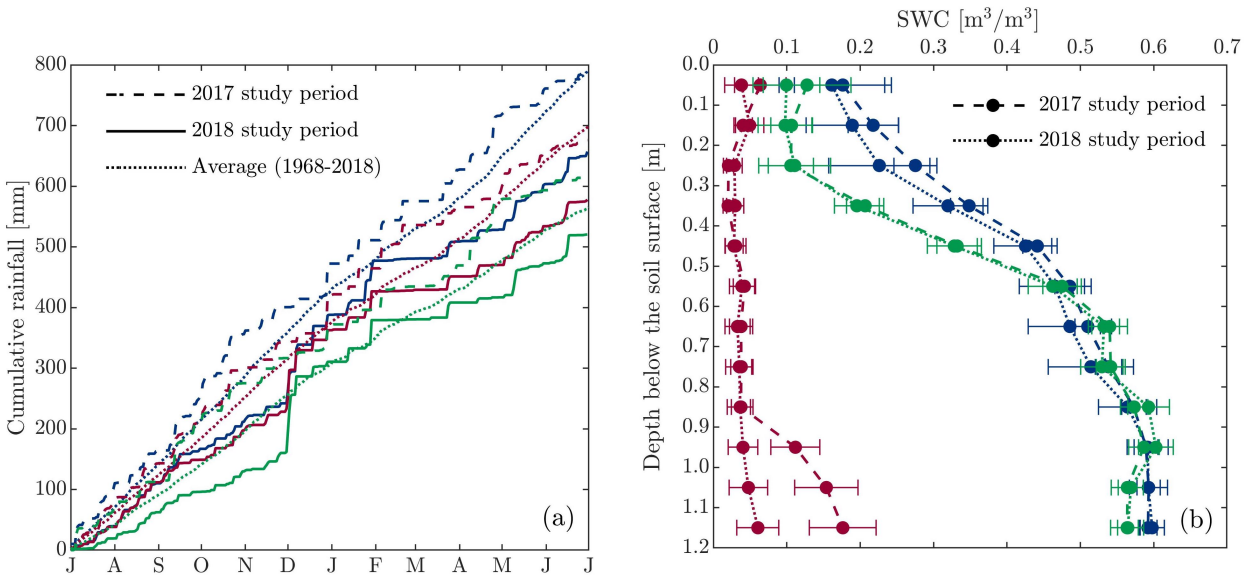

Figure 4.2: Comparison of (a) cumulative rainfall during the 2017-2018 study period with the 50-year average (1968-2018) and (b) temporal-averaged soil volumetric water content (θ) in the first 1.2 m of soil profile for: National Drive (blue), Alex Wilkie (red), and Napier Park (green).

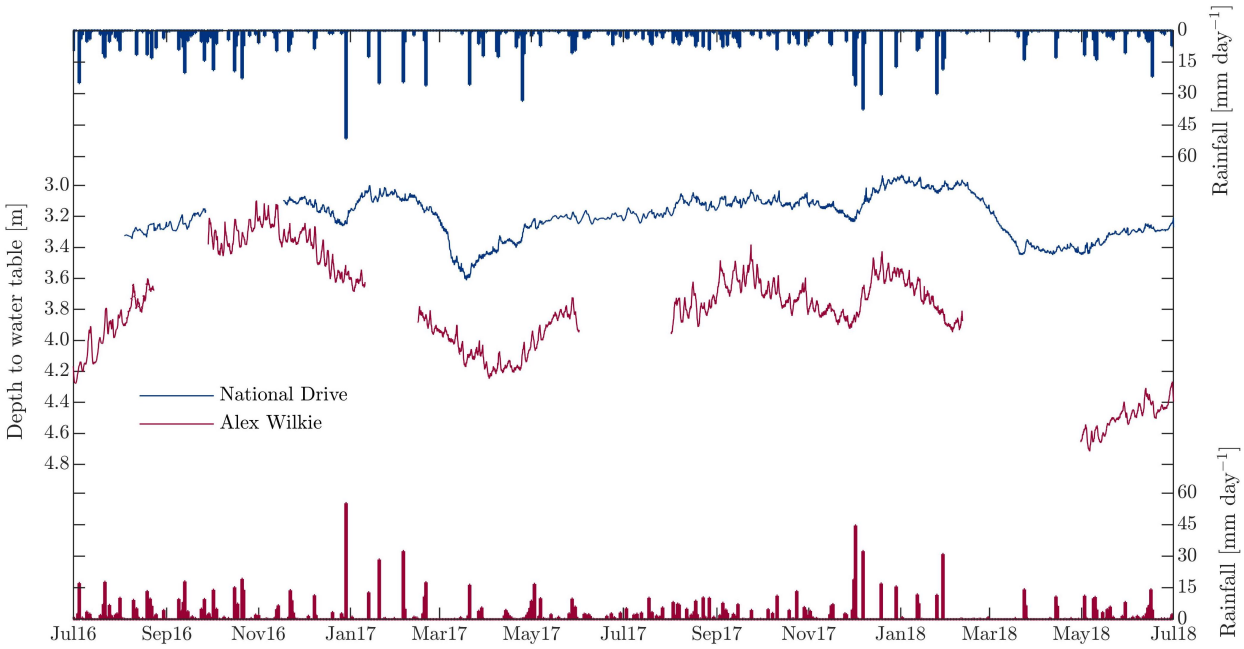

Figure 4.3: Dynamics of rainfall events and depth to water table observed at National Drive and Alex Wilkie during the study period (groundwater was not monitored at Napier Park).

Table 4.1: Water balance components on an annual (water year) basis[a].

Study Sites	ID	WY	P	Irr	T	$\Delta S_{sw,s}$	ΔS_{gw}	ET+$\Delta S_{sw,d}$+ϵ[b]
National Drive	ND	2017	789	0	332	15	2	441
		2018	657	0	297	9	-1	351
Alex Wilkie	AW	2017	676	0	210	-60	16	510
		2018	578	0	205	20	-31	384
Napier Park	NP	2017	615	50	85	-8	n/a	588
		2018	520	50	91	23	n/a	456

[a] WY: Water Year (1 July to 30 June); P: Rainfall; Irr: Imported water (i.e., irrigation); T: Tree transpiration; $\Delta S_{sw,s}$: Change in soil water storage in the first 1.2 m of monitored soil; $\Delta S_{sw,d}$: Change in soil water storage in the deep soil (below 1.2 m); ΔS_{gw}: Change in groundwater water storage; ET: evapotranspiration (ET = ET_{floor} + E_i) which includes floor evapotranspiration (ET_{floor}), including grass, ferns, and small shrubs, as well as soil evaporation, and canopy interception (E_i); ϵ: Water balance errors; n/a: data not available. All water variables are in mm yr^{-1}.
[b] Surface runoff (Q) negligible in all sites.

The annual water balance closure, ET+ΔS_{sw}+ϵ, varied from 351 to 588 mm yr^{-1}, representing 56, 75, and 96% of P during the wet year 2017 and 53, 66, and 88% during the dry year 2018 for National Drive, Alex Wilkie, and Napier Park, respectively. These values are further discussed in section 4.3.

4.2.3 Groundwater uptake by vegetation

Diurnal fluctuations in the depth to the groundwater table were observed during several consecutive rain-free days for both 2017 and 2018 at National Drive (Figure 4.4a and Figure 4.4c). Prolonged periods without rain are not uncommon for Melbourne, especially during the summer months. Specifically, 8 days were selected within two prolonged rain-free periods in both 2017 and 2018, during which the depth to the groundwater table had an observable pattern of daily fluctuations.

As SFD increased during the daylight hours, the depth to groundwater table declined, while during the night a reduction in tree transpiration coincided with a rise in the water table, indicating a recovery flux toward the bore. These patterns of water table are often associated with groundwater uptake by tree roots for transpiration (Loheide et al., 2005; Orellana et al., 2012). Using Eq. (3.4), groundwater uptake (T_{gw}) was estimated to range between 0.4 and 1.1 mm d^{-1}, for a total of 5 mm during the 2017 rain-free period, and between 0.04 and 0.6 mm d^{-1}, for a total of 2.6 mm during the 2018 rain-free period. Therefore, about 42% (SD ± 16%) and 29% (SD ± 15%) of transpiration was estimated to be from groundwater in those periods (Figure 4.4b and Figure 4.4d).

It was not possible to detect a clear diurnal water table signal at Alex Wilkie. The delay

in the downward propagation of air pressure through the pores of the unsaturated zone generated water fluctuations in the bore that overshadowed the diurnal signal. Examining the trends in soil water content (Figure 4.2b) and transpiration rates during the prolonged rain-free periods in 2017 and 2018 suggested that transpiration rates were not limited by the modest soil water availability. The diurnal shrinking and swelling of the tree trunk for EV1 along with sustained SFD also supported the presence of T_{gw} at Alex Wilkie (Figure 4.5). Swelling started in the late afternoon when the evaporative demand decreased considerably, and continued throughout the night due to the water uptake; as evapotranspiration demand increased during the daylight hours, shrinkage occurred. The contribution of groundwater uptake to the total transpiration was quantified by estimating the change in water table depth attributed to the specific rain-free period. Using this method, a total of 2.8 mm of T_{gw} was estimated for the 8 days between February and March 2017, being about 47% of total transpiration. A small data gap did not allow T_{gw} to be estimated for the 2018 summer rain-free period.

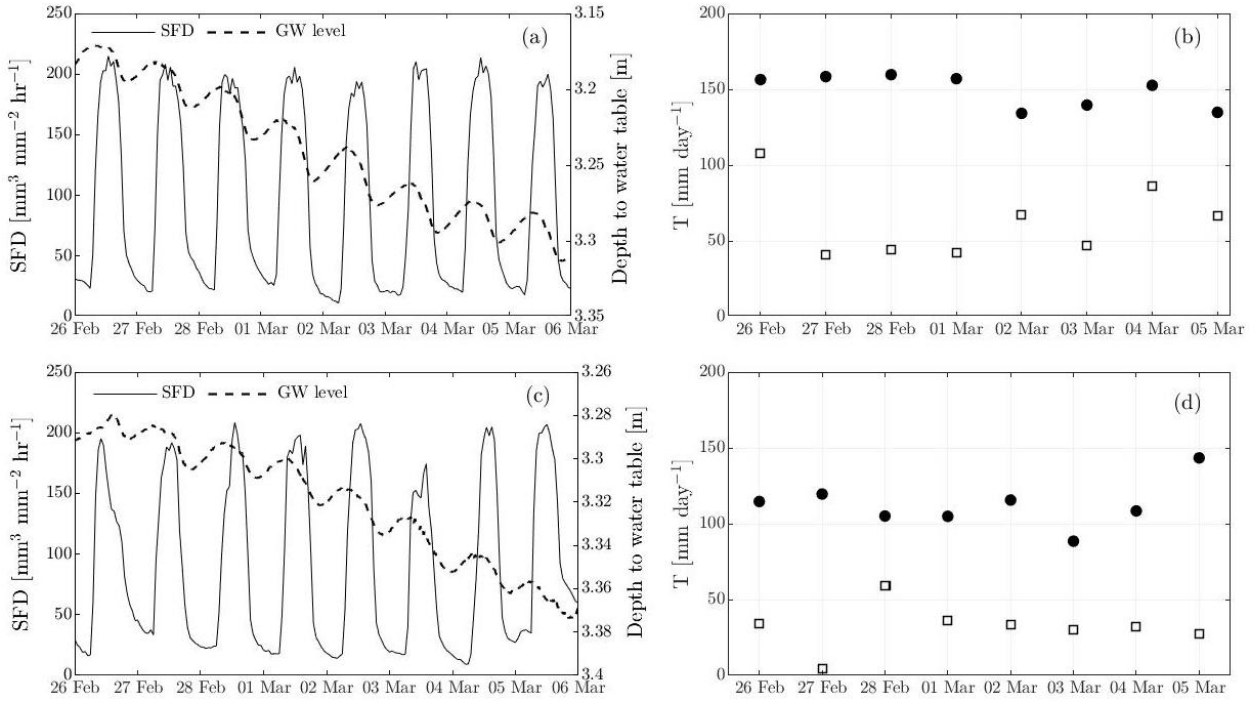

Figure 4.4: Diurnal groundwater fluctuations and sap flux density (SFD) for a selection of 8 rain-free days for the (a) 2017 and (c) 2018 water years at National Drive. Daily groundwater uptake from the fluctuation method (T_{gw}) (open square) and transpiration fluxes (solid circle) for the 8 days rain-free period of the (b) 2017 and (d) 2018 water years at National Drive.

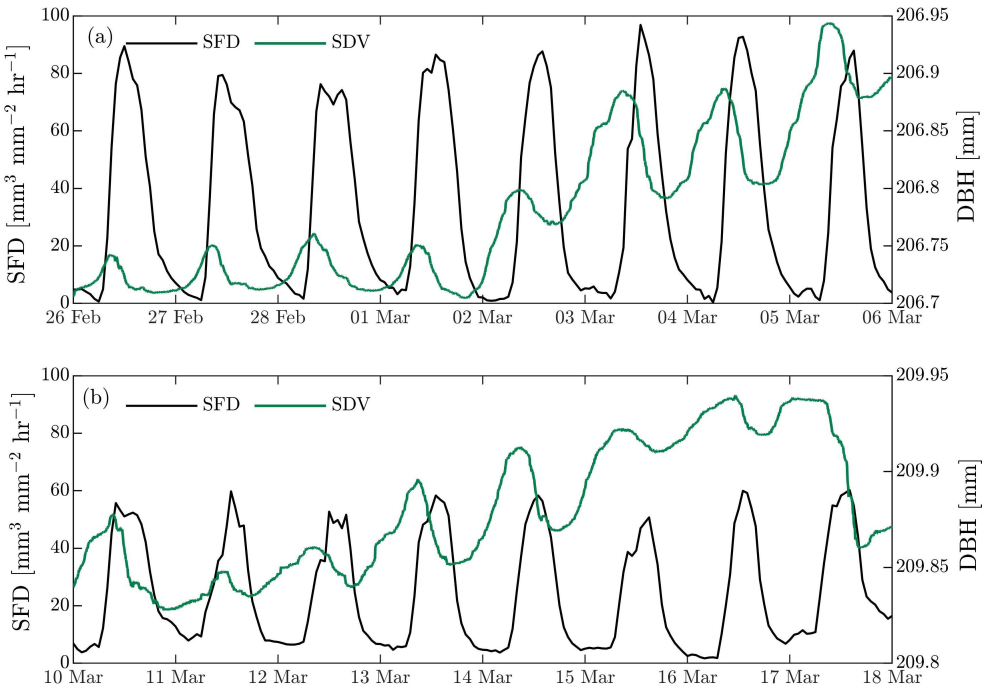

Figure 4.5: Sap flux density (SFD) and DBH for a selection of 8 rain-free days for the (a) 2017 and (b) 2018 water years at Alex Wilkie.

4.2.4 Night-time tree water use

Warm summer nights with temperatures above 25°C following days with temperatures above 35°C occurred a few times within the two years of this study. In most circumstances, trees under observation coped well with these short heat events and did not lose their hydraulic functions. Substantial night-time SFD was recorded in both EV1 and EV3 during the nights between 7 and 8 of January and between 8 and 9 of February 2017 (Figure 4.6a and Figure 4.6d). The high temperatures on these nights were associated with consequent high VPD, which likely led to transpiration during the night. During the two recorded warm summer nights SFD_n was found to be about 11% (EV1) and 16% (EV3) of the daily water use for January 2017, and about 3% (EV1) and 13% (EV3) for February 2017.

Measurements of diurnal shrinking and swelling of the tree trunk also verified the presence of night-time water use. During the first warm night, swelling, usually occurring near sunset when the evaporative demand decreased, coincided with a reduced amplitude due to the night-time transpiration, causing an even larger shrinkage when the evaporative demand increased during the following daylight hours (Figure 4.6b and Figure 4.6c). This phenomenon was also present during the second warm night even though recent rainfall events affected the diurnal signal of DBH (Figure 4.6e and Figure 4.6f).

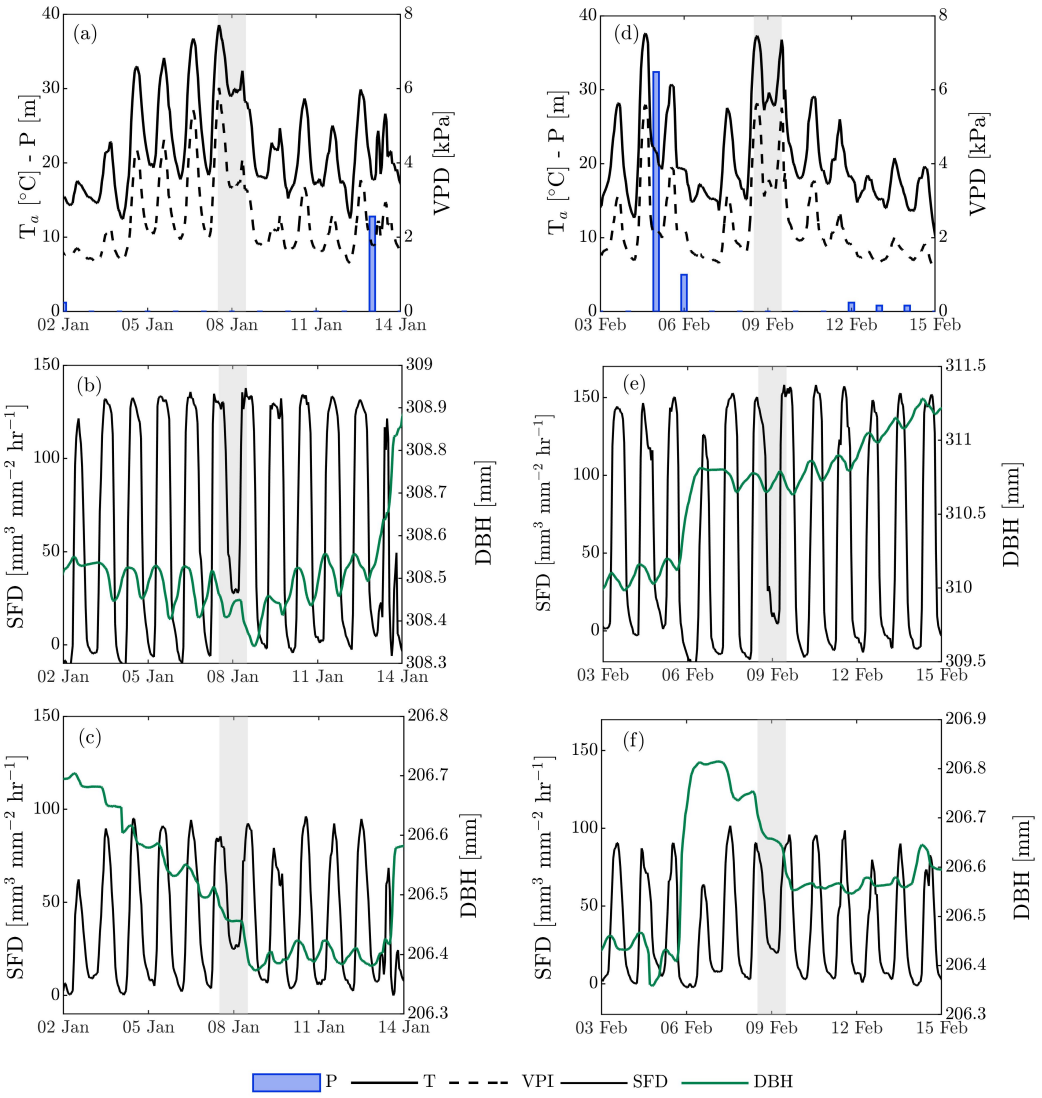

Figure 4.6: Time evolution of environmental factors, sap flux density (SFD), and DBH during the night-time heat stress events observed in January and February 2017 at Alex Wilkie: (a, d) air temperature (T_a), vapor pressure deficit (VPD), and rainfall (P); (b, e) SFD and DBH for the EV1 tree; and (c, f) SFD and DBH for the EV3 tree.

4.3 Discussion

This study attempts to understand and quantify the water balance and tree water use of small urban reserves. In two of the study sites (i.e., National Drive and Alex Wilkie) groundwater was found to play an essential role in supporting tree transpiration, especially during the driest periods of the year and heat events. At Napier Park, groundwater not being easily accessible, the water stored in the shallow clay layer of the duplex soil supported transpiration rates, as observed in other similar conditions (Verma et al., 2014).

Observed transpirations rates were found to be comparable to estimates from other *Eucalyptus* stands in natural areas (e.g., Zeppel et al., 2006; Doody et al., 2015). Transpiration rates at National Drive ranged from 1.3 to 0.5 mm day^{-1} during summer and winter, while at Alex Wilkie they were from 0.9 to 0.25 mm day^{-1}; at Napier Park, T ranged between 0.3 mm day^{-1} during summer and 0.1 mm day^{-1} in winter. In both years, T was about 44% (ND), 33% (AW), and 16% (NP) of total annual rainfall, showing large inter-site variability due to different natural rainfall regimes and stand density (Table 3.1; Table 4.1); on the contrary, small inter-annual variability was observed, although annual rainfall in 2018 was about 15% lower than 2017.

In both years, a large portion of the water balance closure was attributed to ET (i.e., ET_{floor} + E_i) and $\Delta S_{sw,d}$. The magnitude of ET and $\Delta S_{sw,d}$ can be estimated from previous studies conducted on similar vegetation cover and hydrologic regime (Benyon and Doody, 2015).

Specifically, ET_{floor} may represent more than 50% of total ET (Zeppel et al., 2006) and about 23-37% of the annual rainfall (Benyon and Doody, 2015), whereas E_i may be between 15 to 26% of the total annual rainfall (Dunin et al., 1988; Farrington and Bartle, 1991; Hutley et al., 2000; Bulcock and Jewitt, 2012). Accordingly, considering ET_{floor} + E_i about 50% of the annual rainfall, this term accounted for 89% (National Drive), 66% (Alex Wilkie), and 52% (Napier Park) of the water balance closure for the 2017 water year, and 94% (ND), 75% (AW), and 57% (NP) for the 2018 water year.

These estimates support the water balance in Table 4.1, especially for National Drive, in which $\Delta S_{sw,d}$ is expected to be small due to the clayey nature of the soil, which enhances the capillary rise up to the monitored soil layers (as also shown in Figure 4.2b). At Alex Wilkie, higher proportions of interception losses (E_i) should be considered due to the dense understory cover. As well, higher $\Delta S_{sw,d}$ may be expected because of the highly sandy soil which increases the movement of water beyond the monitored soil profile. At Napier Park the water balance was only conducted for the monitored soil (0 - 1.2 m), with $\Delta S_{sw,d}$

representing the downward drainage below this depth; at this site, extensive grassy and bare soil areas may also contribute to a larger percentage of floor evaporation.

Most of the uncertainties in the estimates of the water balance components are related to the underestimation of canopy transpiration. Accounting for an underestimation of T of 35% would result in an annual water balance closure of 41, 65, and 91% of P during 2017 and 38, 54, and 81% in 2018 for National Drive, Alex Wilkie, and Napier Park, respectively. This may involve, in particular at National Drive, a different water balance closure partitioning with less water lost through ET_{floor}.

Groundwater use by vegetation at the National Drive and Alex Wilkie reserves illustrates the important role that groundwater resources may have in supporting tree transpiration in urban areas, where arduous growing conditions and abiotic stress factors, such as heat stress and low moisture conditions, affect the health of trees. Several studies have detected similar behaviors, but commonly with reference to large bio-diverse ecosystems and often in natural environments or environments mildly affected by human activities (e.g., Fan et al., 2014a; Fan et al., 2016; Balugani et al., 2017). In this study, groundwater transpiration (T_{gw}) was estimated to contribute about 30-40% of total T in the driest period of the year; this is consistent with the findings from other studies, showing that groundwater was a source of water for vegetation (Orellana et al., 2012). The annual value of T_{gw} is difficult to estimate precisely because of the assumptions in the definition of Eq. 4. The difficulties in the estimation of S_y (Gehman et al., 2009; Dietrich et al., 2018) and the lack of information on the groundwater flows in and out of the reserves introduce uncertainties in the estimation of T_{gw} (Loheide et al., 2005). However, the water table patterns during dry periods and the sustained transpiration rates during and following warm nights strongly support the assumption that trees are using groundwater at National Drive and Alex Wilkie.

As shown in Drake et al. (2018), water availability played an essential role during heat events. During the study period, the monitored trees successfully coped with warm summer nights with temperatures above 25°C and did not lose their hydraulic functions. In particular, T_n ranged from 3 to 16% of the daily transpiration, which is comparable to those found in eucalyptus woodland in Western Australia (∼15-20%) (Dawson et al., 2007) and in New South Wales (∼6-8% and up to 19% on some days) (Zeppel et al., 2010; Fan et al., 2016).

4.4 Summary

Urbanization and the associated land use changes greatly impact natural ecosystems, causing small natural reserves in urban areas to face changes in their hydrologic regime. This

chapter provides a comprehensive analysis of the water balance and tree water use dynamics over a two-year period in three urban reserves hosting remnant native vegetation and experiencing different rainfall patterns in Melbourne, Australia. The water balances (2017-2018) showed that the three urban reserves had enough water to sustain transpiration rates despite the urban surrounding. Two of the reserves of this study appeared to be dependent on groundwater and the other one relied on water stored in a clay layer of its duplex soil. Groundwater played an essential role in sustaining transpiration rates. During the driest periods of the year, transpiration from groundwater was estimated to be about 30-40 % of the total transpiration. During warm nights following days with temperatures above 35°C, groundwater allows trees to transpire between 3 and 16 % of the total daily transpiration. Therefore, these results highlight the importance of soil water resources in urban areas to support green spaces.

Chapter 5

Groundwater buffers drought effects and climate variability

This chapter is an extract from the manuscript **"Groundwater buffers drought effects and climate variability in urban reserves"** submitted to *Water Resources Research*.

The chapter investigates, through a series of numerical experiments, how groundwater availability controls the water balance and vegetation productivity of two of the three study sites: National Drive and Alex Wilkie. Using a mechanistic ecohydrological model supported by field observations, long-term simulations were used to explore the ecosystem relationship to water availability in the recent climatic conditions, including the Millennium Drought (2001-2009), and in response to perturbations in key environmental variables (i.e., air temperature, atmospheric CO_2 concentrations, and rainfall). The presence of a water table and its capillary fringe within the root depths were found to support ecosystem transpiration and vegetation productivity. The effects of declining groundwater were found to be more severe in predominantly sandy soils because of the lower water-holding capacity, identifying that the water status of vegetation differs significantly depending on soil type. Differences in rooting strategies and groundwater availability also had a pivotal role in helping plants soften the impacts of increased air temperature (T_a) and make use of higher atmospheric CO_2 concentrations. Increased T_a strongly affected evapotranspiration, enhancing the competition for water between different vegetation types. These results provide quantitative insights on how vegetation responds to groundwater depletion and climate variability, highlighting the essential role of groundwater resources in urban ecosystems characterized by seasonally dry climates.

5.1 Introduction

A notable fraction of the global land area has the water table (WT) or its capillary fringe within the reach of plants roots (Fan et al., 2013). Therefore, groundwater is a key source of water for a wide range of terrestrial vegetation across different climatic regions, especially those characterized by pronounced dry seasons lasting for months (Lowry and Loheide, 2010; Fan, 2015). Consequently, groundwater could become increasingly important under a rapidly changing climate, as more frequent and severe extremes, such as droughts and hotter temperatures, increase the risk of plant mortality and reduce productivity (Soylu et al., 2011; Allen et al., 2015; Breshears et al., 2005; Mcdowell et al., 2016). Groundwater may therefore become crucial in supporting ecosystem resilience to seasonal and inter-annual droughts and in buffering the impact of warming predicted by climate models (Taylor et al., 2013; Skinner et al., 2018).

Groundwater depth has been found to control energy fluxes at the land-surface, especially when the WT depth ranges between 1 and 5 m (Maxwell and Kollet, 2008; Kollet and Maxwell, 2008). In semiarid regions, for example, shallow WT near river corridors allow vegetation establishment and help plants to cope with extended dry seasons (Scott et al., 2006). Other evidence of groundwater supporting plant water demand can be found in Mediterranean climates (Zencich et al., 2002; Murray et al., 2003; Eamus et al., 2006; Barbeta et al., 2015), where groundwater represents a large source of water for transpiration, possibly being the sole contribution to total transpiration in parts of the year (Miller et al., 2010; Orellana et al., 2012). The contribution of the WT to forest transpiration has also been found in humid temperate climates (Love et al., 2018), even during cool and wet winter months (Vincke and Thiry, 2008).

The focus of most studies related to groundwater dependent ecosystems is on large biodiverse ecosystems, often in natural environments or areas mildly affected by human activities. However, the role of groundwater in the water balance of urban ecosystems has received considerably less attention. In cities, vegetated surfaces become often fragmented into small and isolated patches of native species, which are surrounded by impervious surfaces and embedded in a highly disturbed environment (McKinney, 2002). This complex mosaic of urban land use and cover strongly influences the water cycle (Newcomer et al., 2014; Cho et al., 2009; Xiao et al., 2007; Shields and Tague, 2015; Bhaskar et al., 2016) having impacts on rainfall partitioning into infiltration and runoff, plant-available soil moisture and, consequently, ecosystem health and productivity. Moreover, changes in air temperature associated with the urban heat island (UHI) can increase the duration of the growing season of urban

trees (Zipper et al., 2016), enhancing their transpiration rates when and where sufficient soil water is available to sustain the higher evapotranspirative demand (Zipper et al., 2017a). In addition to these environmental changes, the need for fresh water in urban areas has exacerbated the pressure on groundwater resources, especially in fast-growing cities (Flörke et al., 2018). Because groundwater withdrawals and diversions may decrease groundwater levels, there is the need to evaluate if urban groundwater dependent plants can be affected by more frequent, rapid, and extended WT declines and fluctuations than those in pristine environments (Naumburg et al., 2005).

Overall, cities are recognized to be major contributors to climate change but, at the same time, are extremely vulnerable to its impacts (Van Loon et al., 2016a), making them ideal natural laboratories for testing ecosystems resilience to extreme conditions. Specifically, while the role of urban trees in supporting urban ecosystem functionality through the provision of ecosystem services is well documented (Chiesura, 2004; Tyrväinen et al., 2005; Dobbs et al., 2014; Livesley et al., 2016a; Song et al., 2018; Richards and Thompson, 2019), less is known about their response to these environmental changes. In particular, groundwater-supported trees might cope with short-term droughts and hotter temperatures (Drake et al., 2018; Marchionni et al., 2019a) better than with long-term groundwater storage declines due to climate shifts or direct anthropogenic manipulations (Kløve et al., 2014; Eamus et al., 2015). Investigating the interactions and feedback between WT dynamics and terrestrial vegetation becomes crucial to managing and maintaining healthy urban ecosystems, and in gaining an understanding of possible impacts on land surface fluxes (Naumburg et al., 2005; Orellana et al., 2012).

This chapter aims at evaluating the vulnerability of urban vegetation to changes in environmental variables by using simulations of present conditions, tested against observations and a series of numerical experiments, for two of the three urban reserves that are part of this project. The recent Millennium Drought (Freund et al., 2017), a prolong period of dry conditions spanning from 2001 to 2009, provides a unique opportunity to explore ecosystem responses to changes in water variability. During this prolonged drought, below median rainfall, since at least 1900, was recorded with regional declines in WT depths (Leblanc et al., 2012; van Dijk et al., 2013) and reductions of observed vegetation biomass (Sawada and Koike, 2016). The specific questions addressed are: (1) How do different scenarios of groundwater availability control tree transpiration and vegetation productivity under both present and variable climate? (2) How can different vegetation types (tree-shrubs-grass) coexist and is this coexistence threatened? (3) How can soil properties amplify or dampen the ecosystem dependence on groundwater?

5.2 Ecohydrological modeling

Numerical simulations were carried out using the ecohydrological model Tethys-Chloris, which is extensively described in section 3.3.

5.2.1 Model setup and parameter calibration

The most influential model parameters for both soil and vegetation (e.g., root depth) were calibrated at hourly time steps to reproduce soil water dynamics using the data available for the 19 month period between December 2016 and June 2018. The atmospheric forcing consisted of meteorological data observed locally for National Drive, and at the Moorabbin and Melbourne Airport weather stations for Alex Wilkie (no. 086077, 086282). Consistent with the hypothesis of representing average reserve-scale processes, a 1-D soil domain was assumed with soil depths limited to 15 m and 7.2 m for National Drive and Alex Wilkie, respectively. The modeled soil stratigraphy follows the one that was measured during the installation of the groundwater bores (Table 5.1), with layers progressively coarsening with depth. No-flow conditions were assigned at the bottom of the domain.

To account for local groundwater flow towards or from the sites, a net lateral flow (q) was added to the soil water budget. To calculate the amount of subsurface water entering and exiting the system, a simulation with q set to zero was first run, meaning that the system is one-dimensional and there is no lateral flux of water. In such a case plants can only use water stored in the root zone coming from rainfall. The term q was then obtained by matching the volume of water that the system needed in order to maintain the WT beneath the root zone at the observed depth. The values of q (represented by the dots in Figure 5.1), which can be either a source or a sink term in the subsurface dynamics, showed a clear seasonal pattern at National Drive. By fitting these points with a sinusoidal function, the seasonal variation of q were then taken into account.

This seasonality was particularly relevant at National Drive, where the predominantly clayey soil responds to small variations in volume of water with larger WT fluctuations; on the contrary, seasonal variations of q did not appear to significantly affect the groundwater dynamics at Alex Wilkie, for which a constant positive value of q (source) was assumed throughout the year. The values of q obtained during calibration are reported and discussed in section 5.3.1. This approach allowed a simulated WT to be maintained, with fluctuations close to the ones measured, and to estimate the local net contribution of groundwater flow to the reserves.

Soil moisture and vegetation carbon pool initial conditions for the calibration simulations

Table 5.1: Main soil parameters used in the simulations.

Depth (m)	**Soil Discretization**	**Soil sand/silt/clay fractions** Saxton and Rawls (2006)	***van Genuchten* coefficients** (θ_s, θ_r, α, **n**)	**Saturated hydraulic conductivity** ($\mathbf{k_s}$; **mm** $\mathbf{h^{-1}}$)
National Drive:				
0.0-0.3	Silty Clay	55/3/12	-	38
0.3-0.6	Silty Clay	30/4/40	-	10
0.6-1.2	Clay	8/1/80	-	0.86
1.2-15	Clay	10/0.1/80	-	0.67
Alex Wilkie:				
0.0-3.2	Loamy Sand	-	0.39, 0.025, 0.014 mm^{-1}, 1.95	250
3.2-4.0	Silty Sand	-	0.40, 0.070, 0.010 mm^{-1}, 1.60	4
4.0-7.2	Sandy Clay	-	0.40, 0.120, 0.005 mm^{-1}, 1.10	1

Saturated hydraulic conductivity is assumed variable with depth as k_s=-5.11 ln(z)+46.36 mm h^{-1} at National Drive
Saturated hydraulic conductivity is assumed variable with depth as k_s=-39.62 ln(z)+339.32 mm h^{-1} at Alex Wilkie

Table 5.2: Main vegetation parameters used in the simulations.

Parameters	**Unit**	**National Drive**		**Alex Wilkie**		
		Trees	**Grass**	**Trees**	**Shrubs**	**Grass**
$Z_{R,50}$	m	0.35	0.15	0.60	0.50	0.20
$Z_{R,95}$	m	1.00	0.20	2.00	1.50	0.40
ZR_{max}	m	3.00	0.30	4.00	3.80	0.50
h_c	m	20.00	0.20	20.00	10.00	0.20
a_1	-	8.00	7.00	8.00	6.00	7.00
ψ_{S2}	MPa	-0.70	-0.60	-0.70	-0.50	-0.60
ψ_{S50}	MPa	-1.50	-2.00	-1.50	-5.00	-2.00
S_L	m^2/gC	0.009	0.016	0.009	0.012	0.016
r	gC/gN/d	0.042	0.038	0.042	0.036	0.038
$A_{L,cr}$	d	365	180	365	730	180
d_{mg}	d	20	20	20	15	20
T_{rr}	gC/m^2/d	1.00	2.50	1.00	0.40	2.50
L_{tr}	-	0.80	0.40	0.80	0.50	0.40
ϵ_{ac}	-	0.60	0.50	0.60	0.80	0.50
$1/K_{lf}$	d	40	40	40	50	40
$V_{c,max25}$	-	45	54	45	62	54
r_{JV}	-	2.00	2.10	2.00	2.00	2.10

$Z_{R,50}$: root depth 50 percentile, $Z_{R,95}$: root depth 95 percentile, $Z_{R,max}$: maximum root depth, h_c: canopy height, a_1: empirical parameter connecting stomatal aperture and net assimilation, ψ_{S2}: water potential at 2% stomatal closure, ψ_{S50}: water potential at 50% stomatal closure, S_L: specific leaf area, r: respiration rate at 10°C, $A_{L,cr}$: critical leaf age, d_{mg}: days of maximum growth, T_{rr}: translocation rate from carbohydrate reserve, L_{tr}: leaf to root biomass maximum ratio, ϵ_{ac}: parameter for allocation to carbon reserves, $1/K_{lf}$: dead leaf fall turnover, $V_{c,max25}$: maximum Rubisco capacity at 25°C leaf level, r_{JV}: scaling J_{max}- $V_{c,max}$.

were generated by running a 1 year spin-up simulation starting from soil moisture conditions coinciding with field capacity. Vegetation parameters (Table 5.2) were chosen based on literature and previous model applications (Fatichi and Pappas, 2017). In particular, two

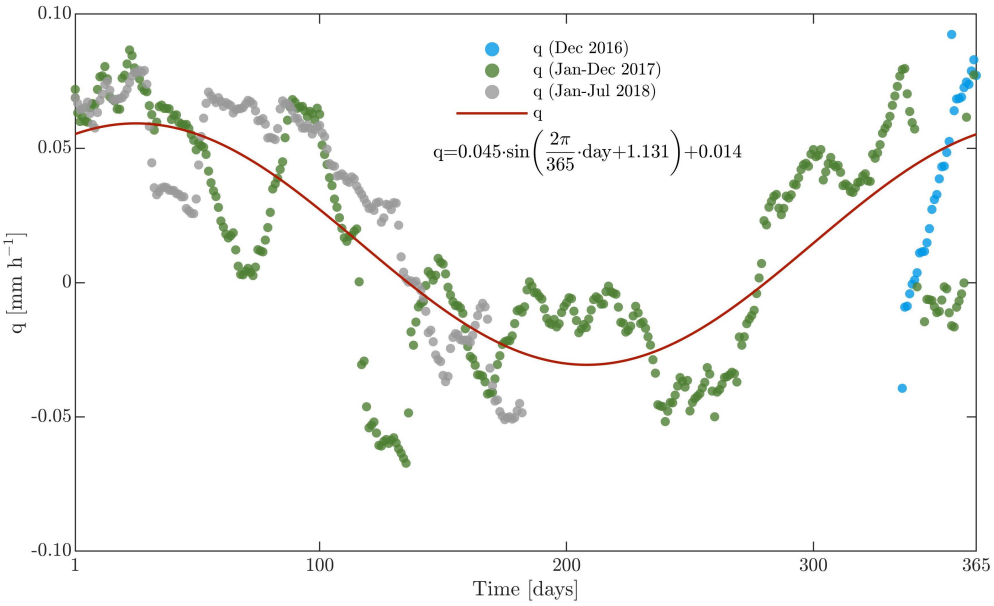

Figure 5.1: Net lateral flow (q) necessary to maintain the water table depth at the level of observations for the 19-month calibration period at National Drive Reserve. Values are shown for December 2016 (blue dots), January to December 2017 (green dots), and January to July 2018 (grey dots). A sinusoidal function (red line) was then fitted to smooth annual variation of q and its observational uncertainty.

PFTs (i.e., trees and grass) were considered at National Drive covering 40% and 60% of the reserve, respectively; at Alex Wilkie, the coexistence of trees, shrubs, and grass was represented with three PFTs covering 20%, 20%, and 60% of the reserve, respectively. These fractions were based on local observations.

Soil hydraulic properties were obtained through pedotransfer functions (Saxton and Rawls, 2006) for National Drive, while the *Van Genuchten* model (Van Genuchten, 1980; Carsel and Parrish, 1988) was used for Alex Wilkie, as the hydraulic parameters obtained by Saxton and Rawls, 2006 pedotransfer functions led to unrealistic soil moisture dynamics in such a highly sandy soil (Table 5.1). In both cases, soil hydraulic parameters were manually adjusted during calibration. A linear dose response profile with tap roots (Collins and Bras, 2007) was used to describe the root depth distribution. This required specification of the rooting depth that contains 50% and 95% of fine root biomass ($Z_{R,50}$ and $Z_{R,95}$), as well as the maximum rooting depth ($Z_{R,max}$).

The values of the parameters obtained in the model calibration for National Drive and Alex Wilkie, including q, were then used to run long-term (July 1999 - June 2018) simulations to confirm the model performance in reproducing groundwater dynamics. For both sites, the long-term time series of meteorological data at the Moorabbin Airport weather station

was used as meteorological forcing, with the exception of the solar radiation data taken from Melbourne Airport weather station. Results in terms of WT depths were then compared with the long-term observations available from the groundwater bores nearby the sites. Anomalies with respect to the mean value were evaluated to minimize the influence of topographic differences and spatial variability in the characteristics of the aquifers.

5.2.2 Recent and variable climate

A series of numerical experiments were designed to investigate the effects of changes in soil water availability (both in the unsaturated and saturated zones) on hydrological fluxes and vegetation productivity. Simulations were carried out from 1 July 1999 to 30 June 2018 using the long-term time series of meteorological data available at the Moorabbin Airport weather station, in combination with the solar radiation data available from Melbourne Airport weather station.

The sensitivity to groundwater availability was determined by imposing different values of q, leading to different WT depths: 0, 42, 63, 126, 252, and 378 mm y^{-1} for National Drive, and 0, 50, 100, 200, 300, and 400 mm y^{-1} for Alex Wilkie. These scenarios were performed by assigning no-flow conditions at the bottom of the soil domain. A further scenario with free-drainage conditions and q=0 mm y^{-1} (indicated as 0_{FD}) was also considered, for a total of seven scenarios in each site.

Moreover, the impacts of the Millennium Drought on vegetation dynamics were analyzed by running a scenario with a lower q during the drought, thus taking into account a possible reduction of local groundwater flow towards the sites. Specifically, values of q equal to 63 and 100 mm y^{-1} were assumed between 2001 and 2009 (representing half of the estimated net groundwater flow) for National Drive and Alex Wilkie, respectively, while for the remaining years q was set equal to 126 mm y^{-1} for National Drive and 200 mm y^{-1} for Alex Wilkie. Although mainly a numerical experiment, these reductions result in water table depletions similar to those observed in the monitoring bores within 7 km radius of the study sites during the Millennium Drought.

The effects of altered environmental drivers due to expected climate change were then investigated by imposing changes to air temperature, atmospheric CO_2 concentrations, and rainfall with respect to the present climate values. Simulations were run by changing only one environmental driver at a time to analyze their influence on vegetation response and hydrological fluxes. Specifically, four scenarios of increased temperature (+1.5, 2.0, 3.0, 4.0 °C), two scenarios with increased atmospheric CO_2 concentrations (+200 and +400 ppm), and two different rainfall conditions (+15% and -15%) were simulated. In all simulations soil

moisture and vegetation carbon pool initial conditions were generated by running a spin-up simulation of 19 years.

5.3 Results

5.3.1 Model calibration and confirmation

A satisfactory match between observed and simulated soil water dynamics was achieved for an average q equal to 126 mm y^{-1} for National Drive and 200 mm y^{-1} for Alex Wilkie, after tuning soil hydraulic properties and root depths (Table 5.1 and Table 5.2). The smaller value of q found for National Drive likely reflected local conditions and a predominantly clay soil that affects groundwater transmissivity.

Overall, the model reproduced the magnitude and timing of the WT fluctuations for the 19 month calibration period at both sites. At National Drive, simulations exceeded the observed saturated zone during wet months, where the WT responded with a larger rise to less intense, more frequent rainfall events (Figure 5.2b). Soil layers in the unsaturated zone were strongly affected by the proximity to the WT, as shown at depths between 0.7 to 1.2 m (Figure 5.2e); conversely, the surface soil layers (0-0.3 m) were more sensitive to rainfall events. As shown in Figures 5.3a-c, a better match between observed and simulated soil water dynamics was achieved in the first layers of soil. At Alex Wilkie, soil water dynamics in the top soil (i.e., between 0 to 1.2 m) were quite sensitive to rainfall events (Figure 5.2f), but disconnected from the saturated zone dynamics because of the coarse sandy soil (Figure 5.2d). A good match between observed and simulated soil water dynamics was achieved in the first 1.2 m of the soil domain, as shown in Figure 5.3d).

Although the model was not calibrated against transpiration rates, it was able to capture the magnitude of annual transpiration with an overestimation during summers and underestimating in winter (Figure 5.2g and Figure 5.2h). However, the errors in the measurements of sap flow using HPV sensors, as explained in section 3.2.4, along with those occurring during the upscaling as well as the strong variability in the measurements collected in the different trees at both sites may lead to uncertainties in the observed daily transpiration.

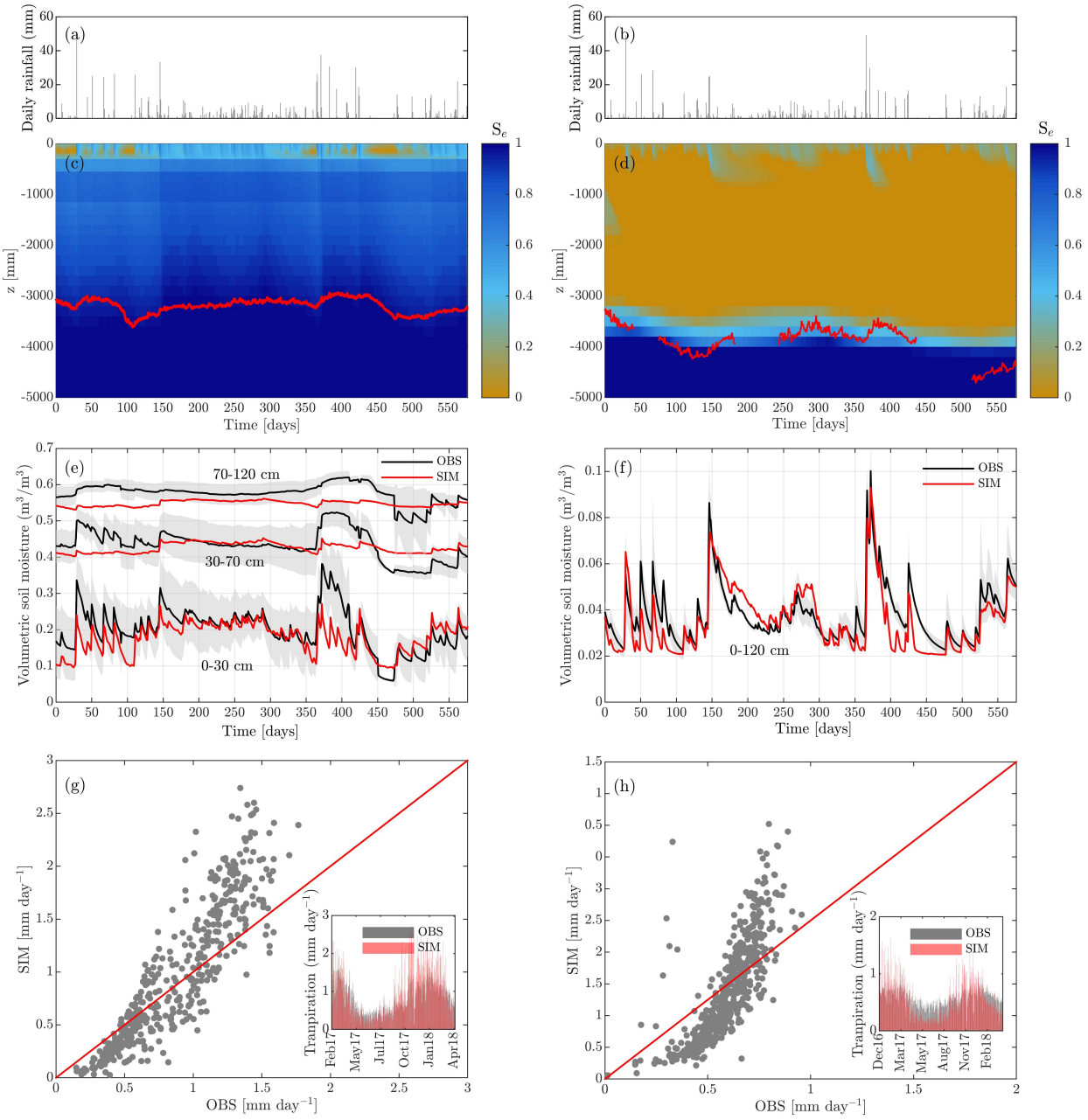

Figure 5.2: Daily rainfall recorded for the 19 month period between December 2016 and July 2018 at the (a) weather station located in National Drive Reserve and (b) Moorabbin Airport weather station for Alex Wilkie Reserve. A comparison between simulated effective saturation (S_e) and observed groundwater depths (red line) in the calibration period for (c) National Drive Reserve and (d) Alex Wilkie Reserve is presented. Simulated and observed ($\pm$ SD; grey areas) volumetric soil moisture in the calibration period for (e) National Drive (at depth 0-30; 30-70;70-120 cm) and (f) Alex Wilkie (depth 0-120 cm) are also shown, along with simulated and observed transpiration (g) between February 2017 and April 2018 for National Drive and (h) between December 2016 and April 2018 for Alex Wilkie.

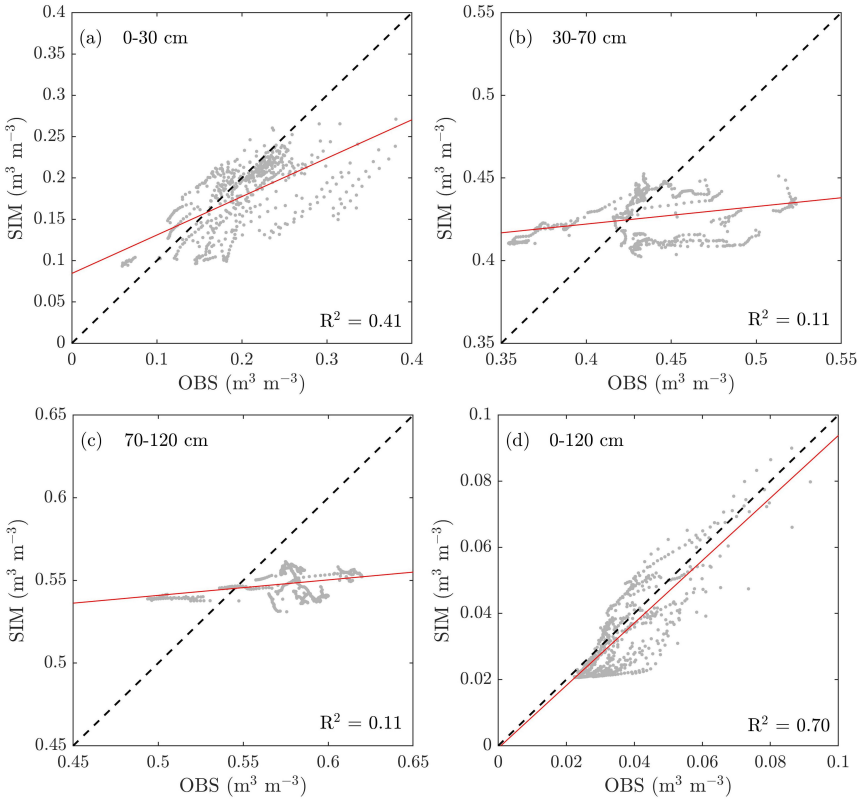

Figure 5.3: Simulated and observed volumetric soil moisture in the calibration period (a-c) for National Drive Reserve and (d) Alex Wilkie Reserve.

A further confirmation of the model performance was achieved for the long-term (July 1999 - June 2016) WT fluctuations, expressed as hourly anomalies relative to the mean value (Figure 5.4). The model performed better at Alex Wilkie, whereas the amplitudes of the simulated anomalies were much more pronounced for National Drive, where the representation of the very clayey soil generated large changes in WT depths for small changes of water added or removed from the soil (e.g., a very small specific yield). In such a soil, it was observationally and numerically challenging to distinguish between actual WT depth and depth of the capillary fringe.

5.3.2 Ecohydrological response to soil water availability

The simulated effects of different groundwater levels on hydrological and energy fluxes as well as on plant water stress (β) and gross primary productivity (GPP), are shown in Figure 5.5, expressed as mean values of the 19 years analyzed, with the latter weighted and integrated over the entire vegetated area.

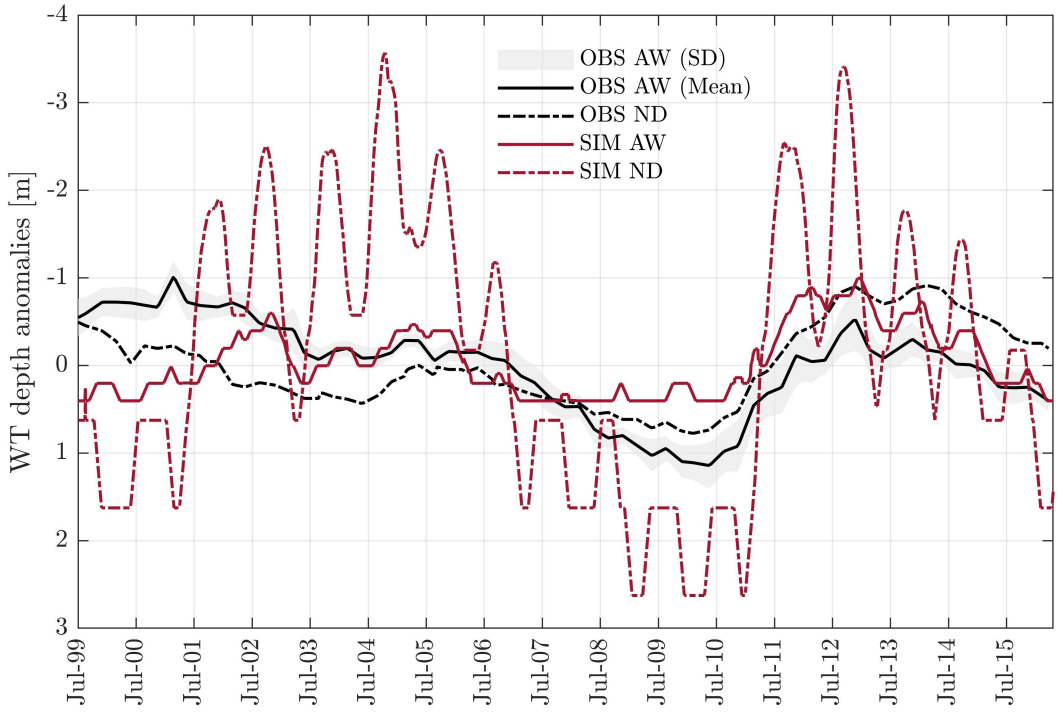

Figure 5.4: Simulated and observed water table (WT) depth fluctuations expressed as hourly anomalies (relative to the mean value) at both the observation bores within 7 km radius of and within the study sites.

Groundwater availability, regulated by q, noticeably affected evapotranspiration fluxes (ET), which varied between 641 and 935 mm y^{-1} at National Drive (Figure 5.5a) and 640 and 985 mm y^{-1} at Alex Wilkie (Figure 5.5b) across the different simulation scenarios. The groundwater contribution led ET to exceed the mean annual precipitation, i.e., 640 mm y^{-1}. In both reserves, results showed that an annual net lateral flow of 126 mm y^{-1} for National Drive and 200 mm y^{-1} for Alex Wilkie was sufficient to largely eliminate tree water stress. The WT depths obtained with these values of q (i.e., 6.9 m at National Drive and 3.9 m at Alex Wilkie) were considered the reference conditions for each site. At National Drive, grass transpiration (T_G) followed the same pattern as total ET, while tree transpiration (T_T) reached a maximum for q=126 mm y^{-1} and then decreased slightly, as the WT was closer to the top soil layers and favors ground evaporation. At Alex Wilkie, the presence of shrubs led to more complex dynamics associated with the competition for soil water resources, with T_G always below the shrubs transpiration (T_S) despite both having 20% of the areal cover. When the WT was 0.6 m below the ground, T_G reached its maximum (374 mm y^{-1}; +62%). T_T and T_S also increased considerably (110% and 71%, respectively) when compared to the scenario 0_{FD} corresponding to a completely unsaturated soil column.

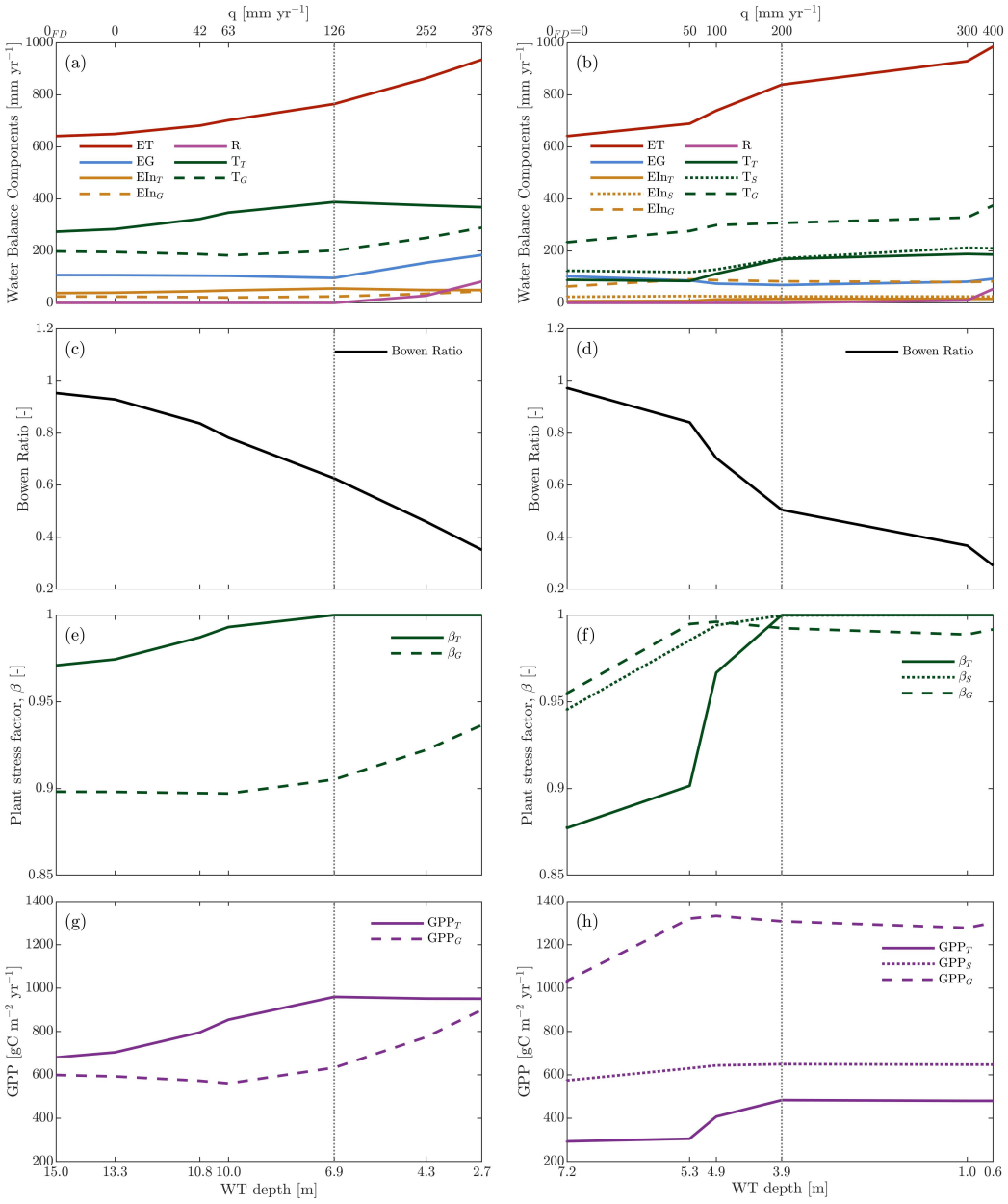

Figure 5.5: Simulation results averaged over the 19-year period (July 1999-June 2018) illustrating water and energy fluxes as well as vegetation productivity with respect to different average water table (WT) depth scenarios (corresponding to different values of net lateral flow, q) at National Drive Reserve (left column) and Alex Wilkie Reserve (right column). (a-b) Water balance components (i.e., ET: evapotranspiration, EG: ground evaporation, EIn: evaporation from interception, R: runoff, T: transpiration; subscripts T, G, S are referred to trees, grass, and shrubs, respectively), (c-d) Bowen ration (Bo=H/LE), (e-f) plant water stress (β), and (g-h) gross primary productivity (GPP; for unit of total ground area) are expressed as a function of both the average WT depth and average net lateral flow (q). The WT depth reference value, corresponding to the calibration period (dotted lines), is identified with q equal to 126 mm y^{-1} for National Drive Reserve and 200 mm y^{-1} for Alex Wilkie Reserve.

When groundwater was shallower than the reference value, a distinct increase in ground evaporation (EG) was modeled at National Drive, while groundwater did not affect EG at Alex Wilkie due to the sandy soil. Evaporation from interception, including grass (EIn_G), trees (EIn_T), and shrubs (EIn_S) was a relatively minor component of the water balance at both sites, accounting for about 10% and 15% of the total ET at National Drive and Alex Wilkie, respectively. Overland runoff (R) was also quite small at both sites and it was mostly affected by the proximity of the WT to the surface at National Drive. The thicker capillary fringe due to the particularly clayey soil of National Drive affected R even when the long-term average WT was below 3 m (going from 0 to 80 mm y^{-1} when the WT depth changed from 6.9 m to 2.7 m), while at Alex Wilkie the WT had to be on average only 0.6 m below the ground to generate runoff. Changes in ET also affected the surface energy budget. Increasing groundwater availability led to higher latent heat (LE) and lower sensible heat (H) fluxes, resulting in a considerably different partitioning of energy at the land surface (i.e., lower Bowen ratio, Bo = H/LE) (Figures 5.5c and 5.5d).

In terms of plant water stress, results suggested that trees are more susceptible to water stress when deep roots do not have access to groundwater or its capillary fringe. In particular at Alex Wilkie (Figure 5.5f), β for trees (β_T) strongly decreased (from 1 to 0.87) when the WT depth went below the reference value; on the contrary, at National Drive (Figure 5.5e) β_T remained overall above 0.97, due to the enhanced water-holding capacity of the clay soil, which buffered the decline of the WT. At both sites, grass was stressed in specific periods in all scenarios. While at National Drive β for grass (β_G) increased from 0.90 to 0.94 when groundwater availability increased, at Alex Wilkie it reached a maximum value (0.99) when the WT was on average 4.9 m below the ground, representing the best compromise in term of competition with trees. Shrubs at Alex Wilkie were less stressed than trees, with β for shrubs (β_S) always above 0.94 across the scenarios; this reflects a higher drought tolerance as specified in the model parameters, despite shallower roots than trees.

The impacts of groundwater availability were quite pronounced in terms of vegetation productivity. At both sites, the trajectories of gross primary productivity (GPP) with groundwater availability followed a similar trajectory as T_G, T_T, and T_S, with peaks in water use corresponding to peaks in productivity (Figures 5.5g and 5.5h). At National Drive, GPP of both grass (GPP_G) and trees (GPP_T) increased with groundwater availability (+41% and +50%, respectively). At Alex Wilkie (Figure 5.5h), GPP_T strongly decreased (-64%) when the average WT fell below 3.9 m, while GPP of shrubs (GPP_S) varied little with groundwater, remaining fairly constant across scenarios.

To explore the possible effects of the Millennium Drought (2001-2009) on the water fluxes

and GPP, the time series of annual values of the main water fluxes and GPP were presented assuming the flux q to be as in the calibration period (Figure 5.6). At both sites, the simulated annual ET exceeded the annual precipitation (P) in most years. As the drought intensified between 2007 and 2009, grass cover at both sites appeared to be more stressed, leading to lower rates of transpiration and GPP; trees on the other hand, having access to groundwater, coped well with the drought, maintaining their unstressed transpiration rates and productivity. During the driest years of the Millennium Drought, i.e., from 2007 to 2009, trees and shrubs reduced their transpiration at Alex Wilkie (Figure 5.6b), despite the constant net lateral flow of 200 mm y^{-1}.

When a decrease in local groundwater flow towards the sites was also taken into account during the prolonged drought (i.e., by reducing q by half), vegetation dynamics differed considerably compared to the scenario with constant q (Figure 5.7). In particular, trees appeared more stressed between 2007 and 2009 at Alex Wilkie, due to the dry conditions in the unsaturated zone and the very thin capillary fringe that could not buffer the groundwater drawdown. Simulations showed a rapid decrease in LAI_T (-26%) and GPP_T (-43%) between 2007 and 2009, followed by a slow recovery, returning in 2018 to the value that would have been obtained considering a constant q (Figures 5.7a and 5.7d). On the contrary, groundwater drawdown did not have a strong impact on shrubs and grass dynamics due to the prolonged drought. Shrubs exhibited an increase in LAI between 2002 and 2008, due to the reduced competition with trees, followed by a steeper decrease compared to the constant q scenario (Figures 5.7b); in terms of GPP, simulations showed a slight decrease in GPP_S (-10%) in 2009 (Figures 5.7e). Both grass LAI_G and GPP_G (Figures 5.7c and 5.7f) were only slightly affected by the groundwater depletion, with an actual softening of water stress because of a minor competition with trees during the 2009-2011 period.

5.3.3 Sensitivity to climate variations

Simulations using different environmental drivers, i.e., air temperature (T_a), atmospheric CO_2 concentrations, and rainfall (P), illustrate the possible role of groundwater in supporting these urban reserves to cope with plausible climatic variations. Results are shown with reference to two different groundwater availability scenarios: shallow groundwater (reference WT values, corresponding to the calibrated q) and without groundwater (completely unsaturated soil, corresponding to q sets to zero). Comparing these results with the simulation using observed climate, hereafter defined as control, groundwater availability strongly affects the water balance and vegetation productivity in both sites, even though soil properties and vegetation composition mediate the ecosystems response. Figure 5.8 and Figure 5.9 show

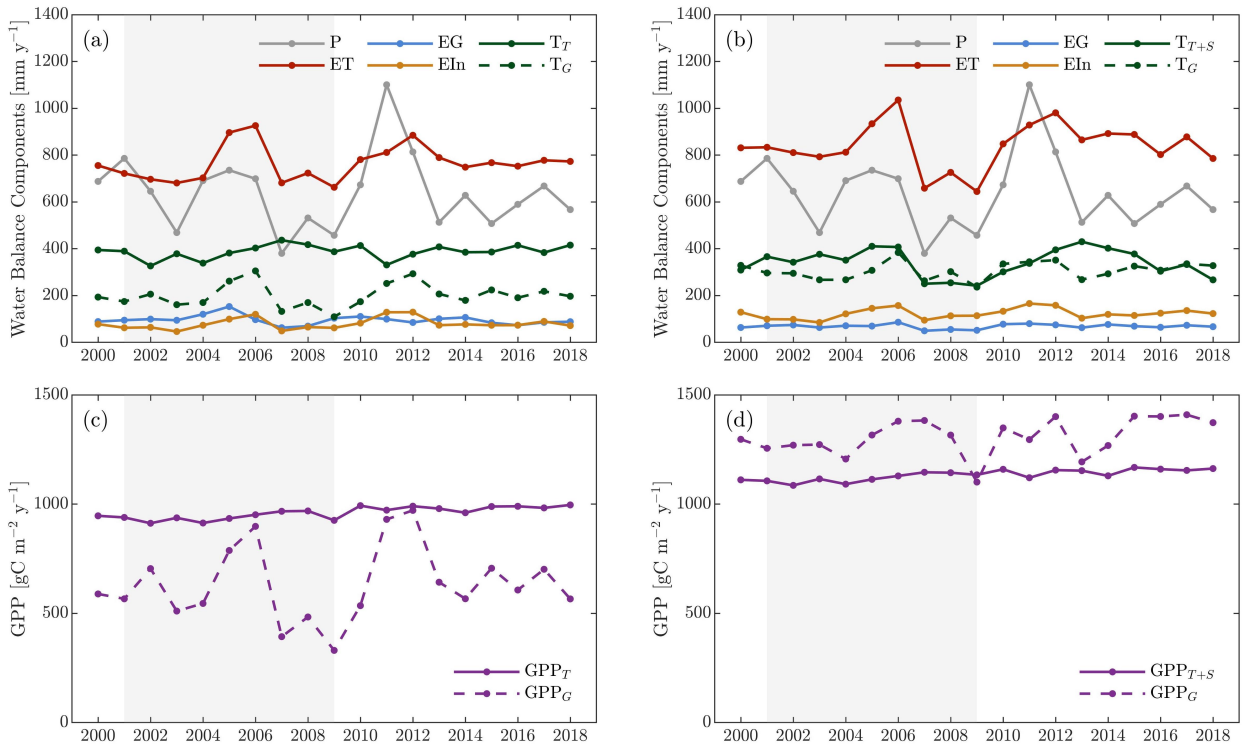

Figure 5.6: Simulation results for the 19 year period (July 1999-June 2018) corresponding to the calibrated net lateral flow (q) of 126 mm y^{-1} for National Drive Reserve (left column) and 200 mm y^{-1} for Alex Wilkie Reserve (right column). (a-b) Annual values of the water balance components, i.e., evaporation (ET), ground evaporation (EG), evaporation from interception from all PFTs (EIn), and transpiration from trees (T_T), grass (T_G), and trees and shrubs (T_{T+S}) combined. (c-d) Total annual values of gross primary productivity (GPP; for unit of ground area) for trees (GPP_T), grass (GPP_S), as well as trees and shrubs (GPP_{T+S}) combined. Grey regions indicate the period of the Millennium Drought.

the results of the scenario analysis for National Drive and Alex Wilkie, respectively.

At National Drive, in shallow groundwater condition (Figure 5.8a), T_G and EG increased with T_a (22% and 43%, respectively), while T_T decreased (-17%). Without groundwater (Figure 5.8d), trees strongly reduced their transpiration (-31%), while T_G increased (31%) as a consequence of minor competition, thus in the simulation grass was outcompeting trees in the access to the water in the top soil layers. Overall, T_a increases had a greater impact on plant water stress when deep roots did not have access to groundwater or its capillary fringe. While β_T decreased by 4% in the shallow groundwater scenario and by 8% in the scenario without groundwater (Figures 5.8b and 5.8e), β_G was not affected by groundwater presence, thus showing the same decrease (3%) in both scenarios. Changes in water availability and air temperature were linked to changes in vegetation productivity, with GPP_T more affected

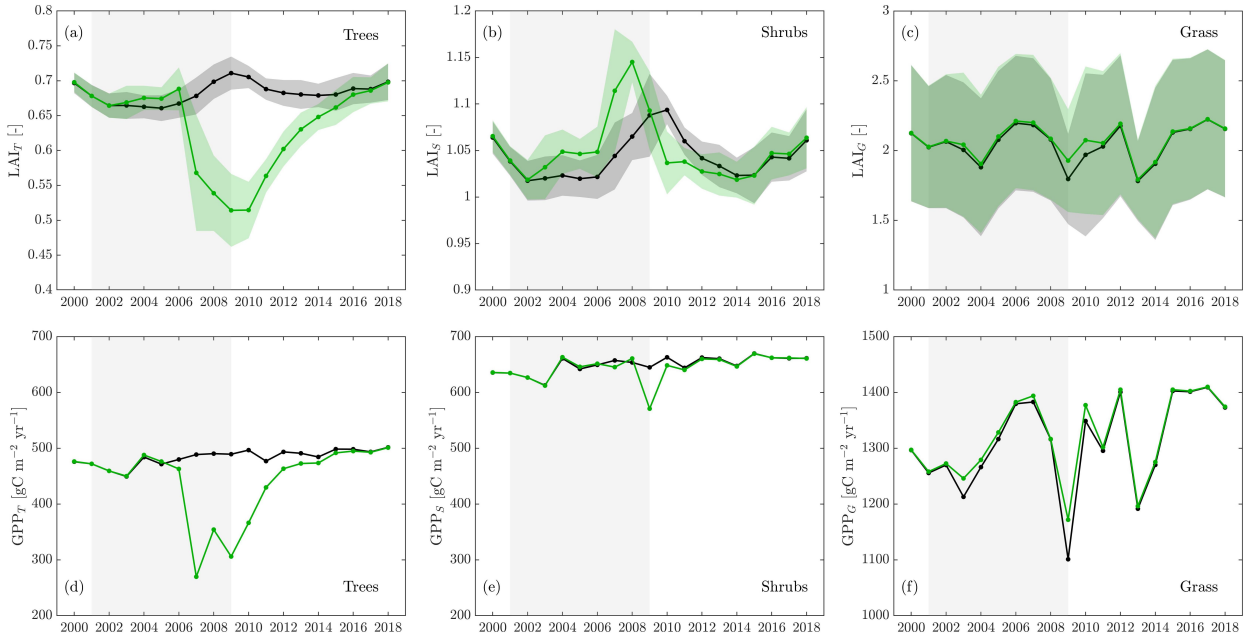

Figure 5.7: Simulation results for Alex Wilkie related to the 19 year period (July 1999-June 2018) corresponding to a constant net lateral flow (q) of 200 mm y^{-1} (black lines) and a variable q (green lines), i.e., 100 mm y^{-1} between 2001 and 2009 (Millennium Drought) and 200 mm y^{-1} in the remaining years. (a-c) Mean annual values (± SD) of Leaf Area Index (LAI; for unit of ground area) for (a) trees, (b) shrubs, and (c) grass. (d-f) Total annual values of gross primary productivity (GPP; per unit of ground area) for (d) trees, (e) shrubs, and (f) grass. Grey regions indicate the period of the Millennium Drought.

than GPP_G. Results showed a steep decrease in GPP_T when T_a increased in both groundwater scenarios, decreasing by 56% with shallow WT (Figure 5.8c) and 18% with deep WT (Figure 5.8f). GPP_T overcame GPP_G when tree roots had access to groundwater, although in the +4°C scenario the two values were similar; on the contrary, GPP_G overcame GPP_T across all temperature scenarios when groundwater was not accessible by tree roots.

In both scenarios, results indicated that with increased atmospheric CO_2 both grass and trees were able to assimilate carbon with a lower stomatal conductance and thus lower transpiration rate, leading to higher ecosystem water-use efficiency ($WUE=GPP/ET$). Specifically, by doubling the actual atmospheric CO_2 concentrations (+400 ppm), larger increases in GPP were found for the grass in the deep groundwater scenario (from 632 to 1208 gC m^2 y^{-1}; +91%) and for the trees when groundwater was shallow (from 680 to over 1164 gC m^2 y^{-1}; +71%). Overall, the increases in WUE were 59% and 74% in the shallow groundwater scenario and 71% and 67% in the scenario without groundwater, for grass and trees, respectively. When they did not have access to groundwater, trees were more sensitive to rainfall

variability, i.e., a decrease in rainfall (-15%) led to -27% of T_T, while its increase (+15%) led to +26% of T_T; the same variations occurred in the GPP_T. Grass cover appeared to be more sensitive to rainfall variability for shallow WT depths. In particular, a decrease in rainfall (-15%) led to -20% of T_G and GPP_G, while its increase (+15%) generated a 23% increase of T_G and GPP_G.

Simulations in the shallow groundwater scenario at Alex Wilkie indicated that transpiration from trees and shrubs decreased when temperatures increased from the actual value (control simulation) to +4°C, leading to -52% for T_T and -40% for T_S; at the same time, grass transpiration increased (+24%) (Figure 5.9a). Without groundwater (Figure 5.9d), T_G remained fairly constant as the temperatures increased, while T_T and T_S exhibited a behavior consistent with the shallow groundwater scenario (-43% and -15%, respectively). Overall, simulations indicated that grass and shrubs could cope quite well with T_a increases, in particular when the WT was within the reach of shrubs roots, with β_G remaining constant and β_S decreasing by 1%. Without the groundwater support, trees suffered most from the increases in T_a, with β_T decreasing by 13% (Figure 5.9b). In terms of vegetation productivity, trees were more susceptible to temperature increases than shrubs and grass, with GPP_T decreasing from 483 to 359 gC m^2 y^{-1} and from 295 to 137 gC m^2 y^{-1} for the shallow and no groundwater scenarios, respectively. Conversely, shrubs were affected very little by the changes in T_a, increasing by 1% when the WT is shallow and decreasing by 8% without groundwater (Figures 5.9c and 5.9f).

Similarly to National Drive, simulations for Alex Wilkie showed that changes in atmospheric CO_2 concentrations mainly influenced plant transpiration and productivity, thus affecting plant WUE. Higher increases in GPP were found for trees, shrubs, and grass in the deep groundwater scenario, i.e., +63%, +27%, and +45%, respectively. Without groundwater, a decrease in rainfall considerably affected an already stressed ecosystem, leading to a reduction in T_T (-29%), T_S (-17%), and T_G (-15%). In contrast, a rainfall increase of 15% had a positive impact on trees, shrubs, and grass transpiration (+27%, +15%, and +16%, respectively).

5.4 Discussion

5.4.1 Dependence on groundwater

The results of the numerical experiments showed how the presence of the WT or its capillary fringe within the root zone supported urban ecosystems against inter-annual rainfall

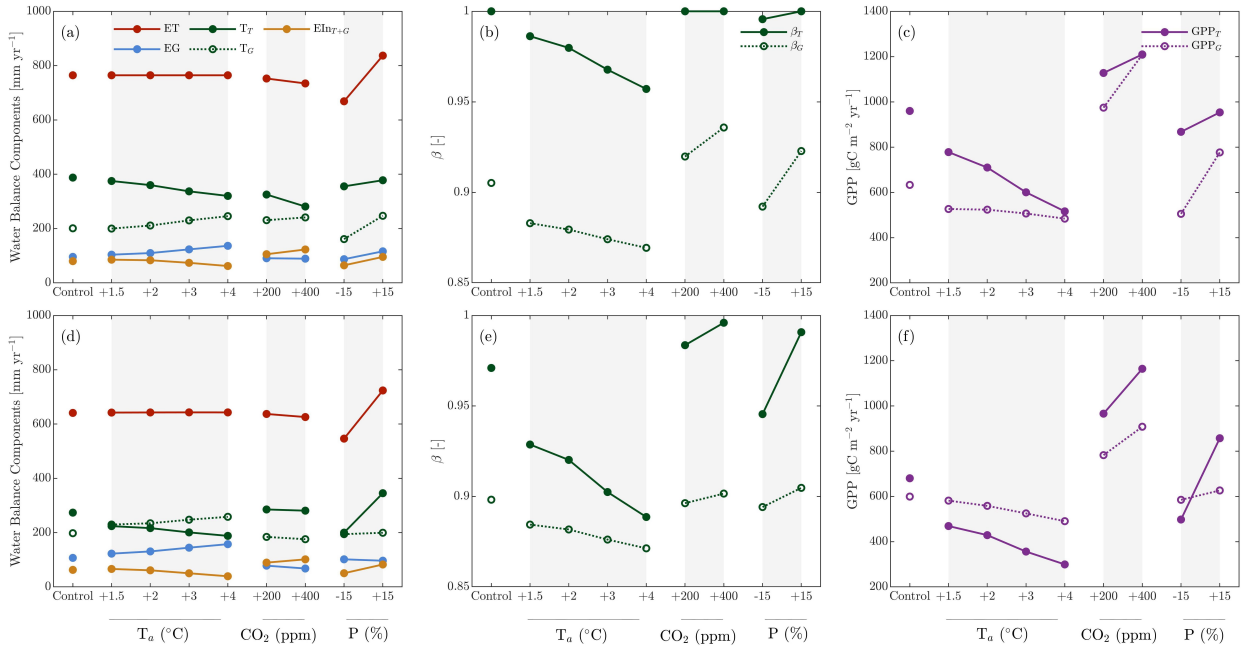

Figure 5.8: (a)-(f) Effects of altered environmental drivers at National Drive for two different groundwater availability scenarios: (a)-(c) shallow groundwater (i.e., depth to groundwater at 6.9 m, corresponding to a net lateral flow of 126 mm y^{-1}) and (d)-(f) without groundwater (i.e., groundwater beneath the soil domain, corresponding to a net lateral flow of 0 mm y^{-1} and free drainage to the bottom of the soil domain). Simulation results show (a, d) water balance components (symbols as in Figure 5.5), (b, e) plant water stress (β), and (c, f) gross primary productivity (GPP; for unit of total ground area) for the actual climate and eight climate scenarios: four scenarios of increased air temperature T_a (+1.5 °C, +2.0 °C, +3.0 °C, +4.0 °C), two scenarios with increased atmospheric CO_2 concentrations (+200 ppm, +400 ppm), and two different rainfall (P) scenarios (+15% and -15%).

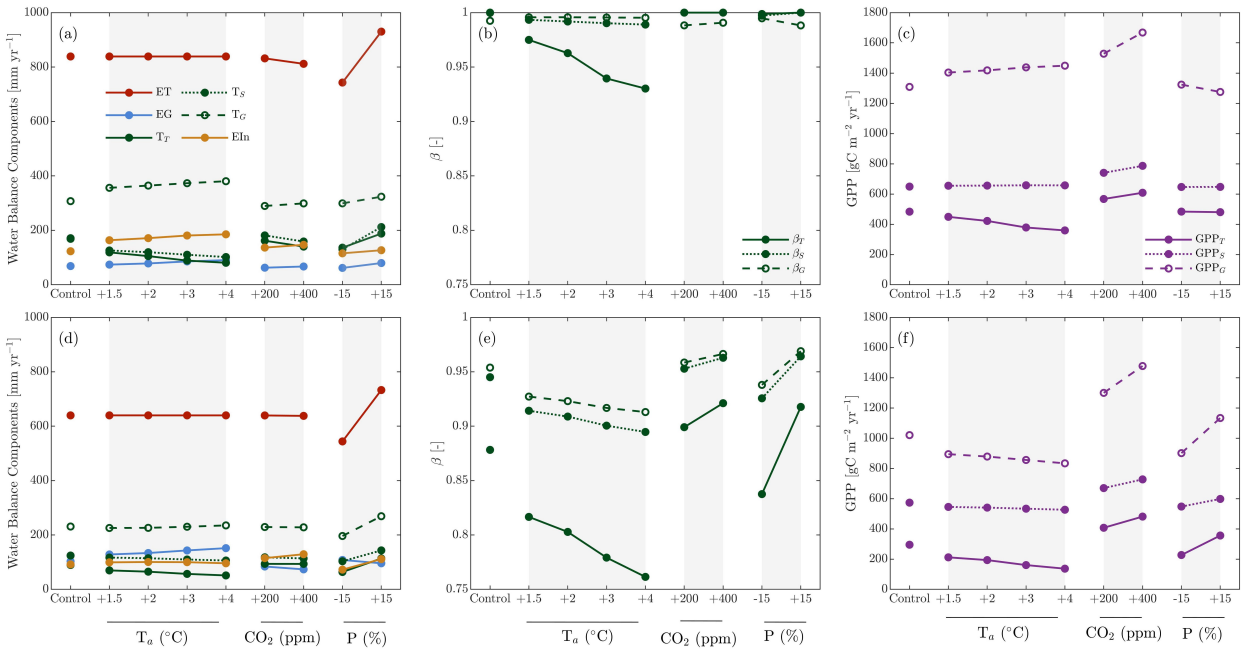

Figure 5.9: (a)-(f) Effects of altered environmental drivers at Alex Wilkie for two different groundwater availability scenarios: (a)-(c) shallow groundwater (i.e., depth to groundwater at 3.9 m, corresponding to a net lateral flow of 200 mm y^{-1}) and (d)-(f) deep groundwater (i.e., groundwater beneath the soil domain, corresponding to a net lateral flow of 0 mm y^{-1} and free drainage to the bottom of the soil domain). Simulation results show (a, d) water balance components (symbols as in Figure 5.5), (b, e) plant water stress (β), and (c, f) gross primary productivity (GPP; for unit of ground area) for the actual climate and eight climate scenarios: four scenarios of increased temperature T$_a$ (+1.5 °C, +2.0 °C, +3.0 °C, +4.0 °C), two scenarios with increased atmospheric CO$_2$ concentrations (+200 ppm, +400 ppm), and two different rainfall (P) scenarios (+15% and -15%).

variability. Groundwater availability was also found to have a pivotal role in helping plants soften the impacts of increased air temperature and atmospheric CO_2 concentrations, as well as buffering the effects of local rainfall decrease. The presence of a shallow WT as well as the seasonal and inter-annual variations in WT depths arise from the variable balance between P, ET, and net lateral subsurface flow (q). Simulations showed that both National Drive and Alex Wilkie needed a considerable groundwater inflow at catchment scale to maintain the observed WT beneath the root zone, i.e., 126 mm yr^{-1} and 200 mm yr^{-1} at National Drive and Alex Wilkie, respectively, which is roughly 20-30% of annual rainfall. These values of q led to a WT depth (expressed as mean value for the 19 year period of analysis) of 6.9 m and 3.9 m for National Drive and Alex Wilkie, respectively, leading to an increase in total ET of 19% and 31% respectively. These levels of groundwater were sufficient to minimize the water stress and maximize plant productivity. Such result also highlighted the importance of including groundwater in ecohydrological analysis, given their essential role in controlling plant water stress in certain ecosystems (Brolsma and Bierkens, 2007; Brolsma et al., 2010).

Simulations indicated that woody plants overall transpired more (+42% at National Drive and +90% at Alex Wilkie, Figure 5.5) in scenarios where the WT depth was maintained within the reach of the plant roots. This was experimentally confirmed at the two study sites, where shallow WT depths were found to support transpiration during dry months as well as hot days and nights (Marchionni et al., 2019a). The fact that groundwater represents such a large source of the water needed for trees is consistent with the results from previous studies on groundwater dependent vegetation. Using stable isotope analysis or water balance methods, it has been shown that the contribution of groundwater to the total transpiration in seasonally dry ecosystems can range from 15% up to 100% (Orellana et al., 2012). As groundwater approaches the soil surface, the strong capillary rise from the shallow WT also enhances the amount of water transpired by grasses (Soylu et al., 2011), as reflected in the model results here.

At National Drive, the high water-holding capacity of clay soil played a crucial role in amplifying the capillary rise even with an average WT 2.7 m below the soil surface, thus increasing grass transpiration by 46%. At Alex Wilkie, where the soil is predominantly sandy and the capillary fringe is practically absent, the WT needed to be almost within the grass roots (<1m) in order to enhance significantly grass transpiration. At both sites, the trajectories of GPP with groundwater availability followed patterns similar to transpiration for all the vegetation types. As the WT deepened, declines in GPP were predicted in trees, shrubs, and grass, with trees experiencing a more consistent increase in water stress and hence a reduction in GPP relative to grass. In particular, tree productivity decreased by

about 40% (National Drive) and 64% (Alex Wilkie) when the WT was assumed to be out of reach (absent) compared to the reference WT scenario.

5.4.2 Vegetation competition

Results from this study indicate that the presence of groundwater strongly affects the competition for water between woody plants (i.e., trees and shrubs) and grasses. Differences in terms of rooting depth and tolerance to low water potentials are critical for plant water access, canopy transpiration, and carbon assimilation, thus allowing for coexistence of woody plants and grasses (Eggemeyer et al., 2009). Shallow-rooted grass species only access soil moisture in the shallow soil layers, while trees and shrubs have access to the water in both shallow and deep soil layers (Kim and Eltahir, 2004; Rossatto et al., 2012). When groundwater is available, these differences in rooting and water uptake depths help buffer the competition for water (Grossiord et al., 2018). When the WT depth falls below a certain threshold level, capillary rise from the WT becomes inadequate to supply moisture to the woody plants, affecting their productivity and competitive performance. This can be noticed especially at Alex Wilkie, where, in addition to the higher species competition (i.e., coexistence of trees, shrubs, and grass), the effects of declining groundwater were more severe due to the sandy soil and low water-holding capacity. Therefore, trees were more stressed at Alex Wilkie compared to National Drive when the WT is beneath their root zone, suggesting that the water status and competitiviness of vegetation may differ significantly depending on soil type (Naumburg et al., 2005). Overall, grasses appeared less affected by groundwater fluctuations than woody plants in all scenarios, because grasses rely on rainfall rather than groundwater resources. Groundwater drawdown can benefit grasses because of a reduced competitive capability of the other vegetation types. Furthermore, unlike trees and shrubs, which try to maintain a consistent leaf-area strongly regulating stomata (McDowell et al., 2008), grasses wilted reducing their leaf-area and became almost inactive during dry periods.

5.4.3 Millennium Drought

During the Millennium Drought between 2001 and 2009, grass was more tolerant to changes in soil water availability (Craine et al., 2013). Even in such a prolonged dry period, trees and shrubs reliance on groundwater was sufficient to largely support ecosystem productivity and transpiration to levels similar to normal years. When, in addition to the rainfall shortage, a possible reduction in the groundwater flow towards the sites and thus a decrease in the WT depth were imposed, trees started showing signs of stress, manifested by a reduction in

LAI, especially as drought conditions intensified between 2007 and 2009. The extremely dry sandy soil at Alex Wilkie did not provide any buffer to the groundwater drawdown, which was instead simulated at National Drive. After the Millennium Drought, a higher than average rainfall in 2010 in many parts of southeast Australia helped trees to recover from the water stress (van Dijk et al., 2013). However, simulations showed a full tree recovery only 5-6 years later, suggesting long-term impacts on vegetation due to groundwater depletion combined with drought conditions.

5.4.4 Changing climate

Groundwater availability was also found to have remarkable implications for ecosystems under different climatic conditions. The focus here was to explore the role of groundwater in affecting ecosystem response to a single stressor, such as higher air temperatures, increased atmospheric CO_2 concentrations, and different rainfall regimes. When subjected to warmer air temperatures, both urban reserves exhibited altered hydrologic regimes, especially when groundwater was out of reach. Although an increase in air temperature did not affect total evapotranspiration, it strongly affected its partitioning, in particular at National Drive, triggering an active competition for water sources between vegetation types. In all simulations, grass appeared to be able to cope better with increased temperature and maintain its transpiration and productivity levels. Without groundwater, the root water uptake also changed, thus resulting in higher competition for shallow soil water, as also shown by Grossiord et al. (2018). In these scenarios, grass was able to cope with modified conditions better than trees, profiting from the fact that the trees were more stressed. Already stressed by the lack of groundwater sources, trees quickly worsened their water stress under the warming climate. This was more evident at Alex Wilkie, where the low soil water-holding capacity did not help to buffer the decline in groundwater. Warmer temperatures also contribute to lower photosynthesis rates (GPP), confirming that a warming climate combined with limited water availability reduces vegetation productivity (Grossiord et al., 2017). In response to increased atmospheric CO_2, plants were able to photosynthesize with a lower stomatal conductance and thus with lower transpiration rates, leading to increased WUE, as expected (Keenan et al., 2013; Frank et al., 2015; Mastrotheodoros et al., 2017), regardless of the groundwater availability. This finding confirms that the high-CO_2 environment expected for the future may partially alleviate water stress through increased WUE (Conley et al., 2001; Swann et al., 2016).

5.5 Summary

In this chapter a mechanistic ecohydrological model was used to simulate different scenarios of groundwater availability in two of the three urban reserves that are part of this project. Results from the numerical simulations confirmed that these ecosystems strongly depend on groundwater, with woody plants (trees and shrubs) transpiring more than 40% when the WT was maintained within the reach of the plant roots, when compared to scenarios without groundwater. The fact that groundwater represented such a large source of water for these ecosystems emphasizes their vulnerability to its depletion, which could result in reductions of plants transpiration (-56%) and productivity (-45%), and in extreme cases, in drought-induced mortality (Eamus et al., 2015). Therefore, to be effective a proper management of urban ecosystems should also account for catchment scale subsurface water dynamics. The most significant impacts of declining groundwater occurred in predominantly sandy soils because of their lower water-holding capacity compared to clay soils.

Changes in environmental variables, such as increased air temperature and atmospheric CO_2 concentrations as well as a rainfall reduction, were found to alter ecosystems hydrologic regime and the competition among vegetation types, especially when groundwater was not available. These findings suggest that groundwater has a pivotal role in sustaining urban reserves, and even more so during major droughts or changes in climate.

Human-induced land use change combined to a rapidly changing climate might threaten groundwater availability, with possible profound impacts on the conservation of natural urban ecosystems. Hence, extensive groundwater monitoring networks and robust quantifications of vegetation responses to groundwater depletion and climate variability, as computed here by means of ecohydrologic simulations, are crucial to evaluate appropriate management practices.

Chapter 6

Ecohydrological Effects of Management

This chapter is largely from the research paper **"Ecohydrological modelling for urban reserves management"** to be submitted to *Landscape and Urban Planning*.

The chapter investigates how different vegetation cover and irrigation scenarios might affect hydrological fluxes and vegetation productivity in one of the three study sites, Napier Park. Napier Park was chosen for this analysis because of the extensive irrigation system already in use that covers about 85% of the reserve. Results are obtained using the model Tethys-Chloris. The model is calibrated and confirmed to reproduce, at the reserve-scale, the soil water content observed in several locations within the reserve where soil moisture probes were installed (Figure 3.6d). A series of numerical experiments are then designed to simulate different vegetation cover and irrigation scenarios. In particular, the sensitivity to different vegetation covers is simulated by imposing different percentages of tree cover (10%, 20%, and 30%), while three different irrigation scenarios are imposed by increasing the duration fo each rainfall event by 1, 2, and 3 hours. Results show that irrigation might have helped trees soften the impacts of the Millennium Drought (2001-2009), decreasing the losses of the water store within the entire soil domain.

6.1 Introduction

Worldwide, cities are facing issues associated with rapid environmental changes. The increase in the number of extreme weather events, such as floods and droughts, and the more frequent and severe heat waves, often exacerbated by the presence of the urban heat island (UHI), have dramatic and costly impacts on cities' services and infrastructure as well as the quality of life of urban residents. At the same time, cities are recognized to be major contributors to global environmental changes, mainly because of their impacts on water and energy fluxes, and their greenhouse gas emissions. In this context, there is a growing interest in the creation of green-blue cities in which green (e.g., trees and parks) and blue assets (e.g., stormwater harvesting) can help make cities more resilience to the negative impacts of both urbanization and climate change.

City dwellers can benefit from the presence of urban green spaces. Their role in promoting ecosystem health and resilience, contributing to biodiversity conservation, and enhancing urban ecosystem functionality through the provision of ecosystem services is well known, as extensively described in section 2.2. However, to be able to effectively deliver this full range of benefits, urban green spaces are typically managed assets in the urban landscape. Among the management practices, irrigation plays a crucial role in supporting vegetation and soil health. Especially in arid and semi-arid regions, the coexistence of remaining native vegetation and introduced non-native species may create unique biotic communities highly dependent on irrigation (McCarthy and Pataki, 2010; Pataki et al., 2011a).

The use of technologies and approaches, such as low impact development (LID), water sensitive urban design (WSUD), and sustainable urban drainage systems (SUDS), can provide precious sources of water for supporting urban green spaces, while providing benefits to downstream receiving environments (e.g., Fletcher et al., 2015). Among these technologies, also known as blue-green infrastructure, stormwater harvesting systems provide numerous benefits, including the water retention within the urban landscape to provide water for irrigation during periods of water restriction, the reduction of stormwater pollutant loads to urban water bodies, and the shift of the hydrological cycle closer to pre-developed conditions, only to name a few (e.g., Poff, 1997; Hamel et al., 2013; Coutts et al., 2013b).

The need for irrigation to maintain ecosystems health and biodiversity may be intensified by increasing drought and extreme heat events, which in turn exacerbate the pressure on water resources, already strongly impacted by the climatic trends and population growth. In this context, there is the need for a better understanding of the potential benefits of using blue-green infrastructure. Other actions may include the choice of appropriate irrigation

practices, irrigation-scheduling depending on plant water demands, and water-conserving landscape designs (Pataki et al., 2011b; Volo et al., 2014; Litvak and Pataki, 2016; Breyer et al., 2018). McCarthy et al. (2011), for instance, suggested the water-use efficiency (WUE) (i.e., the ratio of water used in plant metabolism to water lost by the plant through transpiration) as a measurable indicator of the trade-off between the water use and the ecosystem services related to the growth rate to help maximizing the growth while conserving water.

These issues are particularly relevant in southeast Australia where the recent Millennium Drought have resulted in below median rainfall since at least 1900 (van Dijk et al., 2013), reductions in vegetation biomass (Sawada and Koike, 2016), and prolonged water restrictions. In the Melbourne metropolitan area, for example, more than a decade of severe water restrictions and periods of extreme heat resulted in declining vegetation health recorded both during the drought and in the following years. These events led to plan and design several green-blue infrastructure across the Melbourne metropolitan area to improve water resources management and liveability.

Napier Park, one of the urban reserves included in this study, is a good example of this. As previously described in section 3.1.3, Napier Park is equipped with an extensive irrigation system covering about 85% of the reserve that uses stormwater harvesting from an upstream urbanized catchment of about 16.3 ha to recharge the soil stores throughout the site. The stormwater harvesting and irrigation system was design to include a vegetated swale that conveys the event based flows (whenever there is rainfall resulting in runoff from the upstream drainage catchment) into an underground storage tank; from the tank, at the end of each rainfall event, the water is pumped to supply the reticulated distribution system throughout the reserve. Recharge bores (30 cm diameter; 45 cm depth) are used as part of the irrigation distribution network to promote direct infiltration into the clay layer at 50 cm. The irrigation strategy is based on increasing the volume of each rainfall event by lengthening the duration of each rainfall event up to 3 hours. Irrigation started irregularly in January 2016, becoming more consistent towards the end of the same year.

To quantify the benefits of such design in terms of hydrological fluxes and vegetation productivity, a series of numerical experiments were carried out using the ecohydrologycal model Tethys-Chloris. Different vegetation cover and irrigation scenarios as well as the impacts of the Millennium Drought were investigated. Results from this study are expected to improve the understanding of how urban reserves, and more in general urban green spaces, can be effectively managed ensuring both vegetation health and water savings.

6.2 Model setup

The ecohydrological model Tethys-Chloris (Section 3.3) was calibrated to reproduce, at the reserve-scale and at hourly time steps, soil water dynamics observed in several locations within the study site (Figure 3.6d). Specifically, the probes SM1, SM2, and SM3 were used for this task (Figures 6.1a-c); on the contrary, the probes SM4, SM5, and SM6 were not considered due to the absence of vegetation in their surroundings as well as data gaps and anomalies in the time series (Figures 6.1d-f).

The 1-D soil domain was assumed to be limited to 1.8 m with a stratigraphy that follows the one that was measured during the site investigation works between March and April 2010 and layers progressively coarsening with depth; soil hydraulic parameters were obtained through the *van Genuchten* model (Van Genuchten, 1980; Carsel and Parrish, 1988) (Table 6.1).

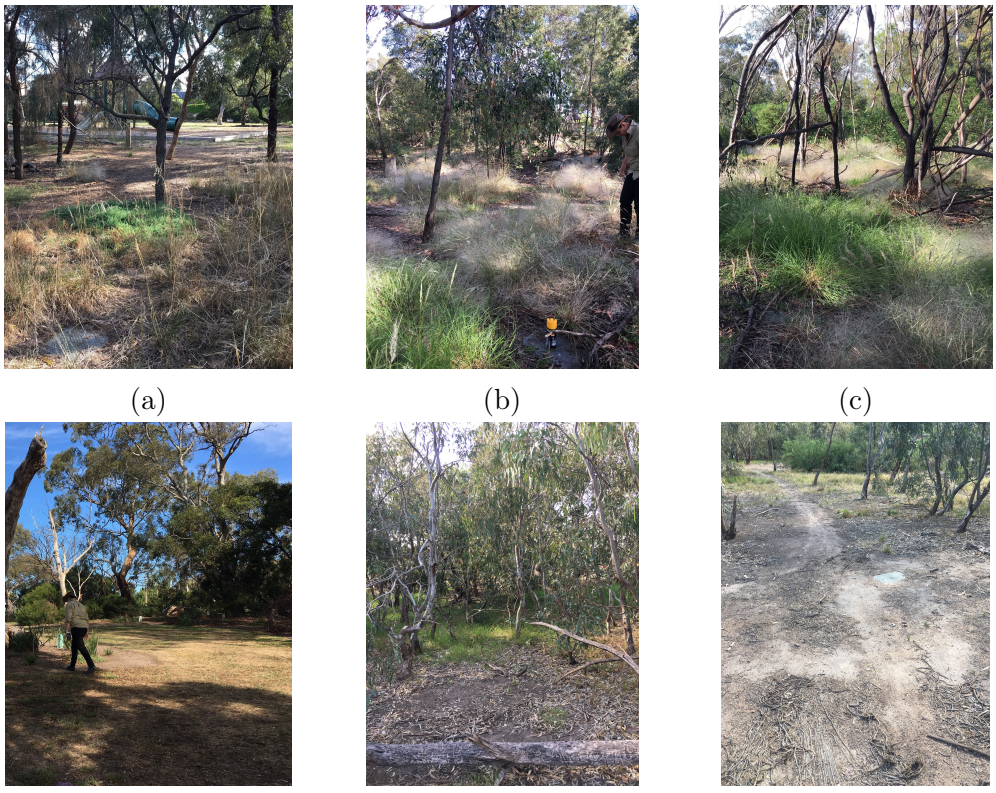

Figure 6.1: Vegetation cover surrounding the soil moisture probes (a) SM1, (b) SM2, (c) SM3, (d) SM4, (e) SM5, and (f) SM6.

Table 6.1: Main soil parameters used in the simulations.

Depth (m)	**Soil Discretization**	***van Genuchten* coefficients** (θ_s, θ_r, α, **n**)	**Saturated hydraulic conductivity**[(a)] ($\mathbf{k_s}$; **mm h**$^{-1}$)
0.0-0.4	Sandy Silt	0.30, 0.09, 0.020 mm^{-1}, 1.70	80
0.4-1.8	Clay	0.57, 0.20, 0.0006 mm^{-1}, 1.10	0.10

[(a)] Saturated hydraulic conductivity is assumed variable with depth as: k_s=-15.39 ln(z)+115.43 [mm h^{-1}]

Table 6.2: Main vegetation parameters used in the simulations.

Parameter	**Unit**	**Trees**	**Grass**
$Z_{R,50}$	m	0.50	0.15
$Z_{R,95}$	m	1.60	0.30
h_c	m	20.00	0.10
a_1	-	8.00	7.00
ψ_{S2}	MPa	-0.10	-0.07
ψ_{S50}	MPa	-1.50	-0.15
S_L	m^2/gC	0.009	0.016
r	gC/gN/d	0.042	0.038
$A_{L,cr}$	d	365	180
d_{mg}	d	20	20
T_{rr}	gC/m^2/d	1.00	2.50
L_{tr}	-	0.80	0.40
ϵ_{ac}	-	0.60	0.50
$1/K_{lf}$	d	40	40
$V_{c,max25}$	-	45	54
r_{JV}	-	2.00	2.10

$Z_{R,50}$: root depth 50 percentile, $Z_{R,95}$: root depth 95 percentile, h_c: canopy height, a_1: empirical parameter connecting stomatal aperture and net assimilation, ψ_{S2}: water potential at 2% stomatal closure, ψ_{S50}: water potential at 50% stomatal closure, S_L: specific leaf area, r: respiration rate at 10°C, $A_{L,cr}$: critical leaf age, d_{mg}: days of maximum growth, T_{rr}: translocation rate from carbohydrate reserve, L_{tr}: leaf to root biomass maximum ratio, ϵ_{ac}: parameter for allocation to carbon reserves, $1/K_{lf}$: dead leaf fall turnover, $V_{c,max25}$: maximum Rubisco capacity at 25°C leaf level, r_{JV}: scaling J_{max}- $V_{c,max}$.

During calibration and confirmation, the PFTs grass and trees were considered covering 80% and 10% of the reserve, respectively, while the remaining 10% was considered as bare soil. These fractions were based on local observations of the areas in which soil moisture profiles were monitored, as shown in Figure 6.1. To describe the root depth distribution, a linear dose response profile was used (Collins and Bras, 2007). This required the specification of the rooting depth that contains 50% and 95% of fine root biomass ($Z_{R,50}$ and $Z_{R,95}$). Free-drainage conditions were assigned at the bottom of the soil domain. Vegetation parameters (Table 6.2) were chosen based on literature and model experience (Fatichi and Pappas, 2017).

Performance in reproducing soil water dynamics in the first 1.2 m of the soil domain was tested against the observations for the 12 month period between June 2015 and June 2016; the model was then confirmed for the 12 month period between June 2016 and June 2017. The atmospheric forcing consisted of meteorological data collected at the Melbourne Airport

weather station (no. 086282). Initial condition of soil moisture and vegetation carbon pool for the calibration simulations were generated by running a 9 months (i.e., between September 2014 and June 2015) spin-up simulation starting from soil moisture conditions coinciding with field capacity at the bottom of the clay layer and a linear soil water potential with no flux within the soil domain.

As shown in Figure 6.2, the model was able to reproduce the magnitude and timing of the volumetric soil moisture. Overall, a satisfactory match between observed and simulated soil water dynamics was achieved after tuning soil hydraulic properties (Table 6.1) and root depths (Table 6.2) for both calibration and confirmation periods (Figure 6.3).

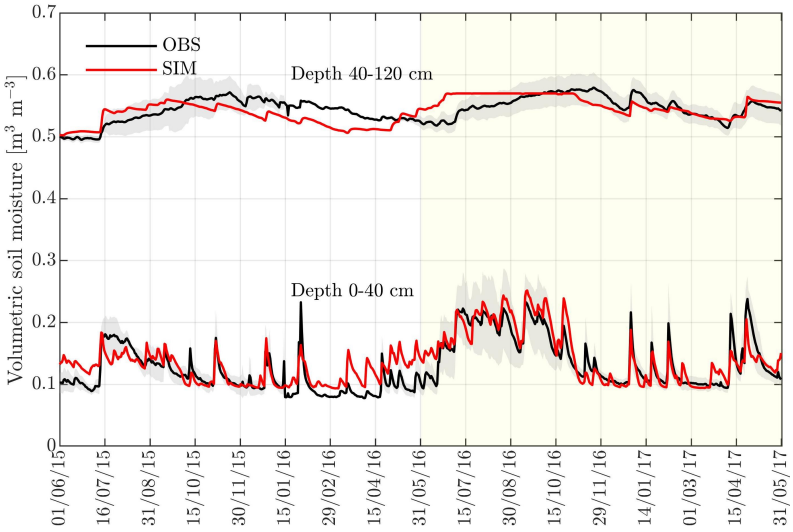

Figure 6.2: Simulated and observed volumetric soil moisture in the calibration and confirmation (yellow area) periods at depths of 0-40 cm and 40-120 cm. Observed volumetric soil moisture is represented as the mean values (± SD; grey areas) from the probes SM1, SM2, and SM3.

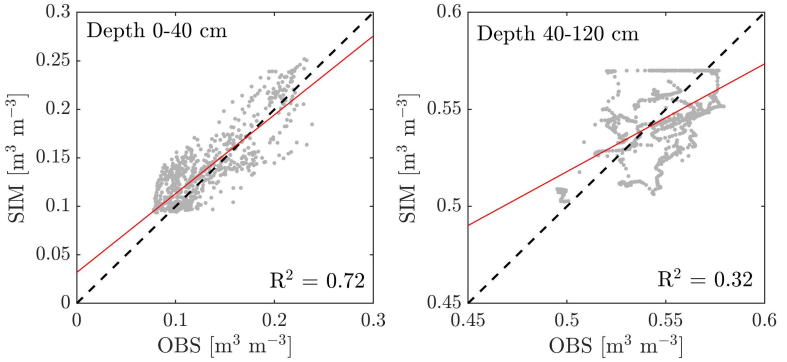

Figure 6.3: Simulated and observed volumetric soil moisture in the calibration and confirmation periods at depths of 0-40 cm and 40-120 cm.

6.3 Design of the experiment

A series of numerical experiments were designed to investigate the effects of vegetation cover and irrigation scenarios on hydrological fluxes and vegetation productivity. Simulations were carried out from 1 July 1999 to 30 June 2018 using the long-term time series of data available at the Melbourne Airport weather station as meteorological forcing.

The sensitivity to different vegetation covers was analyzed by imposing different percentages of tree cover (i.e., 10%, 20%, and 30%); the increase in tree cover was obtained by decreasing the percentage of grass cover while the percentage of bare soil cover (i.e., 10%) was maintained constant throughout all simulations, as shown in Table 6.3. Among the selected vegetation cover scenarios, the tree cover of 20% can be assumed as representative of the overall tree cover of the reserve based on local observations of tree density.

According to the design of the irrigation system at Napier Park, irrigation strategy was set to increase the length of each rainfall event by up to 3 hours with an application rate of 0.5 mm/h applied at a depth of 50 cm below the ground surface. Specifically, three different scenarios with duration of each rainfall event increased by 1, 2, and 3 hours were imposed for an annual average of additional rainfall to the site of about 98, 197, and 295 mm/y, respectively. A further scenario with no irrigation was also considered, for a total of four scenarios for each vegetation cover (Table 6.3).

In all simulations, free-drainage conditions were assigned at the bottom of the soil domain. Soil moisture and vegetation carbon pool initial conditions were generated by running a spin-up simulation of 19 years, starting from the soil at field capacity at the bottom of the clay layer and a linear water potential with no flux within the soil domain.

Table 6.3: List of the numerical experiments used for testing the effects of irrigation scenarios for different vegetation cover. The annual average of the additional water to the site is also specified for each irrigation scenario (mm/y).

Vegetation Scenarios			**Irrigation Scenarios**			
% Grass	**% Bare Soil**	**% Trees**	**No irrigation**	**+1h**	**+2h**	**+3h**
80	10	10				
70	10	20	0	98	197	295
60	10	30				

6.4 Results and Discussion

6.4.1 Effects on hydrological fluxes

The simulated effects of different vegetation cover and irrigation scenarios on hydrological fluxes are shown in Figure 6.4, expressed as mean values of the 19 years analyzed.

Overall average total evapotranspiration strongly increased with the percentage of tree cover (+26% with 30% of tree cover compared to the scenario with 10% of tree cover; Figure 6.4a), mainly in response to the increase in tree transpiration (+156% with 30% of tree cover compared to the scenario with 10% of tree cover; Figure 6.4c). In terms of irrigation scenarios, tree transpiration was found less affected than grass transpiration by the amount of water available through irrigation (Figure 6.4b and Figure 6.4c). Ground evaporation decreased of about 6% with increasing tree cover, while it increased of about 18% with increasing irrigation (Figure 6.4d).

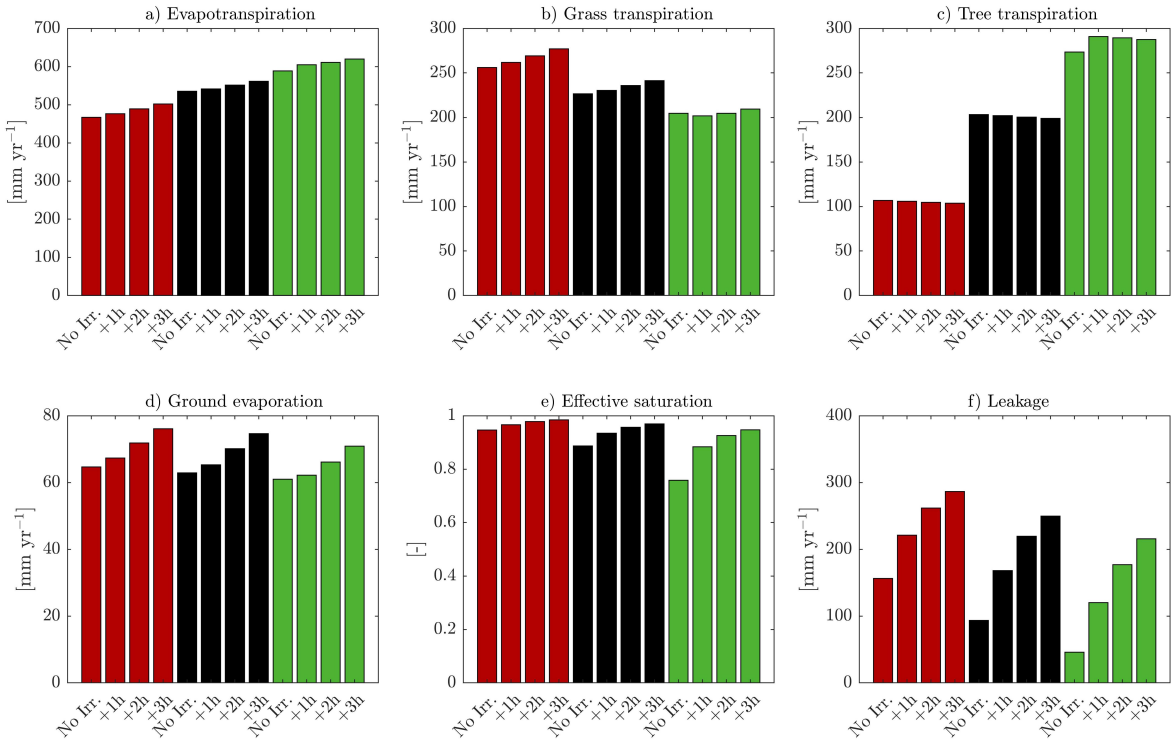

Figure 6.4: Sensitivity of hydrological fluxes to vegetation cover scenarios, i.e., 10% (red bars), 20% (black bars), and 30% (greens bars) tree cover, and irrigation scenarios, i.e., No Irrigation, +1h, +2h, and +3h, over the simulation period of 19 years (July 1999-June 2018). (a) Evapotranspiration, (b) Leakage from the bottom of the soil domain, (c) Ground evaporation, (d) Effective saturation, (e) Grass transpiration, and (f) Tree transpiration.

The vertically integrated effective saturation in the clay layer (i.e., from 0.4 m to the bottom of the soil domain) was influenced mainly by the irrigation with the tree cover appearing to have milder impact especially when irrigation was considered (Figure 6.4e). In particular, highest values of effective saturation were obtained regardless of the irrigation scenario for the 10% tree cover, mainly because grass roots do not have access to the water stored in the clay layer. However, most pronounced impacts of irrigation were obtained for the 30% tree cover scenario. Leakage from the bottom of the soil domain (Figure 6.4f) was strongly influenced by both the tree cover and the amount of water available through irrigation. Specifically, leakage increased of about +80%, +180%, and +370% for a +3h irrigation scenario compared to the scenario with no irrigation when tree cover was set to 10%, 20%, and 30%, respectively, whereas it decreased of about 40% and 70% when tree cover was set to 20% and 30%, respectively, compared to the scenario with 10% of tree cover (Figure 6.4f).

Analyzing the annual changes in evaporation, transpiration, leakage from the bottom of the soil domain, runoff, and soil water storage for the 19 years simulated (Figure 6.5), results showed overall higher values of evaporation and transpiration when irrigation is considered. Benefits of irrigation can also be noticed in the lower losses in the soil water storage, especially during the Millennium Drought between 2001 and 2009. In particular, during the driest years, i.e., 2003 and 2007, results showed that irrigation increased the recharge of the soil store, thus helping both trees and grass to maintain their transpiration rates. When a +3h irrigation scenario was considered, as shown in Figure 6.5d, excess water was mostly lost through leakage from the bottom of the soil domain and runoff. Accordingly, a threshold value for the irrigation can be set with regards to the +2h irrigation scenario. Once this threshold was exceeded, adding further water through irrigation did not increase the soil water storage but rather it was lost through leakage from the bottom of the soil domain and runoff, in particular during very wet years (e.g., 2011).

These results highlighted the pivotal role of irrigation in supporting tree transpiration, also helping trees soften the impacts of the Millennium Drought as well as decreasing the losses of the water store within the entire soil domain.

6.4.2 Effects on vegetation productivity

To explore the simulated effects of different vegetation cover scenarios and the Millennium Drought (2001-2009) on vegetation productivity, the time series of annual values of gross primary productivity (GPP), leaf area index (LAI), and plant water stress (β) are presented for the scenario without irrigation with respect to the 10%, 20%, and 30% tree cover (Fig-

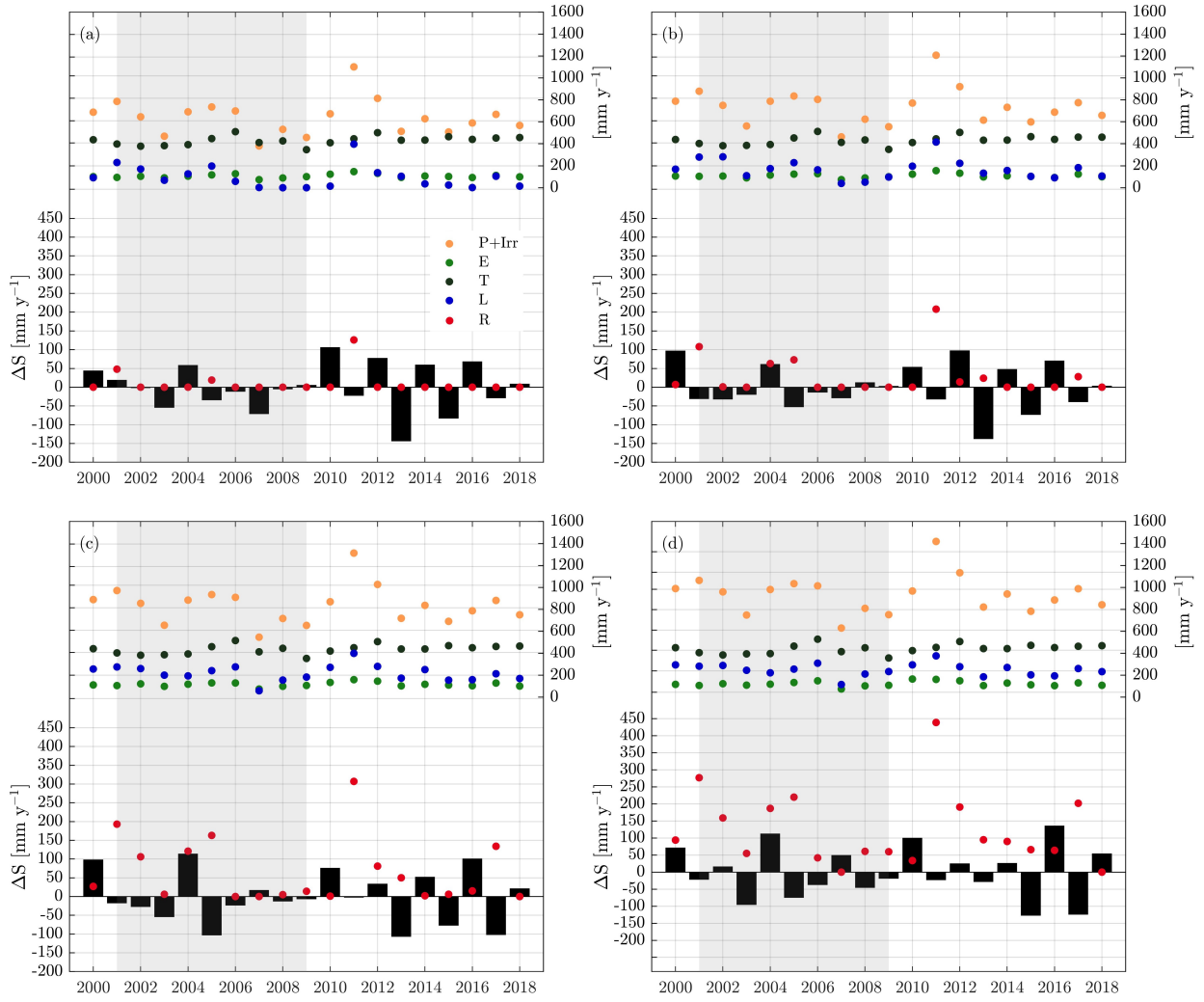

Figure 6.5: Simulation results for the 19 year period (July 1999-June 2018) showing annual changes in the water balance components, i.e., rainfall and irrigation (P + Irr), evapotranspiration, i.e., evaporation from interception by canopy and ground evaporation (E), transpiration, i.e., grass and tree transpiration (T), leakage from the bottom of the soil domain (L), runoff (R), and soil water storage (ΔS). Results correspond to a tree cover of 20% and irrigation scenarios, i.e., (a) No Irrigation, (b) +1h, (c) +2h, and (d) +3h. Grey regions indicate the period of the Millennium Drought.

ure 6.6). For this analysis, GPP and LAI are shown in terms of unit of vegetated area instead of weighted and integrated over the entire vegetated area (as the results were reported in chapter 5) in order to be able to compare the results irrespective of the percentages of tree and grass covers.

Results suggest that tree productivity was negatively affected by the increased tree cover; in particular, during dry years trees reduced their GPP by -24% in 2007 and -21% in 2016 for

the 30% tree cover scenario (Figure 6.6c) compared to the scenario with a tree cover of 10% (Figure 6.6a). On the contrary, grass showed overall higher GPP with increasing tree cover. Similar patterns were found in terms of LAI for both grass and trees, with small variations of LAI for trees across all scenarios. Overall, trees coped well with the drought with respect to the 10% tree cover scenario; however, with respect to the 30% tree cover scenario, trees appeared more stressed as drought intensified between 2007 and 2009, reaching the lowest plant water stress (i.e., 0.90) in 2007 (Figure 6.6i). On the contrary, grass showed a strongly variable LAI during the simulated period with respect to all vegetation cover scenarios, reducing LAI by -37%, -39%, and -25% in 2009 compared to the beginning of the drought in 2001 with respect to the 10%, 20%, and 30% tree cover, respectively.

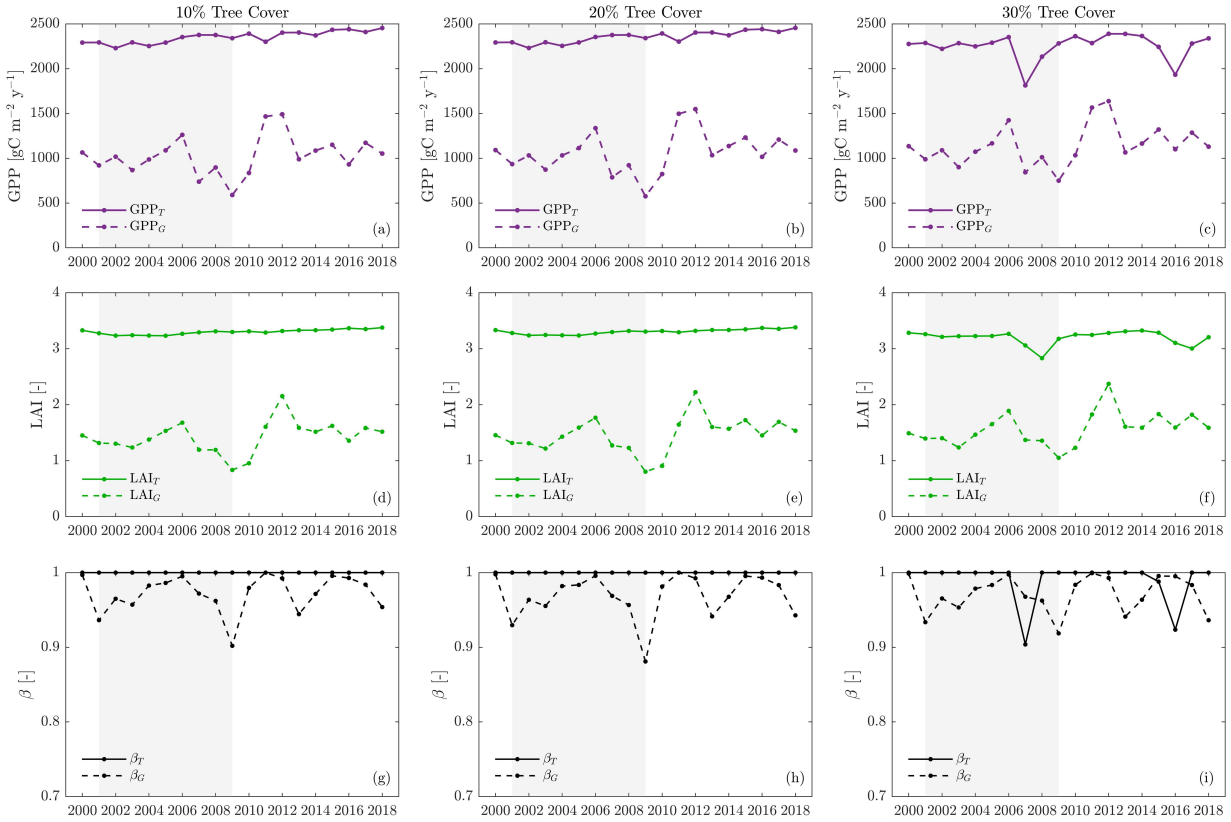

Figure 6.6: Simulation results for the 19 year period (July 1999-June 2018) corresponding to tree covers of 10% (a, d, g), 20% (b, e, h) and 30% (c, f, i) without irrigation. (a-c) Total annual values of gross primary productivity (GPP; for unit of vegetated area) for trees (GPP_T) and grass (GPP_S). (d-f) Mean annual values of leaf area index (LAI; for unit of vegetated area) for trees (LAI_T) and grass (LAI_S). (g-i) Mean annual values of plant water stress for trees (β_T) and grass (β_S). Grey regions indicate the period of the Millennium Drought.

When an increase in soil water availability was considered through irrigation (Figure 6.7), vegetation dynamics differed considerably from the scenario without irrigation. Irrigation helped trees to overall increase their productivity and LAI, especially during the driest years, as well as to cope better with a prolonged drought period, thus allowing trees to maintain unstressed values of β (Figure 6.7f).

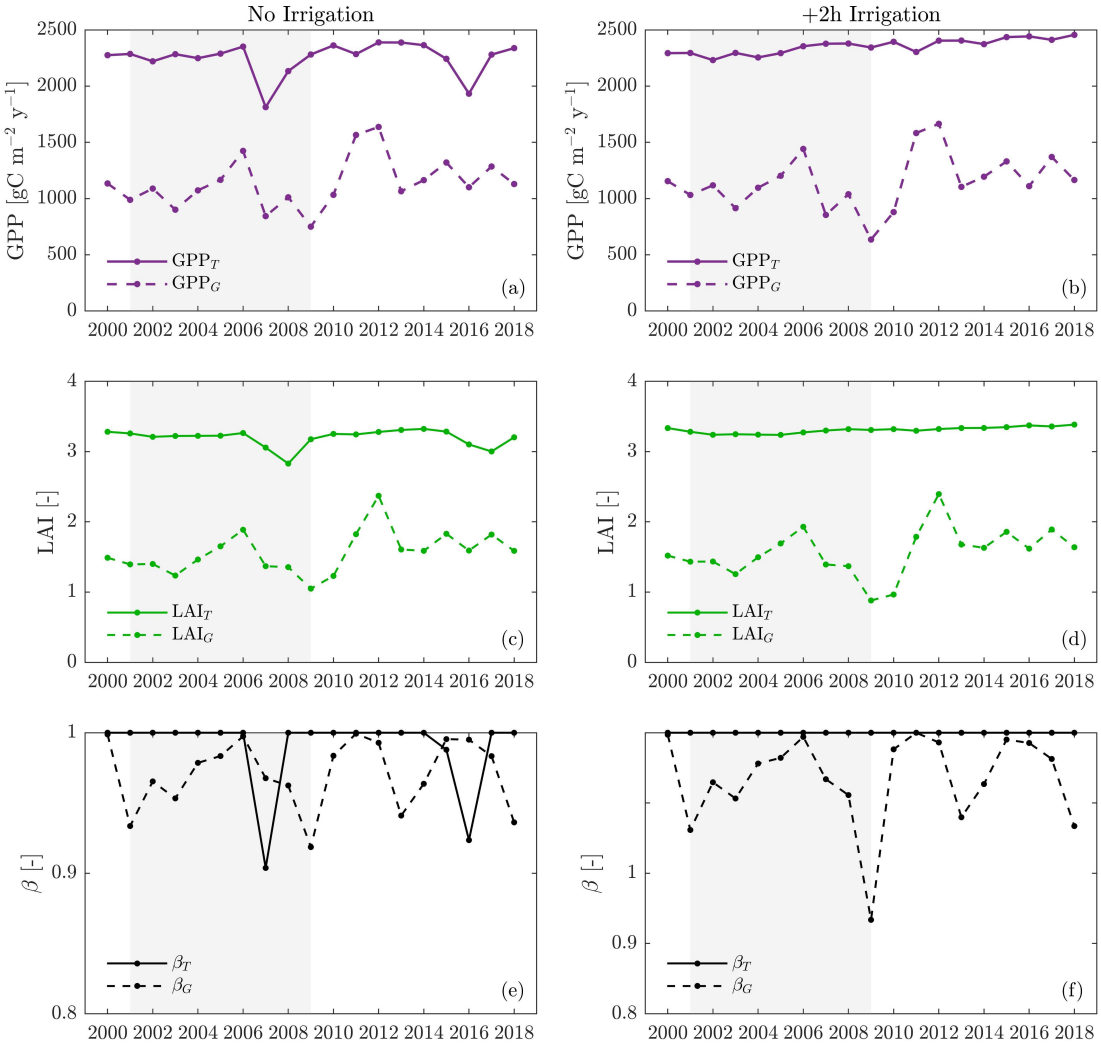

Figure 6.7: Simulation results for the 19 year period (July 1999-June 2018) corresponding to a 30% tree cover without irrigation (a, c, e) and with respect to a +2h irrigation scenario (b, d, f). (a-b) Total annual values of gross primary productivity (GPP; for unit of vegetated area) for trees (GPP$_T$) and grass (GPP$_S$). (c-d) Mean annual values of leaf area index (LAI; for unit of vegetated area) for trees (LAI$_T$) and grass (LAI$_S$). (e-f) Mean annual values of plant water stress for trees (β_T) and grass (β_S). Grey regions indicate the period of the Millennium Drought.

6.5 Summary

In this chapter, the ecohydrological model Tethys-Chloris, once calibrated and confirmed, was used to run a series of numerical experiments to analyze the effects of different vegetation cover and irrigation scenarios on hydrological fluxes and vegetation productivity in a small urban reserve, Napier Park. The site has a stormwater harvesting and irrigation system that allows for the collection of water from an urbanized upstream drainage catchment to reuse it for irrigating most of the area of the reserve. The implementation of this kind of blue-green infrastructure is becoming increasingly popular worldwide. However, the quantification of the benefits they can provide in terms of hydrological fluxes and vegetation dynamics has received considerable less attention. In this context, using an ecohydrological modeling approach may help to overcome the constraints of experimental studies, thus providing additional information on the management of urban green spaces. Specifically, results indicate the following:

1. Changing the vegetation cover, for example by increasing tree cover, may produce benefits in terms of urban cooling (e.g., Coutts et al., 2013b), but at the same time it has considerable impacts on rainfall partitioning into infiltration and runoff, plant-available soil moisture and, consequently, ecosystem health and productivity.

2. Retaining water in the urban landscape through stormwater harvesting systems to provide water for irrigation can be crucial for preserving vegetation health in urban areas, especially during periods of water restriction. In particular, irrigation was found to help trees soften the impacts of the Millennium Drought (2001-2009), while decreasing the losses of the water store within the entire soil domain.

3. Adjusting irrigation schedule in response to meteorological conditions and plant water stress can be really useful to optimize the outdoor water use. For example, in this study a threshold value for the irrigation was found, beyond which adding further water through irrigation does not increase the soil water storage but rather the losses through leakage from the bottom of the soil domain increase.

Chapter 7

Conclusion

7.1 Summary of results

Natural habitats and biodiversity are increasingly removed to accommodate the rapid expansion of cities and metropolitan regions. Land transformations associated with urbanization generate a fragmented and heterogeneous landscape where small vegetated areas, often with remnant native plants, are surrounded by artificial surfaces and embedded in a highly disturbed environment. The urban surrounds often exert negative impacts on the remaining vegetation, by imposing changes in the radiation and energy budget, the hydrologic regime, and ecosystem composition and structure. In this context, while the role of urban trees in supporting urban ecosystem functionality through the provision of ecosystem services is well documented, less is known about their response to these environmental changes. For this reason, an urban ecohydrology perspective allows to place more emphasis on interactions and feedbacks among soil, plant, and atmosphere specifically related to cities.

Although many studies on large bio-diverse ecosystems often in natural environments or mildly affected by human activities are available, the links between the water balance and vegetation health in urban ecosystems has received considerable less attention. This project aims to fill this gap, understanding the environmental water requirements and the response to climate variability of small natural reserves embedded in urban environment.

Overall, cities are major contributors to climate change, being at the same time extremely vulnerable to its impacts. Increased temperatures due to the UHI and more frequent extreme heat events may amplify the water stress of urban trees and lead to higher transpiration rates, especially when soil moisture is not a limiting factor. The complex mosaic of urban land uses and covers strongly influences the water cycle, having impacts on rainfall partitioning into infiltration and runoff, plant-available soil moisture and, consequently, ecosystem health

and productivity. In addition, increasing drought and the need for fresh water, especially in fast-growing cities, may exacerbate the pressure on water resources. In this context, there is an increasing need for evidence related to interactions and feedback between water resources and vegetation health in urban areas.

Addressing the problem of a sustainable balance between urban development and the natural environment, this project focused on three urban reserves located in the Melbourne metropolitan area in southeast Australia: National Drive Reserve, Alex Wilkie Reserve, and Napier Park. The sites host predominantly remnant native trees, with some occasional introduced species, and differ for vegetation structure, soil characteristics, and management practices. Combining field measurements and ecohydrological modeling, this project provided a unique and comprehensive analysis of the water dynamics and tree water use in small natural urban reserves.

As shown in Chapter 4, the dataset collected during this project provides novel insights on mechanisms of tree water use in urban areas. The data collected between July 2016 and June 2018 showed that native vegetation had enough water to sustain its transpiration rates despite the urban surrounding. Two of the reserves of this study appeared to be dependent on groundwater and the other one relied on water stored in a clay layer of its duplex soil. Groundwater played an essential role in sustaining transpiration rates. During the driest periods of the year, transpiration from groundwater was estimated to be about 30-40 % of the total transpiration. During warm nights following days with temperatures above 35°C, groundwater allowed trees to transpire between 3 and 16 % of the total daily transpiration. Therefore, these results highlight the importance of groundwater and soil texture in urban areas and may assist government authorities in improving management effectiveness for these ecosystems through measures such as irrigation.

To further investigate ecosystem responses to changes in water variability, in Chapter 5 an ecohydrological model was used to carry out long-term simulations (July 1999 - June 2018) under both present climatic conditions, including the Millennium Drought (2001-2009), and in response to perturbations in key environmental variables (i.e., air temperature, atmospheric CO_2 concentrations, and rainfall). Numerical simulations confirmed that two of the reserves of this study (National Drive Reserve and Alex Wilkie Reserve) strongly depend on groundwater, with woody plants transpiring more than 40% when the water table was maintained within the reach of the plant roots compared to scenarios without groundwater. The presence of a threshold water table depth, below which vegetation was found to be more susceptible to water stress, emphasizes the vulnerability of trees in the reserves to groundwater depletion, which could result in reduction of plant transpiration (-56%) and

productivity (-45%), and, in extreme cases, in drought-induced mortality. During the Millennium Drought, groundwater played an essential role in supporting ecosystem productivity and transpiration to levels similar to normal years. When a decrease in the groundwater availability was imposed in the simulations, trees showed major signs of stress, in particular at Alex Wilkie where the particularly sandy soil did not provide any buffer to the groundwater drawdown. Results also suggested that groundwater might control trees-shrubs-grass coexistence and competition for resources, with soil properties playing a crucial role in amplifying and dampening these dynamics. Finally, groundwater (or its capillary fringe) was found to have a crucial role in affecting ecosystem response to a single stressor, such as higher air temperature, increased atmospheric CO_2 concentrations, and different rainfall regimes. As computed here by means of ecohydrologic simulations, quantifications of vegetation responses to groundwater depletion and climate variability may be crucial to evaluate appropriate management practices in order to maintain healthy urban ecosystems.

When groundwater is not available, as for the case of Napier Park, irrigation may be a useful management practice to sustain ecosystem dynamics, even more so during major droughts. Also in this case, an ecohydrological model was used to carry out long-term simulations (July 1999 - June 2018) to test how vegetation cover and irrigation scenarios affect hydrological fluxes and vegetation productivity. As shown in Chapter 6, numerical simulations confirmed that trees at Napier Park mostly rely on the water stored in the clay layer of its duplex soil. In fact, increasing the volume of water for the recharge of this soil layer during all rainfall events helped the trees to maintain unstressed conditions in which transpiration rates increased by 18% when the tree cover was set to 30%. Results also showed that, while grass maintained overall unstressed transpiration rates and productivity, regardless of the vegetation cover and irrigation scenarios, trees needed irrigation to be able to maintained unstressed conditions, especially during dry years. These results put even more emphasis on the need for sustainable management of urban vegetation in order to avoid further ecosystem losses while maximizing the positive impacts on the urban environments.

7.2 Contributions of research

The growing interest worldwide for greener cities presents exciting research opportunities that aim to understand the links between water resources, vegetation health, and climate in urban ecosystems. In this context, this project contributed to address some basic scientific problems related to urban native vegetation, providing at the same time practical knowledge to help support the management of parks and reserves. In particular, the main contributions

of this project are:

- **Identification of groundwater dependent ecosystems in urban areas.** The data collected between July 2016 and June 2018 provided a strong support to this finding, as shown in Chapter 4. In particular, the water available to the trees, via groundwater or duplex soils, was able to sustain tree transpiration during dry periods of the year and hot nights following days with temperatures higher than 35°C.

- **Quantifications of vegetation response to groundwater depletion and climate variability are crucial to evaluate appropriate management practices.** The dependency on groundwater was also confirmed by the T&C model simulations in Chapter 5. In particular, the results support the assumption that water stress in the reserves did occur during the Millennium Drought (2001-2009), when groundwater depths might have dropped outside the reach of the plants roots. Simulations also showed that a full trees recovery happened only 5-6 years later, suggesting long-term impacts on vegetation due to groundwater depletion combined with drought conditions.

- **Irrigation might represent a useful source of water for preserving vegetation health in urban areas.** As shown in Chapter 6, irrigation helped to buffer the effects of local rainfall decrease, especially when groundwater was not available. However, the outdoor water use needs to be optimized to avoid water losses (e.g., evaporation and leakage). This can be achieved by combining local alternative water supply (e.g., rainwater and stormwater harvesting) with irrigation schedules that respond to meteorological conditions and plant water stress.

7.3 Future research

With more than half of the world population living in urban areas and projections showing a population increase up to 66% by 2050, there is a growing need to support sustainable uses of soil, vegetation, and water resources in urban areas, promoting a shift towards greener cities. Sustainable solutions in the use of soil and water resources in urban areas need to be supported by a better understanding of the ecosystem responses to the environmental changes associated with urbanization. Urban ecohydrology thus offers novel perspectives and challenges on coupled human-natural systems.

The potential of UHI-induced changes to impact patterns of water, energy, and carbon cycling within cities is highlighted in several studies (e.g., Zipper et al., 2017a). However, there is the need to improve empirical evidence of urban ET patterns which can be strongly

affected by urbanization and associated changes in vegetation cover, plant functional type, and irrigation (e.g., Litvak et al., 2017). Moreover, the variability in plant response to the UHI should be better understood, along with the potential benefits of the evaporative cooling provided by urban vegetation (e.g., Konarska et al., 2016,Broadbent et al., 2018).

Simulating water, carbon, nutrient, and energy fluxes in urban areas is perhaps the least explored research area. This project used a 1D model, but several existing process-based distributed models, which couple hydrological processes and vegetation dynamics (e.g., Tethys-Chloris, Fatichi et al., 2012; tRIBS-VEGGIE, Ivanov et al., 2008; CATHY-NoahMP, Niu et al., 2014), could be extended to urban areas to model the coupled urban-hydrological-biosphere system dynamics. In addition, coupling radiative models with hydrological models and perhaps C and N cycle models at different scales, taking into account for example the UHI impacts, would bring an integrated and more complete evaluation of urban ecohydrological processes (e.g., Nice et al., 2018).

The complex role of shallow groundwater in sustaining urban ecosystems must be further investigated, in particular in relation to its impacts on ecosystem services and in combination with climate variability (Qiu et al., 2019). Moreover, despite numerous cities around the world exhibit a high level of dependence on groundwater for urban water-supply, the impacts of urbanization on such a resource are not completely clear.

Finally, although the role of urban green spaces in providing environmental, socio-cultural, and economic benefits essential to the quality of life of urban dwellers is well known, more detailed quantitative assessments of these ecosystem services (e.g., microclimate regulation, stormwater runoff management, carbon emission reduction, biodiversity) are needed.

References

Akbari, H. (2002). Shade trees reduce building energy use and CO_2 emissions from power plants. *Environmental Pollution*, 116:S119–S126.

Alarcón, J., Domingo, R., Green, S., Sánchez-Blanco, M. J., Rodríguez, P., and Torrecillas, A. (2000). Sap flow as an indicator of transpiration and the water status of young apricot trees. *Plant and Soil*, 227(1-2):77–85.

Allen, C. D., Breshears, D. D., and McDowell, N. G. (2015). On underestimation of global vulnerability to tree mortality and forest die-off from hotter drought in the anthropocene. *Ecosphere*, 6(8):1–55.

Allen, R. G., Pereira, L. S., Raes, D., and Smith, M. (1998). Guidelines for computing crop water requirements-FAO Irrigation and drainage paper 56, FAO-Food and Agriculture Organisation of the United Nations, Rome (http://www. fao. org/docrep) ARPAV (2000). *Geophysics*, 156:178.

Armson, D., Stringer, P., and Ennos, A. (2012). The effect of tree shade and grass on surface and globe temperatures in an urban area. *Urban Forestry & Urban Greening*, 11(3):245–255.

Arnfield, A. J. (2003). Two decades of urban climate research: a review of turbulence, exchanges of energy and water, and the urban heat island. *International journal of climatology*, 23(1):1–26.

Arora, V. K. and Boer, G. J. (2005). A parameterization of leaf phenology for the terrestrial ecosystem component of climate models. *Global Change Biology*, 11(1):39–59.

Asawa, T., Kiyono, T., and Hoyano, A. (2017). Continuous measurement of whole-tree water balance for studying urban tree transpiration. *Hydrological Processes*, 31(17):3056–3068.

Balling, R. and Brazel, S. (1987). Recent changes in Phoenix, Arizona summertime diurnal precipitation patterns. *Theoretical and Applied Climatology*, 38(1):50–54.

Balling, R. C., Gober, P., and Jones, N. (2008). Sensitivity of residential water consumption to variations in climate: an intraurban analysis of Phoenix, Arizona. *Water Resources Research*, 44(10).

Balugani, E., Lubczynski, M., Reyes-Acosta, L., Van Der Tol, C., Francés, A., and Metselaar, K. (2017). Groundwater and unsaturated zone evaporation and transpiration in a semi-arid open woodland. *Journal of Hydrology*, 547:54–66.

Barbeta, A., Mejía-Chang, M., Ogaya, R., Voltas, J., Dawson, T. E., and Peñuelas, J. (2015). The combined effects of a long-term experimental drought and an extreme drought on the use of plant-water sources in a Mediterranean forest. *Global Change Biology*, 21(3):1213–1225.

Barron, O., Barr, A., and Donn, M. (2013). Effect of urbanisation on the water balance of a catchment with shallow groundwater. *Journal of Hydrology*, 485:162–176.

Bartens, J., Day, S. D., Harris, J. R., Dove, J. E., and Wynn, T. M. (2008). Can urban tree roots improve infiltration through compacted subsoils for stormwater management? *Journal of Environmental Quality*, 37(6):2048–2057.

Benyon, R. and Doody, T. (2015). Comparison of interception, forest floor evaporation and transpiration in *Pinus radiata* and *Eucalyptus globulus* plantations. *Hydrological Processes*, 29(6):1173–1187.

Berland, A., Shiflett, S. A., Shuster, W. D., Garmestani, A. S., Goddard, H. C., Herrmann, D. L., and Hopton, M. E. (2017). The role of trees in urban stormwater management. *Landscape and Urban Planning*, 162:167–177.

Bhaskar, A. S., Jantz, C., Welty, C., Drzyzga, S. A., and Miller, A. J. (2016). Coupling of the water cycle with patterns of urban growth in the Baltimore Metropolitan Region, United States. *JAWRA Journal of the American Water Resources Association*, 52(6):1509–1523.

Bijoor, N. S., McCarthy, H. R., Zhang, D., and Pataki, D. E. (2012). Water sources of urban trees in the Los Angeles metropolitan area. *Urban Ecosystems*, 15(1):195–214.

Boggs, J. and Sun, G. (2011). Urbanization alters watershed hydrology in the Piedmont of North Carolina. *Ecohydrology*, 4(2):256–264.

Bolund, P. and Hunhammar, S. (1999). Ecosystem services in urban areas. *Ecological Economics*, 29(2):293–301.

Bonan, G. B. (1997). Effects of land use on the climate of the United States. *Climatic Change*, 37(3):449–486.

Bonan, G. B., Lawrence, P. J., Oleson, K. W., Levis, S., Jung, M., Reichstein, M., Lawrence, D. M., and Swenson, S. C. (2011). Improving canopy processes in the community land model version 4 (clm4) using global flux fields empirically inferred from fluxnet data. *Journal of Geophysical Research: Biogeosciences*, 116(G2).

Bonan, G. B., Levis, S., Sitch, S., Vertenstein, M., and Oleson, K. W. (2003). A dynamic global vegetation model for use with climate models: concepts and description of simulated vegetation dynamics. *Global Change Biology*, 9(11):1543–1566.

Bonneau, J., Fletcher, T. D., Costelloe, J. F., and Burns, M. J. (2017). Stormwater infiltration and the 'urban karst'–a review. *Journal of Hydrology*, 552:141–150.

Bou-Zeid, E., Overney, J., Rogers, B. D., and Parlange, M. B. (2009). The effects of building representation and clustering in large-eddy simulations of flows in urban canopies. *Boundary-layer Meteorology*, 132(3):415–436.

Bowler, D. E., Buyung-Ali, L., Knight, T. M., and Pullin, A. S. (2010). Urban greening to cool towns and cities: A systematic review of the empirical evidence. *Landscape and Urban Planning*, 97(3):147–155.

Boyd, M., Bufill, M., and Knee, R. (1993). Pervious and impervious runoff in urban catchments. *Hydrological Sciences Journal*, 38(6):463–478.

Bradshaw, C. J. (2012). Little left to lose: Deforestation and forest degradation in Australia since European colonization. *Journal of Plant Ecology*, 5(1):109–120.

Brazel, A., Selover, N., Vose, R., and Heisler, G. (2000). The tale of two climates—Baltimore and Phoenix urban LTER sites. *Climate Research*, 15(2):123–135.

Breshears, D. D., Cobb, N. S., Rich, P. M., Price, K. P., Allen, C. D., Balice, R. G., Romme, W. H., Kastens, J. H., Floyd, M. L., Belnap, J., et al. (2005). Regional vegetation die-off in response to global-change-type drought. *Proceedings of the National Academy of Sciences*, 102(42):15144–15148.

Breyer, B., Zipper, S. C., and Qiu, J. (2018). Sociohydrological impacts of water conservation under anthropogenic drought in Austin, TX (USA). *Water Resources Research*, 54(4):3062–3080.

Broadbent, A. M., Coutts, A. M., Tapper, N. J., and Demuzere, M. (2018). The cooling effect of irrigation on urban microclimate during heatwave conditions. *Urban Climate*, 23:309–329.

Broadbent, A. M., Coutts, A. M., Tapper, N. J., Demuzere, M., and Beringer, J. (2017). The microscale cooling effects of water sensitive urban design and irrigation in a suburban environment. *Theoretical and Applied Climatology*, pages 1–23.

Brolsma, R. and Bierkens, M. (2007). Groundwater–soil water–vegetation dynamics in a temperate forest ecosystem along a slope. *Water Resources Research*, 43(1).

Brolsma, RJ, v., Van Beek, L., and Bierkens, M. (2010). Vegetation competition model for water and light limitation. ii: Spatial dynamics of groundwater and vegetation. *Ecological Modelling*, 221(10):1364–1377.

Bruse, M. and Fleer, H. (1998). Simulating surface–plant–air interactions inside urban environments with a three dimensional numerical model. *Environmental Modelling & Software*, 13(3-4):373–384.

Bulcock, H. and Jewitt, G. (2012). Field data collection and analysis of canopy and litter interception in commercial forest plantations in the KwaZulu-Natal Midlands, South Africa. *Hydrology and Earth System Sciences*, 16(10):3717–3728.

Burgess, S. S., Adams, M. A., Turner, N. C., Beverly, C. R., Ong, C. K., Khan, A. A., and Bleby, T. M. (2001). An improved heat pulse method to measure low and reverse rates of sap flow in woody plants. *Tree Physiology*, 21(9):589–598.

Burian, S. J. and Shepherd, J. M. (2005). Effect of urbanization on the diurnal rainfall pattern in houston. *Hydrological Processes*, 19(5):1089–1103.

Caird, M. A., Richards, J. H., and Donovan, L. A. (2007). Nighttime stomatal conductance and transpiration in C3 and C4 plants. *Plant Physiology*, 143(1):4–10.

Carsel, R. F. and Parrish, R. S. (1988). Developing joint probability distributions of soil water retention characteristics. *Water Resources Research*, 24(5):755–769.

Changnon, S. (1981). *METROMEX: A review and summary*, volume 18. Springer.

Chapin III, F. S., Schulze, E., and Mooney, H. A. (1990). The ecology and economics of storage in plants. *Annual review of ecology and systematics*, 21(1):423–447.

Chapman, S., Watson, J. E. M., Salazar, A., Thatcher, M., and McAlpine, C. A. (2017). The impact of urbanization and climate change on urban temperatures: a systematic review. *Landscape Ecology*, 32(10):1921–1935.

Chen, L., Zhang, Z., Li, Z., Tang, J., Caldwell, P., and Zhang, W. (2011). Biophysical control of whole tree transpiration under an urban environment in Northern China. *Journal of Hydrology*, 402(3-4):388–400.

Cheng, X., Wei, B., Chen, G., Li, J., and Song, C. (2014). Influence of park size and its surrounding urban landscape patterns on the park cooling effect. *Journal of Urban Planning and Development*, 141(3):A4014002.

Chiesura, A. (2004). The role of urban parks for the sustainable city. *Landscape and Urban Planning*, 68(1):129–138.

Cho, J., Barone, V., and Mostaghimi, S. (2009). Simulation of land use impacts on groundwater levels and streamflow in a virginia watershed. *Agricultural Water Management*, 96(1):1–11.

Chow, W. T., Pope, R. L., Martin, C. A., and Brazel, A. J. (2011). Observing and modeling the nocturnal park cool island of an arid city: horizontal and vertical impacts. *Theoretical and Applied Climatology*, 103(1-2):197–211.

Cohen, P., Potchter, O., and Matzarakis, A. (2012). Daily and seasonal climatic conditions of green urban open spaces in the mediterranean climate and their impact on human comfort. *Building and Environment*, 51:285–295.

Collatz, G. J., Ball, J. T., Grivet, C., and Berry, J. A. (1991). Physiological and environmental regulation of stomatal conductance, photosynthesis and transpiration: a model that includes a laminar boundary layer. *Agricultural and Forest meteorology*, 54(2-4):107–136.

Collatz, G. J., Ribas-Carbo, M., and Berry, J. (1992). Coupled photosynthesis-stomatal conductance model for leaves of C4 plants. *Functional Plant Biology*, 19(5):519–538.

Collier, C. G. (2006). The impact of urban areas on weather. *Quarterly Journal of the Royal Meteorological Society*, 132(614):1–25.

Collins, D. and Bras, R. (2007). Plant rooting strategies in water-limited ecosystems. *Water Resources Research*, 43(6).

Conley, M. M., Kimball, B., Brooks, T., Pinter Jr, P., Hunsaker, D., Wall, G., Adam, N., LaMorte, R., Matthias, A., Thompson, T., et al. (2001). CO_2 enrichment increases water-use efficiency in sorghum. *New Phytologist*, 151(2):407–412.

Costa, K. H. and Groffman, P. M. (2013). Factors regulating net methane flux by soils in urban forests and grasslands. *Soil Science Society of America Journal*, 77(3):850–855.

Costanza, R., d'Arge, R., De Groot, R., Farber, S., Grasso, M., Hannon, B., Limburg, K., Naeem, S., O'neill, R. V., and Paruelo, J. (1997). The value of the world's ecosystem services and natural capital. *Nature*, 387(6630):253–260.

Costanza, R., de Groot, R., Sutton, P., Van der Ploeg, S., Anderson, S. J., Kubiszewski, I., Farber, S., and Turner, R. K. (2014). Changes in the global value of ecosystem services. *Global Environmental Change*, 26:152–158.

Coutts, A. M., Beringer, J., and Tapper, N. J. (2007). Characteristics influencing the variability of urban CO_2 fluxes in Melbourne, Australia. *Atmospheric Environment*, 41(1):51–62.

Coutts, A. M., Daly, E., Beringer, J., and Tapper, N. J. (2013a). Assessing practical measures to reduce urban heat: Green and cool roofs. *Building and Environment*, 70:266–276.

Coutts, A. M., Tapper, N. J., Beringer, J., Loughnan, M., and Demuzere, M. (2013b). Watering our cities: The capacity for Water Sensitive Urban Design to support urban cooling and improve human thermal comfort in the Australian context. *Progress in Physical Geography*, 37(1):2–28.

Coutts, A. M., White, E. C., Tapper, N. J., Beringer, J., and Livesley, S. J. (2016). Temperature and human thermal comfort effects of street trees across three contrasting street canyon environments. *Theoretical and applied climatology*, 124(1-2):55–68.

Craine, J. M., Ocheltree, T. W., Nippert, J. B., Towne, E. G., Skibbe, A. M., Kembel, S. W., and Fargione, J. E. (2013). Global diversity of drought tolerance and grassland climate-change resilience. *Nature Climate Change*, 3(1):63.

Crawford, B., Grimmond, C., and Christen, A. (2011). Five years of carbon dioxide fluxes measurements in a highly vegetated suburban area. *Atmospheric Environment*, 45(4):896–905.

Cregg, B. M. (1995a). Plant moisture stress of green ash trees in contrasting urban sites. *Journal of Arboriculture*, 21:271–276.

Cregg, B. M. (1995b). Plant moisture stress of green ash trees in contrasting urban sites. *Journal of Arboriculture*, 21:271–276.

Cregg, B. M. and Dix, M. E. (2001a). Tree moisture stress and insect damage in urban areas in relation to heat island effects. *Journal of Arboriculture*, 27(1):8–17.

Cregg, B. M. and Dix, M. E. (2001b). Tree moisture stress and insect damage in urban areas in relation to heat island effects. *Journal of Arboriculture*, 27(1):8–17.

Cuthbert, M., Gleeson, T., Moosdorf, N., Befus, K., Schneider, A., Hartmann, J., and Lehner, B. (2019). Global patterns and dynamics of climate–groundwater interactions. *Nature Climate Change*, 9(2):137.

Dai, Y., Dickinson, R. E., and Wang, Y.-P. (2004). A two-big-leaf model for canopy temperature, photosynthesis, and stomatal conductance. *Journal of Climate*, 17(12):2281–2299.

Daly, E., Deletic, A., Hatt, B., and Fletcher, T. (2012). Modelling of stormwater biofilters under random hydrologic variability: a case study of a car park at Monash University, Victoria (Australia). *Hydrological Processes*, 26(22):3416–3424.

Daly, E., Porporato, A., and Rodriguez-Iturbe, I. (2004). Coupled dynamics of photosynthesis, transpiration, and soil water balance. Part I: Upscaling from hourly to daily level. *Journal of Hydrometeorology*, 5(3):546–558.

Dawson, T. E., Burgess, S. S., Tu, K. P., Oliveira, R. S., Santiago, L. S., Fisher, J. B., Simonin, K. A., and Ambrose, A. R. (2007). Nighttime transpiration in woody plants from contrasting ecosystems. *Tree Physiology*, 27(4):561–575.

Day, S. D., Eric Wiseman, P., Dickinson, S. B., and Roger Harris, J. (2010a). Tree root ecology in the urban environment and implications for a sustainable rhizosphere. *Journal of Arboriculture*, 36(5):193.

Day, S. D., Wiseman, P. E., Dickinson, S. B., and Harris, J. R. (2010b). Contemporary concepts of root system architecture of urban trees. *Arboriculture & Urban Forestry*, 36(4):149–159.

Decina, S. M., Hutyra, L. R., Gately, C. K., Getson, J. M., Reinmann, A. B., Gianotti, A. G. S., and Templer, P. H. (2016). Soil respiration contributes substantially to urban carbon fluxes in the greater Boston area. *Environmental Pollution*, 212:433–439.

Declet-Barreto, J., Knowlton, K., Jenerette, G. D., and Buyantuev, A. (2016). Effects of urban vegetation on mitigating exposure of vulnerable populations to excessive heat in Cleveland, Ohio. *Weather, Climate, and Society*, 8(4):507–524.

DeFries, R. and Eshleman, K. N. (2004). Land-use change and hydrologic processes: a major focus for the future. *Hydrological Processes*, 18(11):2183–2186.

DELWP (2016). Victoria in future 2016. The State of Victoria Department of Environment, Land, Water and Planning.

Dietrich, S., Carrera, J., Weinzettel, P., and Sierra, L. (2018). Estimation of specific yield and its variability by electrical resistivity tomography. *Water Resources Research*, 54(11):8653–8673.

Dimoudi, A. and Nikolopoulou, M. (2003). Vegetation in the urban environment: microclimatic analysis and benefits. *Energy and Buildings*, 35(1):69–76.

Dobbs, C., Nitschke, C. R., and Kendal, D. (2014). Global drivers and tradeoffs of three urban vegetation ecosystem services. *PLoS One*, 9(11):e113000.

Doick, K. J., Peace, A., and Hutchings, T. R. (2014). The role of one large greenspace in mitigating London's nocturnal urban heat island. *Science of the Total Environmentotal*, 493:662–671.

Doody, T. M., Barron, O. V., Dowsley, K., Emelyanova, I., Fawcett, J., Overton, I. C., Pritchard, J. L., Van Dijk, A. I., and Warren, G. (2017). Continental mapping of groundwater dependent ecosystems: A methodological framework to integrate diverse data and expert opinion. *Journal of Hydrology: Regional Studies*, 10:61–81.

Doody, T. M., Colloff, M. J., Davies, M., Koul, V., Benyon, R. G., and Nagler, P. L. (2015). Quantifying water requirements of riparian river red gum (Eucalyptus camaldulensis) in the Murray–Darling Basin, Australia–implications for the management of environmental flows. *Ecohydrology*, 8(8):1471–1487.

Dover, J. W. (2015a). *Green infrastructure: Incorporating plants and enhancing biodiversity in buildings and urban environments*. Routledge.

Dover, J. W. (2015b). *Green infrastructure: Incorporating plants and enhancing biodiversity in buildings and urban environments*. Routledge.

Dow, C. L. and DeWalle, D. R. (2000). Trends in evaporation and Bowen ratio on urbanizing watersheds in eastern United States. *Water Resources Research*, 36(7):1835–1843.

Drake, J. E., Tjoelker, M. G., Vårhammar, A., Medlyn, B. E., Reich, P. B., Leigh, A., Pfautsch, S., Blackman, C. J., López, R., Aspinwall, M. J., et al. (2018). Trees tolerate an extreme heatwave via sustained transpirational cooling and increased leaf thermal tolerance. *Global Change Biology*, 24(6):2390–2402.

Dunin, F., O'loughlin, E., and Reyenga, W. (1988). Interception loss from eucalypt forest: Lysimeter determination of hourly rates for long term evaluation. *Hydrological Processes*, 2(4):315–329.

Duursma, R. A., Medlyn, B. E., et al. (2012). *MAESPA: a model to study interactions between water limitation, environmental drivers and vegetation function at tree and stand levels, with an example application to CO_2 x drought interactions*. Copernicus Publication.

Eamus, D. and Froend, R. (2006). Groundwater-dependent ecosystems: The where, what and why of GDEs. *Australian Journal of Botany*, 54(2):91–96.

Eamus, D., Hatton, T., Cook, P., and Colvin, C. (2006). *Ecohydrology: vegetation function, water and resource management*. CSIRO Publishing.

Eamus, D., Zolfaghar, S., Villalobos-Vega, R., Cleverly, J., and Huete, A. (2015). Groundwater-dependent ecosystems: recent insights from satellite and field-based studies. *Hydrology and Earth System Sciences*, 19(10):4229–4256.

Eggemeyer, K. D., Awada, T., Harvey, F. E., Wedin, D. A., Zhou, X., and Zanner, C. W. (2009). Seasonal changes in depth of water uptake for encroaching trees Juniperus virginiana and Pinus ponderosa and two dominant C4 grasses in a semiarid grassland. *Tree Physiology*, 29(2):157–169.

Elliott, A. and Trowsdale, S. A. (2007). A review of models for low impact urban stormwater drainage. *Environmental Modelling & Software*, 22(3):394–405.

Elmqvist, T., Fragkias, M., Goodness, J., Güneralp, B., Marcotullio, P. J., McDonald, R. I., Parnell, S., Schewenius, M., Sendstad, M., Seto, K. C., et al. (2013). *Urbanization, biodiversity and ecosystem services: challenges and opportunities: a global assessment*. Springer.

Elmqvist, T., Setälä, H., Handel, S., Van Der Ploeg, S., Aronson, J., Blignaut, J. N., Gomez-Baggethun, E., Nowak, D., Kronenberg, J., and De Groot, R. (2015). Benefits of restoring ecosystem services in urban areas. *Current Opinion in Environmental Sustainability*, 14:101–108.

Endreny, T. A. (2005). Land use and land cover effects on runoff processes: urban and suburban development. *Encyclopedia of hydrological sciences*.

Endter-Wada, J., Kurtzman, J., Keenan, S. P., Kjelgren, R. K., and Neale, C. M. (2008). Situational waste in landscape watering: Residential and business water use in an urban utah community 1. *JAWRA Journal of the American Water Resources Association*, 44(4):902–920.

Escobedo, F. J., Kroeger, T., and Wagner, J. E. (2011). Urban forests and pollution mitigation: Analyzing ecosystem services and disservices. *Environmental Pollution*, 159(8-9):2078–2087.

Fam, D., Mosley, E., Lopes, A., Mathieson, L., Morison, J., and Connellan, G. (2008). Irrigation of urban green spaces: a review of the environmental, social and economic benefits. Technical Report 04/08, CRC for Irrigation Futures Technical Report.

Famulari, D., Nemitz, E., Di Marco, C., Phillips, G. J., Thomas, R., House, E., and Fowler, D. (2010). Eddy-covariance measurements of nitrous oxide fluxes above a city. *Agricultural and Forest Meteorology*, 150(6):786–793.

Fan, J., Oestergaard, K. T., Guyot, A., and Lockington, D. A. (2014a). Estimating groundwater recharge and evapotranspiration from water table fluctuations under three vegetation covers in a coastal sandy aquifer of subtropical Australia. *Journal of Hydrology*, 519:1120–1129.

Fan, J., Oestergaard, K. T., Guyot, A., and Lockington, D. A. (2014b). Measuring and modeling rainfall interception losses by a native Banksia woodland and an exotic pine plantation in subtropical coastal Australia. *Journal of Hydrology*, 515:156–165.

Fan, J., Ostergaard, K. T., Guyot, A., Fujiwara, S., and Lockington, D. A. (2016). Estimating groundwater evapotranspiration by a subtropical pine plantation using diurnal water table fluctuations: Implications from night-time water use. *Journal of Hydrology*, 542:679–685.

Fan, Y. (2015). Groundwater in the Earth's critical zone: Relevance to large-scale patterns and processes. *Water Resources Research*, 51(5):3052–3069.

Fan, Y., Li, H., and Miguez-Macho, G. (2013). Global patterns of groundwater table depth. *Science*, 339(6122):940–943.

Farquhar, G. D., von Caemmerer, S. v., and Berry, J. A. (1980). A biochemical model of photosynthetic CO_2 assimilation in leaves of C3 species. *planta*, 149(1):78–90.

Farrington, P. and Bartle, G. (1991). Recharge beneath a Banksia woodland and a Pinus pinaster plantation on coastal deep sands in south Western Australia. *Forest Ecology and Management*, 40(1-2):101–118.

Fatichi, S., Ivanov, V., and Caporali, E. (2012). A mechanistic ecohydrological model to investigate complex interactions in cold and warm water-controlled environments: 1. Theoretical framework and plot-scale analysis. *Journal of Advances in Modeling Earth Systems*, 4(2).

Fatichi, S. and Pappas, C. (2017). Constrained variability of modeled T: ET ratio across biomes. *Geophysical Research Letters*, 44(13):6795–6803.

Fatichi, S., Pappas, C., and Ivanov, V. Y. (2016). Modeling plant–water interactions: an ecohydrological overview from the cell to the global scale. *Wiley Interdisciplinary Reviews: Water*, 3(3):327–368.

Fatichi, S., Zeeman, M. J., Fuhrer, J., and Burlando, P. (2014). Ecohydrological effects of management on subalpine grasslands: From local to catchment scale. *Water Resources Research*, 50(1):148–164.

Fletcher, T., Andrieu, H., and Hamel, P. (2013). Understanding, management and modelling of urban hydrology and its consequences for receiving waters: A state of the art. *Advances in Water Resources*, 51:261–279.

Fletcher, T. D., Shuster, W., Hunt, W. F., Ashley, R., Butler, D., Arthur, S., Trowsdale, S., Barraud, S., Semadeni-Davies, A., and Bertrand-Krajewski, J.-L. (2015). SUDS, LID, BMPs, WSUD and more–The evolution and application of terminology surrounding urban drainage. *Urban Water Journal*, 12(7):525–542.

Flörke, M., Schneider, C., and McDonald, R. I. (2018). Water competition between cities and agriculture driven by climate change and urban growth. *Nature Sustainability*, 1(1):51.

Forster, M. A. (2014). How significant is nocturnal sap flow? *Tree Physiology*, 34(7):757–765.

Frank, D., Poulter, B., Saurer, M., Esper, J., Huntingford, C., Helle, G., Treydte, K., Zimmermann, N., Schleser, G., Ahlström, A., et al. (2015). Water-use efficiency and transpiration across european forests during the anthropocene. *Nature Climate Change*, 5(6):579.

Freund, M., Henley, B. J., Karoly, D. J., Allen, K. J., and Baker, P. J. (2017). Multi-century cool-and warm-season rainfall reconstructions for Australia's major climatic regions. *Climate of the Past*, 13(12):1751–1770.

Friedlingstein, P., Joel, G., Field, C. B., and Fung, I. Y. (1999). Toward an allocation scheme for global terrestrial carbon models. *Global Change Biology*, 5(7):755–770.

Friend, A., Stevens, A., Knox, R., and Cannell, M. (1997). A process-based, terrestrial biosphere model of ecosystem dynamics (hybrid v3. 0). *Ecological Modelling*, 95(2-3):249–287.

Garcia-Fresca, B. and Sharp Jr, J. M. (2005). Hydrogeologic considerations of urban development: Urban-induced recharge. *Reviews in Engineering Geology*, 16:123–136.

Gehman, C. L., Harry, D. L., Sanford, W. E., Stednick, J. D., and Beckman, N. A. (2009). Estimating specific yield and storage change in an unconfined aquifer using temporal gravity surveys. *Water Resources Research*, 45(4).

Georgescu, M., Morefield, P. E., Bierwagen, B. G., and Weaver, C. P. (2014). Urban adaptation can roll back warming of emerging megapolitan regions. *Proceedings of the National Academy of Sciences*, 111(8):2909–2914.

Georgescu, M., Moustaoui, M., Mahalov, A., and Dudhia, J. (2011). An alternative explanation of the semiarid urban area "oasis effect". *Journal of Geophysical Research: Atmospheres*, 116(D24).

Gill, S. E., Handley, J. F., Ennos, A. R., and Pauleit, S. (2007). Adapting cities for climate change: The role of the green infrastructure. *Built Environment*, 33(1):115–133.

Giometto, M., Christen, A., Egli, P., Schmid, M., Tooke, R., Coops, N., and Parlange, M. (2017). Effects of trees on mean wind, turbulence and momentum exchange within and above a real urban environment. *Advances in Water Resources*, 106:154–168.

Giometto, M., Christen, A., Meneveau, C., Fang, J., Krafczyk, M., and Parlange, M. (2016). Spatial characteristics of roughness sublayer mean flow and turbulence over a realistic urban surface. *Boundary-layer Meteorology*, 160(3):425–452.

Girard, P., Nadeau, D. F., Pardyjak, E. R., Overby, M., Willemsen, P., Stoll, R., Bailey, B. N., and Parlange, M. B. (2017). Evaluation of the QUIC-URB wind solver and QESRadiant radiation-transfer model using a dense array of urban meteorological observations. *Urban Climate*.

Golden, H. E. and Hoghooghi, N. (2018). Green infrastructure and its catchment-scale effects: an emerging science. *Wiley Interdisciplinary Reviews: Water*, 5(1):e1254.

Golubiewski, N. E. (2006). Urbanization increases grassland carbon pools: Effects of landscaping in Colorado's front range. *Ecological Applications*, 16(2):555–571.

Gómez-Baggethun, E. and Barton, D. N. (2013). Classifying and valuing ecosystem services for urban planning. *Ecological Economics*, 86:235–245.

Gough, C. M., Flower, C. E., Vogel, C. S., and Curtis, P. S. (2010). Phenological and temperature controls on the temporal non-structural carbohydrate dynamics of Populus grandidentata and Quercus rubra. *Forests*, 1(1):65–81.

Gough, C. M., Flower, C. E., Vogel, C. S., Dragoni, D., and Curtis, P. S. (2009). Whole-ecosystem labile carbon production in a north temperate deciduous forest. *Agricultural and Forest Meteorology*, 149(9):1531–1540.

Grawe, D., Thompson, H. L., Salmond, J. A., Cai, X., and Schlünzen, K. H. (2013). Modelling the impact of urbanisation on regional climate in the Greater London Area. *International Journal of Climatology*, 33(10):2388–2401.

Grimm, N. B., Faeth, S. H., Golubiewski, N. E., Redman, C. L., Wu, J., Bai, X., and Briggs, J. M. (2008). Global change and the ecology of cities. *Science*, 319(5864):756–760.

Grimmond, C., Blackett, M., Best, M., Barlow, J., Baik, J., Belcher, S., Bohnenstengel, S., Calmet, I., Chen, F., and Dandou, A. (2010). The international urban energy balance models comparison project: first results from phase 1. *Journal of applied meteorology and climatology*, 49(6):1268–1292.

Grimmond, C., Oke, T., and Steyn, D. (1986). Urban water balance: 1. A model for daily totals. *Water Resources Research*, 22(10):1397–1403.

Grimmond, C., Salmond, J., Oke, T. R., Offerle, B., and Lemonsu, A. (2004). Flux and turbulence measurements at a densely built-up site in Marseille: Heat, mass (water and carbon dioxide), and momentum. *Journal of Geophysical Research: Atmospheres*, 109(D24).

Groffman, P. M. and Pouyat, R. V. (2009). Methane uptake in urban forests and lawns. *Environmental Science & Technology*, 43(14):5229–5235.

Groffman, P. M., Pouyat, R. V., Cadenasso, M. L., Zipperer, W. C., Szlavecz, K., Yesilonis, I. D., Band, L. E., and Brush, G. S. (2006). Land use context and natural soil controls on plant community composition and soil nitrogen and carbon dynamics in urban and rural forests. *Forest Ecology and Management*, 236(2-3):177–192.

Groffman, P. M., Williams, C. O., Pouyat, R. V., Band, L. E., and Yesilonis, I. D. (2009). Nitrate leaching and nitrous oxide flux in urban forests and grasslands. *Journal of Environmental Quality*, 38(5):1848–1860.

Grossiord, C., Sevanto, S., Bonal, D., Borrego, I., Dawson, T. E., Ryan, M., Wang, W., and McDowell, N. G. (2018). Prolonged warming and drought modify belowground interactions for water among coexisting plants. *Tree Physiology*, 39(1):55–63.

Grossiord, C., Sevanto, S., Dawson, T. E., Adams, H. D., Collins, A. D., Dickman, L. T., Newman, B. D., Stockton, E. A., and McDowell, N. G. (2017). Warming combined with more extreme precipitation regimes modifies the water sources used by trees. *New Phytologist*, 213(2):584–596.

Gunawardena, K., Wells, M., and Kershaw, T. (2017). Utilising green and bluespace to mitigate urban heat island intensity. *Science of the Total Environment*, 584:1040–1055.

Hagedorn, F., Joseph, J., Peter, M., Luster, J., Pritsch, K., Geppert, U., Kerner, R., Molinier, V., Egli, S., Schaub, M., et al. (2016). Recovery of trees from drought depends on belowground sink control. *Nature Plants*, 2(8):16111.

Hahs, A. K. and McDonnell, M. J. (2014). Extinction debt of cities and ways to minimise their realisation: A focus on Melbourne. *Ecological Management & Restoration*, 15(2):102–110.

Hall, S. J., Huber, D., and Grimm, N. B. (2008). Soil N_2O and NO emissions from an arid, urban ecosystem. *Journal of Geophysical Research: Biogeosciences*, 113(G1).

Hallegatte, S., Green, C., Nicholls, R. J., and Corfee-Morlot, J. (2013). Future flood losses in major coastal cities. *Nature Climate Change*, 3(9):802.

Hamel, P., Daly, E., and Fletcher, T. D. (2013). Source-control stormwater management for mitigating the impacts of urbanisation on baseflow: A review. *Journal of Hydrology*, 485:201–211.

Harman, I. N., Best, M. J., and Belcher, S. E. (2004). Radiative exchange in an urban street canyon. *Boundary-Layer Meteorology*, 110(2):301–316.

Hedquist, B. C. and Brazel, A. J. (2006). Urban, residential, and rural climate comparisons from mobile transects and fixed stations: Phoenix, Arizona. *Journal of the Arizona-Nevada Academy of Science*, 38(2):77–87.

Hertwig, D., Patnaik, G., and Leitl, B. (2017a). Les validation of urban flow, part i: flow statistics and frequency distributions. *Environmental Fluid Mechanics*, 17(3):521–550.

Hertwig, D., Patnaik, G., and Leitl, B. (2017b). Les validation of urban flow, part ii: eddy statistics and flow structures. *Environmental Fluid Mechanics*, 17(3):551–578.

Hibbs, B. J. (2016). Groundwater in urban areas. *Journal of Contemporary Water Research & Education*, 159(1):1–4.

Hilaire, R. S., Arnold, M. A., Wilkerson, D. C., Devitt, D. A., Hurd, B. H., Lesikar, B. J., Lohr, V. I., Martin, C. A., McDonald, G. V., and Morris, R. L. (2008). Efficient water use in residential urban landscapes. *HortScience*, 43(7):2081–2092.

Holder, C. D. and Gibbes, C. (2017). Influence of leaf and canopy characteristics on rainfall interception and urban hydrology. *Hydrological Sciences Journal*, 62(2):182–190.

Holmer, B., Thorsson, S., and Eliasson, I. (2007). Cooling rates, sky view factors and the development of intra-urban air temperature differences. *Geografiska Annaler: Series A, Physical Geography*, 89(4):237–248.

Holmer, B., Thorsson, S., and Lindén, J. (2013). Evening evapotranspirative cooling in relation to vegetation and urban geometry in the city of Ouagadougou, Burkina Faso. *International Journal of Climatology*, 33(15):3089–3105.

Huber, W. C., Dickinson, R. E., Barnwell Jr, T. O., and Branch, A. (1988). Storm water management model; version 4. *Environmental Protection Agency, United States.*

Hutley, L., O'Grady, A., and Eamus, D. (2000). Evapotranspiration from Eucalypt open-forest savanna of Northern Australia. *Functional Ecology*, 14(2):183–194.

Hutyra, L. R., Duren, R., Gurney, K. R., Grimm, N., Kort, E. A., Larson, E., and Shrestha, G. (2014). Urbanization and the carbon cycle: Current capabilities and research outlook from the natural sciences perspective. *Earth's Future*, 2(10):473–495.

Idso, C. D., Idso, S. B., and Balling Jr, R. C. (2001). An intensive two-week study of an urban CO_2 dome in Phoenix, Arizona, USA. *Atmospheric Environment*, 35(6):995–1000.

IPCC (2015). *Climate change 2014: mitigation of climate change (Intergovernmental Panel on Climate Change)*, volume 3. Cambridge University Press.

Ivanov, V. Y., Bras, R. L., and Vivoni, E. R. (2008). Vegetation-hydrology dynamics in complex terrain of semiarid areas: 1. A mechanistic approach to modeling dynamic feedbacks. *Water Resources Research*, 44(3).

Jenerette, G., Scott, R., Barron-Gafford, G., and Huxman, T. (2009). Gross primary production variability associated with meteorology, physiology, leaf area, and water supply in contrasting woodland and grassland semiarid riparian ecosystems. *Journal of Geophysical Research: Biogeosciences*, 114(G4).

Jenerette, G. D. and Alstad, K. P. (2010). Water use in urban ecosystems: Complexity, costs, and services of urban ecohydrology. *Urban Ecosystem Ecology*, Agronomy Monographs 55:353–371.

Johnson, A. I. (1963). Compilation of specific yield for various materials. Technical report, USGS Numbered Series.

Kalnay, E. and Cai, M. (2003). Impact of urbanization and land-use change on climate. *Nature*, 423(6939):528–531.

Kanda, M., Inagaki, A., Miyamoto, T., Gryschka, M., and Raasch, S. (2013). A new aerodynamic parametrization for real urban surfaces. *Boundary-layer Meteorology*, 148(2):357–377.

Kaye, J. P., Burke, I. C., Mosier, A. R., and Pablo Guerschman, J. (2004). Methane and nitrous oxide fluxes from urban soils to the atmosphere. *Ecological Applications*, 14(4):975–981.

Kaye, J. P., Groffman, P. M., Grimm, N. B., Baker, L. A., and Pouyat, R. V. (2006). A distinct urban biogeochemistry? *Trends in Ecology & Evolution*, 21(4):192–199.

Kaye, J. P., McCulley, R., and Burke, I. (2005). Carbon fluxes, nitrogen cycling, and soil microbial communities in adjacent urban, native and agricultural ecosystems. *Global Change Biology*, 11(4):575–587.

Keenan, T. F., Hollinger, D. Y., Bohrer, G., Dragoni, D., Munger, J. W., Schmid, H. P., and Richardson, A. D. (2013). Increase in forest water-use efficiency as atmospheric carbon dioxide concentrations rise. *Nature*, 499(7458):324.

Kennedy, C., Steinberger, J., Gasson, B., Hansen, Y., Hillman, T., Havranek, M., Pataki, D., Phdungsilp, A., Ramaswami, A., and Mendez, G. V. (2009). Greenhouse gas emissions from global cities.

Kermavnar, J. and Vilhar, U. (2017). Canopy precipitation interception in urban forests in relation to stand structure. *Urban Ecosystems*, 20(6):1373–1387.

Kim, Y. and Eltahir, E. A. (2004). Role of topography in facilitating coexistence of trees and grasses within savannas. *Water Resources Research*, 40(7).

Kløve, B., Ala-Aho, P., Bertrand, G., Gurdak, J. J., Kupfersberger, H., Kværner, J., Muotka, T., Mykrä, H., Preda, E., Rossi, P., et al. (2014). Climate change impacts on groundwater and dependent ecosystems. *Journal of Hydrology*, 518:250–266.

Koerner, B. and Klopatek, J. (2002). Anthropogenic and natural CO_2 emission sources in an arid urban environment. *Environmental Pollution*, 116:S45–S51.

Koerner, B. A. and Klopatek, J. M. (2010). Carbon fluxes and nitrogen availability along an urban–rural gradient in a desert landscape. *Urban Ecosystems*, 13(1):1–21.

Kollet, S. J. and Maxwell, R. M. (2008). Capturing the influence of groundwater dynamics on land surface processes using an integrated, distributed watershed model. *Water Resources Research*, 44(2).

Konarska, J., Uddling, J., Holmer, B., Lutz, M., Lindberg, F., Pleijel, H., and Thorsson, S. (2016). Transpiration of urban trees and its cooling effect in a high latitude city. *International Journal of Biometeorology*, 60(1):159–172.

Kordowski, K. and Kuttler, W. (2010). Carbon dioxide fluxes over an urban park area. *Atmospheric Environment*, 44(23):2722–2730.

Kozlowski, T. T. and Pallardy, S. G. (1996). *Physiology of woody plants*. Elsevier.

Krayenhoff, E., Christen, A., Martilli, A., and Oke, T. (2014). A multi-layer radiation model for urban neighbourhoods with trees. *Boundary-layer Meteorology*, 151(1):139–178.

Krayenhoff, E. S. and Voogt, J. A. (2007). A microscale three-dimensional urban energy balance model for studying surface temperatures. *Boundary-Layer Meteorology*, 123(3):433–461.

Krinner, G., Viovy, N., de Noblet-Ducoudré, N., Ogée, J., Polcher, J., Friedlingstein, P., Ciais, P., Sitch, S., and Prentice, I. C. (2005). A dynamic global vegetation model for studies of the coupled atmosphere-biosphere system. *Global Biogeochemical Cycles*, 19(1).

Kusaka, H. and Kimura, F. (2004). Thermal effects of urban canyon structure on the nocturnal heat island: Numerical experiment using a mesoscale model coupled with an urban canopy model. *Journal of Applied Meteorology*, 43(12):1899–1910.

Laio, F., Porporato, A., Ridolfi, L., and Rodriguez-Iturbe, I. (2001). Plants in water-controlled ecosystems: active role in hydrologic processes and response to water stress: II. Probabilistic soil moisture dynamics. *Advances in Water Resources*, 24(7):707–723.

Lal, R. and Stewart, B. A. (2017). *Urban Soils*. CRC Press, Milton, UNITED KINGDOM.

Leblanc, M., Tweed, S., Van Dijk, A., and Timbal, B. (2012). A review of historic and future hydrological changes in the Murray-Darling Basin. *Global and Planetary Change*, 80:226–246.

Lee, H., Mayer, H., and Chen, L. (2016). Contribution of trees and grasslands to the mitigation of human heat stress in a residential district of Freiburg, Southwest Germany. *landscape and urban planning*, 148:37–50.

Lee, S.-H. and Park, S.-U. (2008). A vegetated urban canopy model for meteorological and environmental modelling. *Boundary-Layer Meteorology*, 126(1):73–102.

Lemonsu, A., Viguié, V., Daniel, M., and Masson, V. (2015). Vulnerability to heat waves: Impact of urban expansion scenarios on urban heat island and heat stress in Paris (France). *Urban Climate*, 14:586–605.

Leopold, L. B. (1968). *Hydrology for urban land planning: A guidebook on the hydrologic effects of urban land use*, volume 554. US Department of the Interior, Geological Survey.

Lepczyk, C. A., Aronson, M. F., Evans, K. L., Goddard, M. A., Lerman, S. B., and MacIvor, J. S. (2017). Biodiversity in the city: Fundamental questions for understanding the ecology of urban green spaces for biodiversity conservation. *BioScience*, 67(9):799–807.

Lerner, D. N. (1990). Groundwater recharge in urban areas. *Atmospheric Environment. Part B. Urban Atmosphere*, 24(1):29–33.

Lerner, D. N. (2002). Identifying and quantifying urban recharge: a review. *Hydrogeology journal*, 10(1):143–152.

Leuning, R. (1990). Modelling stomatal behaviour and and photosynthesis of eucalyptus grandis. *Functional Plant Biology*, 17(2):159–175.

Lhomme, J., Bouvier, C., and Perrin, J.-L. (2004). Applying a gis-based geomorphological routing model in urban catchments. *Journal of Hydrology*, 299(3-4):203–216.

Lindberg, S., Nielsen, J., Carr, R., et al. (1989). *An integrated PC-modelling system for hydraulic analysis of drainage systems*. Institution of Engineers, Australia.

Litvak, E., Bijoor, N. S., and Pataki, D. E. (2014). Adding trees to irrigated turfgrass lawns may be a water-saving measure in semi-arid environments. *Ecohydrology*, 7(5):1314–1330.

Litvak, E., Manago, K., Hogue, T., and Pataki, D. (2017). Evapotranspiration of urban landscapes in Los Angeles, California at the municipal scale. *Water Resources Research*, 53(5):4236–4252.

Litvak, E., McCarthy, H. R., and Pataki, D. E. (2011). Water relations of coast redwood planted in the semi-arid climate of southern California. *Plant, Cell & Environment*, 34(8):1384–1400.

Litvak, E., McCarthy, H. R., and Pataki, D. E. (2012). Transpiration sensitivity of urban trees in a semi-arid climate is constrained by xylem vulnerability to cavitation. *Tree Physiology*, 32(4):373–388.

Litvak, E. and Pataki, D. E. (2016). Evapotranspiration of urban lawns in a semi-arid environment: An in-situ evaluation of microclimatic conditions and watering recommendations. *Journal of Arid Environments*, 134:87–96.

Liu, M., Tian, H., Yang, Q., Yang, J., Song, X., Lohrenz, S. E., and Cai, W.-J. (2013). Long-term trends in evapotranspiration and runoff over the drainage basins of the Gulf of Mexico during 1901-2008. *Water Resources Research*, 49(4):1988–2012.

Livesley, S., Baudinette, B., and Glover, D. (2014). Rainfall interception and stem flow by eucalypt street trees–the impacts of canopy density and bark type. *Urban Forestry & Urban Greening*, 13(1):192–197.

Livesley, S., McPherson, E., and Calfapietra, C. (2016a). The urban forest and ecosystem services: impacts on urban water, heat, and pollution cycles at the tree, street, and city scale. *Journal of Environmental Quality*, 45(1):119–124.

Livesley, S., Ossola, A., Threlfall, C., Hahs, A., and Williams, N. (2016b). Soil carbon and carbon/nitrogen ratio change under tree canopy, tall grass, and turf grass areas of urban green space. *Journal of Environmental Quality*, 45(1):215–223.

Livesley, S. J., Dougherty, B. J., Smith, A. J., Navaud, D., Wylie, L. J., and Arndt, S. K. (2010). Soil-atmosphere exchange of carbon dioxide, methane and nitrous oxide in urban garden systems: impact of irrigation, fertiliser and mulch. *Urban ecosystems*, 13(3):273–293.

Livesley, S. J., McPherson, G. M., and Calfapietra, C. (2016c). The urban forest and ecosystem services: Impacts on urban water, heat, and pollution cycles at the tree, street, and city scale. *Journal of Environmental Quality*, 45(1):119–124.

Loague, K., Heppner, C. S., Ebel, B. A., and VanderKwaak, J. E. (2010). The quixotic search for a comprehensive understanding of hydrologic response at the surface: Horton, dunne, dunton, and the role of concept-development simulation. *Hydrological Processes*, 24(17):2499–2505.

Locatelli, L., Mark, O., Mikkelsen, P. S., Arnbjerg-Nielsen, K., Deletic, A., Roldin, M., and Binning, P. J. (2017). Hydrologic impact of urbanization with extensive stormwater infiltration. *Journal of Hydrology*, 544:524–537.

Loheide, S. P., Butler Jr, J. J., and Gorelick, S. M. (2005). Estimation of groundwater consumption by phreatophytes using diurnal water table fluctuations: A saturated-unsaturated flow assessment. *Water Resources Research*, 41(7).

Lorenz, K. and Lal, R. (2009). Biogeochemical c and n cycles in urban soils. *Environment International*, 35(1):1–8.

Love, D., Venturas, M., Sperry, J., Brooks, P., Pettit, J., Wang, Y., Anderegg, W., Tai, X., and Mackay, D. (2018). Dependence of aspen stands on a subsurface water subsidy: Implications for climate change impacts. *Water Resources Research*.

Lowry, C. S. and Loheide, S. P. (2010). Groundwater-dependent vegetation: Quantifying the groundwater subsidy. *Water Resources Research*, 46(6).

Lyytimäki, J. (2014). Bad nature: Newspaper representations of ecosystem disservices. *Urban Forestry & Urban Greening*, 13(3):418–424.

Manoli, G., Ivanov, V. Y., and Fatichi, S. (2018a). Dry-season greening and water stress in amazonia: The role of modeling leaf phenology. *Journal of Geophysical Research: Biogeosciences*, 123(6):1909–1926.

Manoli, G., Meijide, A., Huth, N., Knohl, A., Kosugi, Y., Burlando, P., Ghazoul, J., and Fatichi, S. (2018b). Ecohydrological changes after tropical forest conversion to oil palm. *Environmental Research Letters*, 13(6):064035.

Marchionni, V., Guyot, A., Tapper, N., Walker, J., and Daly, E. (2019a). Water balance and tree water use dynamics in remnant urban reserves. *Journal of Hydrology*, 575:343–353.

Marchionni, V., Revelli, R., and Daly, E. (2019b). Ecohydrology of urban ecosystems. In *Dryland Ecohydrology*, pages 533–571. Springer.

Martin, C. and Stabler, L. (2002). Plant gas exchange and water status in urban desert landscapes. *Journal of Arid Environments*, 51(2):235–254.

Masson, V. (2006). Urban surface modeling and the meso-scale impact of cities. *Theoretical and Applied Climatology*, 84(1-3):35–45.

Mastrotheodoros, T., Pappas, C., Molnar, P., Burlando, P., Hadjidoukas, P., and Fatichi, S. (2019). Ecohydrological dynamics in the Alps: Insights from a modelling analysis of the spatial variability. *Ecohydrology*, 12(1):e2054.

Mastrotheodoros, T., Pappas, C., Molnar, P., Burlando, P., Keenan, T. F., Gentine, P., Gough, C. M., and Fatichi, S. (2017). Linking plant functional trait plasticity and the large increase in forest water use efficiency. *Journal of Geophysical Research: Biogeosciences*, 122(9):2393–2408.

Matheny, A. M., Bohrer, G., Garrity, S. R., Morin, T. H., Howard, C. J., and Vogel, C. S. (2015). Observations of stem water storage in trees of opposing hydraulic strategies. *Ecosphere*, 6(9):1–13.

Matthews, T., Lo, A. Y., and Byrne, J. A. (2015). Reconceptualizing green infrastructure for climate change adaptation: Barriers to adoption and drivers for uptake by spatial planners. *Landscape and Urban Planning*, 138:155–163.

Maxwell, R. M. and Kollet, S. J. (2008). Interdependence of groundwater dynamics and land-energy feedbacks under climate change. *Nature Geoscience*, 1(10):665.

McCarthy, H. R. and Pataki, D. E. (2010). Drivers of variability in water use of native and non-native urban trees in the greater Los Angeles area. *Urban Ecosystems*, 13(4):393–414.

McCarthy, H. R., Pataki, D. E., and Jenerette, G. D. (2011). Plant water-use efficiency as a metric of urban ecosystem services. *Ecological Applications*, 21(8):3115–3127.

McDonald, R. I., Douglas, I., Revenga, C., Hale, R., Grimm, N., Grönwall, J., and Fekete, B. (2011). Global urban growth and the geography of water availability, quality, and delivery. *Ambio*, 40(5):437–446.

McDowell, N., Pockman, W. T., Allen, C. D., Breshears, D. D., Cobb, N., Kolb, T., Plaut, J., Sperry, J., West, A., Williams, D. G., et al. (2008). Mechanisms of plant survival and mortality during drought: why do some plants survive while others succumb to drought? *New Phytologist*, 178(4):719–739.

Mcdowell, N. G., Williams, A., Xu, C., Pockman, W., Dickman, L., Sevanto, S., Pangle, R., Limousin, J., Plaut, J., Mackay, D., et al. (2016). Multi-scale predictions of massive conifer mortality due to chronic temperature rise. *Nature Climate Change*, 6(3):295.

McKinney, M. L. (2002). Urbanization, Biodiversity, and Conservation: The impacts of urbanization on native species are poorly studied, but educating a highly urbanized human population about these impacts can greatly improve species conservation in all ecosystems. *Bioscience*, 52(10):883–890.

McPherson, E. G. and Peper, P. J. (2012). Urban tree growth modeling. *Arboriculture & Urban Forestry*, 38(5):175–183.

McPherson, G., Simpson, J. R., Peper, P. J., Maco, S. E., and Xiao, Q. (2005). Municipal forest benefits and costs in five US cities. *Journal of Forestry*, 103(8):411–416.

Meinzer, F. C., James, S. A., and Goldstein, G. (2004). Dynamics of transpiration, sap flow and use of stored water in tropical forest canopy trees. *Tree Physiology*, 24(8):901–909.

Mejía, A., Daly, E., Rossel, F., Jovanovic, T., and Gironás, J. (2014). A stochastic model of streamflow for urbanized basins. *Water Resources Research*, 50(3):1984–2001.

Melaas, E. K., Wang, J. A., Miller, D. L., and Friedl, M. A. (2016). Interactions between urban vegetation and surface urban heat islands: A case study in the Boston metropolitan region. *Environmental Research Letters*, 11(5):054020.

Menz, M. H., Dixon, K. W., and Hobbs, R. J. (2013). Hurdles and opportunities for landscape-scale restoration. *Science*, 339(6119):526–527.

Mezbahuddin, M., Grant, R., and Flanagan, L. B. (2016). Modeling hydrological controls on variations in peat water content, water table depth, and surface energy exchange of a boreal western canadian fen peatland. *Journal of Geophysical Research: Biogeosciences*, 121(8):2216–2242.

Miao, S., Chen, F., Li, Q., and Fan, S. (2011). Impacts of urban processes and urbanization on summer precipitation: a case study of heavy rainfall in Beijing on 1 August 2006. *Journal of Applied Meteorology and Climatology*, 50(4):806–825.

Milesi, C., Running, S. W., Elvidge, C. D., Dietz, J. B., Tuttle, B. T., and Nemani, R. R. (2005). Mapping and modeling the biogeochemical cycling of turf grasses in the United States. *Environmental Management*, 36(3):426–438.

Miller, G. R., Chen, X., Rubin, Y., Ma, S., and Baldocchi, D. D. (2010). Groundwater uptake by woody vegetation in a semiarid oak savanna. *Water Resources Research*, 46(10).

Mitchell, P. J., Veneklaas, E., Lambers, H., and Burgess, S. S. (2009). Partitioning of evapotranspiration in a semi-arid eucalypt woodland in south-western Australia. *Agricultural and Forest Meteorology*, 149(1):25–37.

Morakinyo, T. E., Dahanayake, K. K. C., Ng, E., and Chow, C. L. (2017). Temperature and cooling demand reduction by green-roof types in different climates and urban densities: A co-simulation parametric study. *Energy and Buildings*, 145:226–237.

Murari, K. K., Ghosh, S., Patwardhan, A., Daly, E., and Salvi, K. (2015). Intensification of future severe heat waves in India and their effect on heat stress and mortality. *Regional Environmental Change*, 15(4):569–579.

Murray, B. B. R., Zeppel, M. J., Hose, G. C., and Eamus, D. (2003). Groundwater-dependent ecosystems in Australia: It's more than just water for rivers. *Ecological Management & Restoration*, 4(2):110–113.

Nadezhdina, N., Čermák, J., and Ceulemans, R. (2002). Radial patterns of sap flow in woody stems of dominant and understory species: scaling errors associated with positioning of sensors. *Tree Physiology*, 22(13):907–918.

Naumburg, E., Mata-Gonzalez, R., Hunter, R. G., Mclendon, T., and Martin, D. W. (2005). Phreatophytic vegetation and groundwater fluctuations: a review of current research and application of ecosystem response modeling with an emphasis on great basin vegetation. *Environmental Management*, 35(6):726–740.

Newcomer, M. E., Gurdak, J. J., Sklar, L. S., and Nanus, L. (2014). Urban recharge beneath low impact development and effects of climate variability and change. *Water Resources Research*, 50(2):1716–1734.

Nice, K. A., Coutts, A. M., and Tapper, N. J. (2018). Development of the VTUF-3D v1. 0 urban micro-climate model to support assessment of urban vegetation influences on human thermal comfort. *Urban Climate*, 24:1052–1076.

Niu, G.-Y., Paniconi, C., Troch, P. A., Scott, R. L., Durcik, M., Zeng, X., Huxman, T., and Goodrich, D. C. (2014). An integrated modelling framework of catchment-scale eco-hydrological processes: 1. Model description and tests over an energy-limited watershed. *Ecohydrology*, 7(2):427–439.

Niyogi, D., Pyle, P., Lei, M., Arya, S. P., Kishtawal, C. M., Shepherd, M., Chen, F., and Wolfe, B. (2011). Urban modification of thunderstorms: An observational storm climatology and model case study for the indianapolis urban region. *Journal of Applied Meteorology and Climatology*, 50(5):1129–1144.

Nordbo, A., Järvi, L., Haapanala, S., Wood, C. R., and Vesala, T. (2012). Fraction of natural area as main predictor of net CO_2 emissions from cities. *Geophysical Research Letters*, 39(20).

Nowak, D. J. and Crane, D. E. (2002). Carbon storage and sequestration by urban trees in the USA. *Environmental Pollution*, 116(3):381–389.

Nowak, D. J. and Greenfield, E. J. (2012). Tree and impervious cover in the United States. *Landscape and Urban Planning*, 107(1):21–30.

O'Grady, A., Cook, P., Howe, P., and Werren, G. (2006). Groundwater use by dominant tree species in tropical remnant vegetation communities. *Australian Journal of Botany*, 54(2):155–171.

Oke, T. R. (1982). The energetic basis of the urban heat island. *Quarterly Journal of the Royal Meteorological Society*, 108(455):1–24.

Oke, T. R. (1987). *Boundary layer climates*. Routledge.

Oke, T. R., Crowther, J., McNaughton, K., Monteith, J., and Gardiner, B. (1989). The micrometeorology of the urban forest. *Philosophical Transactions of the Royal Society of London B: Biological Sciences*, 324(1223):335–349.

O'Kelly, B. C. (2004). Accurate determination of moisture content of organic soils using the oven drying method. *Drying Technology*, 22(7):1767–1776.

Orellana, F., Verma, P., Loheide, S. P., and Daly, E. (2012). Monitoring and modeling water-vegetation interactions in groundwater-dependent ecosystems. *Reviews of Geophysics*, 50(3).

Owuor, S. O., Butterbach-Bahl, K., Guzha, A., Rufino, M., Pelster, D., Díaz-Pinés, E., and Breuer, L. (2016). Groundwater recharge rates and surface runoff response to land use and land cover changes in semi-arid environments. *Ecological Processes*, 5(1):16.

Pace, R., Biber, P., Pretzsch, H., and Grote, R. (2018). Modeling ecosystem services for park trees: sensitivity of i-Tree Eco simulations to light exposure and tree species classification. *Forests*, 9(2):89.

Palmer, M. A., Liu, J., Matthews, J. H., Mumba, M., and D'odorico, P. (2015). Manage water in a green way. *Science*, 349(6248):584–585.

Pandeya, B., Buytaert, W., Zulkafli, Z., Karpouzoglou, T., Mao, F., and Hannah, D. (2016). A comparative analysis of ecosystem services valuation approaches for application at the local scale and in data scarce regions. *Ecosystem Services*, 22:250–259.

Passarello, M., Sharp Jr, J., and Pierce, S. (2012). Estimating urban-induced artificial recharge: A case study for Austin, TX. *Environmental & Engineering Geoscience*, 18(1):25–36.

Pataki, D., Boone, C., Hogue, T., Jenerette, G., McFadden, J., and Pincetl, S. (2011a). Socio-ecohydrology and the urban water challenge. *Ecohydrology*, 4(2):341–347.

Pataki, D. E., Carreiro, M. M., Cherrier, J., Grulke, N. E., Jennings, V., Pincetl, S., Pouyat, R. V., Whitlow, T. H., and Zipperer, W. C. (2011b). Coupling biogeochemical cycles in

urban environments: ecosystem services, green solutions, and misconceptions. *Frontiers in Ecology and the Environment*, 9(1):27–36.

Pataki, D. E., McCarthy, H. R., Litvak, E., and Pincetl, S. (2011c). Transpiration of urban forests in the Los Angeles metropolitan area. *Ecological Applications*, 21(3):661–677.

Pawlak, W. and Fortuniak, K. (2016). Eddy covariance measurements of the net turbulent methane flux in the city centre–results of 2-year campaign in Łódź, Poland. *Atmospheric Chemistry and Physics*, 16(13):8281.

Peters, E. B., McFadden, J. P., and Montgomery, R. A. (2010). Biological and environmental controls on tree transpiration in a suburban landscape. *Journal of Geophysical Research: Biogeosciences*, 115(G4).

Peters, R. L., Fonti, P., Frank, D. C., Poyatos, R., Pappas, C., Kahmen, A., Carraro, V., Prendin, A. L., Schneider, L., Baltzer, J. L., et al. (2018a). Quantification of uncertainties in conifer sap flow measured with the thermal dissipation method. *New Phytologist*.

Peters, W., van der Velde, I. R., Van Schaik, E., Miller, J. B., Ciais, P., Duarte, H. F., van der Laan-Luijkx, I. T., van der Molen, M. K., Scholze, M., Schaefer, K., et al. (2018b). Increased water-use efficiency and reduced CO_2 uptake by plants during droughts at a continental scale. *Nature Geoscience*, 11(10):744.

Petrucci, G. and Bonhomme, C. (2014). The dilemma of spatial representation for urban hydrology semi-distributed modelling: Trade-offs among complexity, calibration and geographical data. *Journal of hydrology*, 517:997–1007.

Poff, N. L. (1997). Landscape filters and species traits: towards mechanistic understanding and prediction in stream ecology. *Journal of the north american Benthological society*, 16(2):391–409.

Pokhrel, Y. N., Fan, Y., and Miguez-Macho, G. (2014). Potential hydrologic changes in the Amazon by the end of the 21st century and the groundwater buffer. *Environmental Research Letters*, 9(8):084004.

Porporato, A., D'odorico, P., Laio, F., and Rodriguez-Iturbe, I. (2003). Hydrologic controls on soil carbon and nitrogen cycles. I. Modeling scheme. *Advances in Water Resources*, 26(1):45–58.

Potchter, O., Cohen, P., and Bitan, A. (2006). Climatic behavior of various urban parks during hot and humid summer in the Mediterranean city of Tel Aviv, Israel. *International Journal of Climatology*, 26(12):1695–1711.

Pouyat, R., Groffman, P., Yesilonis, I., and Hernandez, L. (2002). Soil carbon pools and fluxes in urban ecosystems. *Environmental Pollution*, 116:S107–S118.

Pouyat, R. V., Pataki, D. E., Belt, K. T., Groffman, P. M., Hom, J., and Band, L. E. (2007). *Effects of urban land-use change on biogeochemical cycles*, pages 45–58. Springer.

Price, K. (2011). Effects of watershed topography, soils, land use, and climate on baseflow hydrology in humid regions: A review. *Progress in Physical Geography*, 35(4):465–492.

Qiu, J., Zipper, S. C., Motew, M., Booth, E. G., Kucharik, C. J., and Loheide, S. P. (2019). Nonlinear groundwater influence on biophysical indicators of ecosystem services. *Nature Sustainability*, 2(6):475.

Raciti, S. M., Burgin, A. J., Groffman, P. M., Lewis, D. N., and Fahey, T. J. (2011). Denitrification in suburban lawn soils. *Journal of Environmental Quality*, 40(6):1932–1940.

Randelovic, A., Zhang, K., Jacimovic, N., McCarthy, D., and Deletic, A. (2016). Stormwater biofilter treatment model (mpire) for selected micro-pollutants. *Water Research*, 89:180–191.

Redfern, T. W., Macdonald, N., Kjeldsen, T. R., Miller, J. D., and Reynard, N. (2016). Current understanding of hydrological processes on common urban surfaces. *Progress in Physical Geography*, 40(5):699–713.

Revelli, R. and Porporato, A. (2018). Ecohydrological model for the quantification of ecosystem services provided by urban street trees. *Urban Ecosystems*, pages 1–16.

Richards, D. R. and Thompson, B. S. (2019). Urban ecosystems: A new frontier for payments for ecosystem services. *People and Nature*, 1(2):249–261.

Roberts, B. R. (1977). The response of urban trees to abiotic stress [moisture, temperature, light, pesticides]. *Journal of Arboriculture (USA)*.

Rodriguez, F., Morena, F., and Andrieu, H. (2005). Development of a distributed hydrological model based on urban databanks–production processes of urbs. *Water Science and Technology*, 52(5):241–248.

Rosenfeld, D. (2000). Suppression of rain and snow by urban and industrial air pollution. *Science*, 287(5459):1793–1796.

Rossatto, D. R., Silva, L. d. C. R., Villalobos-Vega, R., Sternberg, L. d. S. L., and Franco, A. C. (2012). Depth of water uptake in woody plants relates to groundwater level and vegetation structure along a topographic gradient in a neotropical savanna. *Environmental and Experimental Botany*, 77:259–266.

Ryu, Y.-H., Bou-Zeid, E., Wang, Z.-H., and Smith, J. A. (2016). Realistic representation of trees in an urban canopy model. *Boundary-Layer Meteorology*, 159(2):193–220.

Saaroni, H. and Ziv, B. (2010). Estimating the urban heat island contribution to urban and rural air temperature differences over complex terrain: application to an arid city. *Journal of Applied Meteorology and Climatology*, 49(10):2159–2166.

Salamanca, F., Krpo, A., Martilli, A., and Clappier, A. (2010). A new building energy model coupled with an urban canopy parameterization for urban climate simulations—part i. formulation, verification, and sensitivity analysis of the model. *Theoretical and Applied Climatology*, 99(3-4):331.

Salamanca, F., Zhang, Y., Barlage, M., Chen, F., Mahalov, A., and Miao, S. (2018). Evaluation of the wrf-urban modeling system coupled to noah and noah-mp land surface models over a semiarid urban environment. *Journal of Geophysical Research: Atmospheres*, 123(5):2387–2408.

Salvadore, E., Bronders, J., and Batelaan, O. (2015). Hydrological modelling of urbanized catchments: A review and future directions. *Journal of Hydrology*, 529:62–81.

Sander, H. A. (2016). Assessing impacts on urban greenspace, waterways, and vegetation in urban planning. *Journal of Environmental Planning and Management*, 59(3):461–479.

Sanusi, R., Johnstone, D., May, P., and Livesley, S. J. (2016). Street orientation and side of the street greatly influence the microclimatic benefits street trees can provide in summer. *Journal of Environmental Quality*, 45(1):167–174.

Sawada, Y. and Koike, T. (2016). Ecosystem resilience to the Millennium drought in southeast Australia (2001-2009). *Journal of Geophysical Research: Biogeosciences*, 121(9):2312–2327.

Saxton, K. E. and Rawls, W. J. (2006). Soil water characteristic estimates by texture and organic matter for hydrologic solutions. *Soil Science Society of America Journal*, 70(5):1569–1578.

Schatz, J. and Kucharik, C. J. (2015). Urban climate effects on extreme temperatures in Madison, Wisconsin, USA. *Environmental Research Letters*, 10(9):094024.

Schenk, H. J. and Jackson, R. B. (2002). The global biogeography of roots. *Ecological Monographs*, 72(3):311–328.

Scott, R. L., Huxman, T. E., Williams, D. G., and Goodrich, D. C. (2006). Ecohydrological impacts of woody-plant encroachment: Seasonal patterns of water and carbon dioxide exchange within a semiarid riparian environment. *Global Change Biology*, 12(2):311–324.

Sellers, P., Dickinson, R., Randall, D., Betts, A., Hall, F., Berry, J., Collatz, G., Denning, A., Mooney, H., Nobre, C., et al. (1997). Modeling the exchanges of energy, water, and carbon between continents and the atmosphere. *Science*, 275(5299):502–509.

Seto, K. C., Fragkias, M., Güneralp, B., and Reilly, M. K. (2011). A meta-analysis of global urban land expansion. *PloS One*, 6(8):e23777.

Seto, K. C., Güneralp, B., and Hutyra, L. R. (2012). Global forecasts of urban expansion to 2030 and direct impacts on biodiversity and carbon pools. *Proceedings of the National Academy of Sciences*, 109(40):16083–16088.

Seto, K. C. and Shepherd, J. M. (2009). Global urban land-use trends and climate impacts. *Current Opinion in Environmental Sustainability*, 1(1):89–95.

Shahidan, M. F., Shariff, M. K., Jones, P., Salleh, E., and Abdullah, A. M. (2010). A comparison of Mesua ferrea L. and Hura crepitans L. for shade creation and radiation modification in improving thermal comfort. *Landscape and Urban Planning*, 97(3):168–181.

Shashua-Bar, L., Pearlmutter, D., and Erell, E. (2011). The influence of trees and grass on outdoor thermal comfort in a hot-arid environment. *International Journal of Climatology*, 31(10):1498–1506.

Shem, W. and Shepherd, M. (2009). On the impact of urbanization on summertime thunderstorms in Atlanta: two numerical model case studies. *Atmospheric Research*, 92(2):172–189.

Shepherd, J. M. (2005). A review of current investigations of urban-induced rainfall and recommendations for the future. *Earth Interactions*, 9(12):1–27.

Shepherd, J. M. (2006). Evidence of urban-induced precipitation variability in arid climate regimes. *Journal of Arid Environments*, 67(4):607–628.

Shields, C. and Tague, C. (2015). Ecohydrology in semiarid urban ecosystems: Modeling the relationship between connected impervious area and ecosystem productivity. *Water Resources Research*, 51(1):302–319.

Shiflett, S. A., Liang, L. L., Crum, S. M., Feyisa, G. L., Wang, J., and Jenerette, G. D. (2017). Variation in the urban vegetation, surface temperature, air temperature nexus. *Science of the Total Environment*, 579:495–505.

Shuster, W. D., Bonta, J., Thurston, H., Warnemuende, E., and Smith, D. (2005). Impacts of impervious surface on watershed hydrology: a review. *Urban Water Journal*, 2(4):263–275.

Sieghardt, M., Mursch-Radlgruber, E., Paoletti, E., Couenberg, E., Dimitrakopoulus, A., Rego, F., Hatzistathis, A., and Randrup, T. B. (2005a). *The abiotic urban environment: impact of urban growing conditions on urban vegetation*, pages 281–323. Springer.

Sieghardt, M., Mursch-Radlgruber, E., Paoletti, E., Couenberg, E., Dimitrakopoulus, A., Rego, F., Hatzistathis, A., and Randrup, T. B. (2005b). The abiotic urban environment: impact of urban growing conditions on urban vegetation. In *Urban Forests and Trees*, pages 281–323. Springer.

Simon, H., Lindén, J., Hoffmann, D., Braun, P., Bruse, M., and Esper, J. (2018). Modeling transpiration and leaf temperature of urban trees–a case study evaluating the microclimate model envi-met against measurement data. *Landscape and Urban Planning*, 174:33–40.

Sirakaya, A., Cliquet, A., and Harris, J. (2017). Ecosystem services in cities: Towards the international legal protection of ecosystem services in urban environments. *Ecosystem Services*.

Sitch, S., Smith, B., Prentice, I. C., Arneth, A., Bondeau, A., Cramer, W., Kaplan, J. O., Levis, S., Lucht, W., Sykes, M. T., et al. (2003). Evaluation of ecosystem dynamics, plant geography and terrestrial carbon cycling in the LPJ dynamic global vegetation model. *Global Change Biology*, 9(2):161–185.

Skinner, C. B., Poulsen, C. J., and Mankin, J. S. (2018). Amplification of heat extremes by plant CO_2 physiological forcing. *Nature Communications*, 9(1):1094.

Smith, J. A., Baeck, M. L., Villarini, G., Welty, C., Miller, A. J., and Krajewski, W. F. (2012). Analyses of a long-term, high-resolution radar rainfall data set for the Baltimore metropolitan region. *Water Resources Research*, 48(4).

Sofer, M. and Potchter, O. (2006). The urban heat island of a city in an arid zone: the case of Eilat, Israel. *Theoretical and Applied Climatology*, 85(1-2):81–88.

Song, X. P., Tan, P. Y., Edwards, P., and Richards, D. (2018). The economic benefits and costs of trees in urban forest stewardship: A systematic review. *Urban forestry & urban greening*, 29:162–170.

Soylu, M., Istanbulluoglu, E., Lenters, J., and Wang, T. (2011). Quantifying the impact of groundwater depth on evapotranspiration in a semi-arid grassland region. *Hydrology and Earth System Sciences*, 15(3):787–806.

Spronken-Smith, R. and Oke, T. (1998). The thermal regime of urban parks in two cities with different summer climates. *International Journal of Remote Sensing*, 19(11):2085–2104.

Stabler, L. B., Martin, C. A., and Brazel, A. J. (2005). Microclimates in a desert city were related to land use and vegetation index. *Urban Forestry & Urban Greening*, 3(3):137–147.

Steppe, K., De Pauw, D. J., Doody, T. M., and Teskey, R. O. (2010). A comparison of sap flux density using thermal dissipation, heat pulse velocity and heat field deformation methods. *Agricultural and Forest Meteorology*, 150(7-8):1046–1056.

Swann, A. L., Hoffman, F. M., Koven, C. D., and Randerson, J. T. (2016). Plant responses to increasing CO_2 reduce estimates of climate impacts on drought severity. *Proceedings of the National Academy of Sciences*, 113(36):10019–10024.

Taylor, R. G., Scanlon, B., Döll, P., Rodell, M., Van Beek, R., Wada, Y., Longuevergne, L., Leblanc, M., Famiglietti, J. S., Edmunds, M., et al. (2013). Ground water and climate change. *Nature Climate Change*, 3(4):322.

TEEB (2009). The economics of ecosystems and biodiversity: The ecological and economic foundation. *Earthscan, London and Washington DC*.

Toparlar, Y., Blocken, B., Maiheu, B., and Van Heijst, G. (2017). A review on the CFD analysis of urban microclimate. *Renewable and Sustainable Energy Reviews*, 80:1613–1640.

Toth, F. (2003). *Millennium Ecosystem Assessment: Ecosystems and human well-being: a framework for assessment*. Island press.

Tulloch, A. I., Barnes, M. D., Ringma, J., Fuller, R. A., and Watson, J. E. (2016). Understanding the importance of small patches of habitat for conservation. *Journal of Applied Ecology*, 53(2):418–429.

Tuzet, A., Perrier, A., and Leuning, R. (2003). A coupled model of stomatal conductance, photosynthesis and transpiration. *Plant, Cell & Environment*, 26(7):1097–1116.

Tyrväinen, L., Pauleit, S., Seeland, K., and de Vries, S. (2005). Benefits and uses of urban forests and trees. In *Urban Forests and Trees*, pages 81–114. Springer.

UN (2015). *World Urbanization Prospects: The 2014 Revision, (ST/ESA/SER.A/366)*. United Nations, Department of Economic and Social Affairs, Population Division.

UN, D. (2018). United nations department of economic and social affairs, population division (2018): World population prospects: The 2018 revision, online edition. *Internet: https://www.un.org/development/desa/publications/2018-revision-of-world-urbanization-prospects.html*.

UNEP (1997). World atlas of desertification 2ED. *United Nations Environment Programme*.

Upmanis, H., Eliasson, I., and Lindqvist, S. (1998). The influence of green areas on nocturnal temperatures in a high latitude city (Göteborg, Sweden). *International Journal of Climatology*, 18(6):681–700.

van Delden, L., Larsen, E., Rowlings, D., Scheer, C., and Grace, P. (2016). Establishing turf grass increases soil greenhouse gas emissions in peri-urban environments. *Urban ecosystems*, 19(2):749–762.

van Dijk, A. I., Beck, H. E., Crosbie, R. S., de Jeu, R. A., Liu, Y. Y., Podger, G. M., Timbal, B., and Viney, N. R. (2013). The Millennium Drought in southeast Australia (2001–2009): Natural and human causes and implications for water resources, ecosystems, economy, and society. *Water Resources Research*, 49(2):1040–1057.

Van Genuchten, M. T. (1980). A closed-form equation for predicting the hydraulic conductivity of unsaturated soils 1. *Soil Science Society of America Journal*, 44(5):892–898.

Van Loon, A. F., Gleeson, T., Clark, J., Van Dijk, A. I., Stahl, K., Hannaford, J., Di Baldassarre, G., Teuling, A. J., Tallaksen, L. M., Uijlenhoet, R., et al. (2016a). Drought in the anthropocene. *Nature Geoscience*, 9(2):89.

Van Loon, A. F., Stahl, K., Di Baldassarre, G., Clark, J., Rangecroft, S., Wanders, N., Gleeson, T., Van Dijk, A. I., Tallaksen, L. M., and Hannaford, J. (2016b). Drought in a human-modified world: reframing drought definitions, understanding, and analysis approaches. *Hydrology and Earth System Sciences*, 20(9):3631.

Vandegehuchte, M. W., Guyot, A., Hubeau, M., De Groote, S. R., De Baerdemaeker, N. J., Hayes, M., Welti, N., Lovelock, C. E., Lockington, D. A., and Steppe, K. (2014). Long-term versus daily stem diameter variation in co-occurring mangrove species: Environmental versus ecophysiological drivers. *Agricultural and Forest Meteorology*, 192:51–58.

Verma, P., Loheide II, S. P., Eamus, D., and Daly, E. (2014). Root water compensation sustains transpiration rates in an Australian woodland. *Advances in Water Resources*, 74:91–101.

Vezzaro, L., Eriksson, E., Ledin, A., and Mikkelsen, P. S. (2011). Modelling the fate of organic micropollutants in stormwater ponds. *Science of the Total Environment*, 409(13):2597–2606.

Vezzaro, L., Eriksson, E., Ledin, A., and Mikkelsen, P. S. (2012). Quantification of uncertainty in modelled partitioning and removal of heavy metals (Cu, Zn) in a stormwater retention pond and a biofilter. *Water Research*, 46(20):6891–6903.

Vico, G. and Porporato, A. (2011). From rainfed agriculture to stress-avoidance irrigation: I. a generalized irrigation scheme with stochastic soil moisture. *Advances in water resources*, 34(2):263–271.

Vico, G., Revelli, R., and Porporato, A. (2014). Ecohydrology of street trees: design and irrigation requirements for sustainable water use. *Ecohydrology*, 7(2):508–523.

Vincke, C. and Thiry, Y. (2008). Water table is a relevant source for water uptake by a Scots pine (Pinus sylvestris L.) stand: Evidences from continuous evapotranspiration and water table monitoring. *Agricultural and Forest Meteorology*, 148(10):1419–1432.

Volo, T. J., Vivoni, E. R., Martin, C. A., Earl, S., and Ruddell, B. L. (2014). Modelling soil moisture, water partitioning, and plant water stress under irrigated conditions in desert urban areas. *Ecohydrology*, 7(5):1297–1313.

von Döhren, P. and Haase, D. (2015). Ecosystem disservices research: a review of the state of the art with a focus on cities. *Ecological Indicators*, 52:490–497.

Wachinger, G., Fiedler, S., Zepp, K., Gattinger, A., Sommer, M., and Roth, K. (2000). Variability of soil methane production on the micro-scale: spatial association with hot spots of organic material and archaeal populations. *Soil Biology and Biochemistry*, 32(8-9):1121–1130.

Wagner, I. and Breil, P. (2013). The role of ecohydrology in creating more resilient cities. *Ecohydrology & Hydrobiology*, 13(2):113–134.

Wang, J., Endreny, T. A., and Nowak, D. J. (2008). Mechanistic simulation of tree effects in an urban water balance model. *JAWRA Journal of the American Water Resources Association*, 44(1):75–85.

White, W. N. (1932). *A method of estimating ground-water supplies based on discharge by plants and evaporation from soil: Results of investigations in Escalante Valley, Utah*, volume 659. US Government Printing Office.

Wong, T. and Brown, R. R. (2009). The water sensitive city: principles for practice. *Water Science and Technology*, 60(3):673–682.

Wong, T. H., Fletcher, T. D., Duncan, H. P., Coleman, J. R., and Jenkins, G. A. (2002). A model for urban stormwater improvement: conceptualization. In *Global Solutions for Urban Drainage*, pages 1–14. American Society of Civil Engineers.

Xiao, Q., McPherson, E., Simpson, J., and Ustin, S. (2007). Hydrologic processes at the urban residential scale. *Hydrological Processes: An International Journal*, 21(16):2174–2188.

Xiao, Q. and McPherson, E. G. (2002). Rainfall interception by santa monica's municipal urban forest. *Urban Ecosystems*, 6(4):291–302.

Xiao, Q., McPherson, E. G., Simpson, J. R., and Ustin, S. L. (1998). Rainfall interception by Sacramento's urban forest. *Journal of Arboriculture*, 24:235–244.

Xiao, Q., McPherson, E. G., Ustin, S. L., Grismer, M. E., and Simpson, J. R. (2000). Winter rainfall interception by two mature open-grown trees in Davis, California. *Hydrological Processes*, 14(4):763–784.

Yang, Y., Endreny, T. A., and Nowak, D. J. (2015). Simulating the effect of flow path roughness to examine how green infrastructure restores urban runoff timing and magnitude. *Urban Forestry & Urban Greening*, 14(2):361–367.

Yow, D. M. (2007). Urban heat islands: observations, impacts, and adaptation. *Geography Compass*, 1(6):1227–1251.

Yu, C. and Hien, W. N. (2006). Thermal benefits of city parks. *Energy and Buildings*, 38(2):105–120.

Yu, M. and Liu, Y. (2015). The possible impact of urbanization on a heavy rainfall event in beijing. *Journal of Geophysical Research: Atmospheres*, 120(16):8132–8143.

Zencich, S. J., Froend, R. H., Turner, J. V., and Gailitis, V. (2002). Influence of groundwater depth on the seasonal sources of water accessed by banksia tree species on a shallow, sandy coastal aquifer. *Oecologia*, 131(1):8–19.

Zeppel, M., Tissue, D., Taylor, D., Macinnis-Ng, C., and Eamus, D. (2010). Rates of nocturnal transpiration in two evergreen temperate woodland species with differing water-use strategies. *Tree Physiology*, 30(8):988–1000.

Zeppel, M. J., Yunusa, I. A., and Eamus, D. (2006). Daily, seasonal and annual patterns of transpiration from a stand of remnant vegetation dominated by a coniferous callitris species and a broad-leaved eucalyptus species. *Physiologia Plantarum*, 127(3):413–422.

Zhang, C. L., Chen, F., Miao, S. G., Li, Q. C., Xia, X. A., and Xuan, C. Y. (2009). Impacts of urban expansion and future green planting on summer precipitation in the beijing metropolitan area. *Journal of Geophysical Research: Atmospheres*, 114(D2).

Zhang, W., Wang, K., Luo, Y., Fang, Y., Yan, J., Zhang, T., Zhu, X., Chen, H., Wang, W., and Mo, J. (2014a). Methane uptake in forest soils along an urban-to-rural gradient in Pearl River Delta, South China. *Scientific Reports*, 4:5120.

Zhang, Y., Smith, J. A., Luo, L., Wang, Z., and Baeck, M. L. (2014b). Urbanization and rainfall variability in the Beijing metropolitan region. *Journal of Hydrometeorology*, 15(6):2219–2235.

Zhang, Z., Lv, Y., and Pan, H. (2013). Cooling and humidifying effect of plant communities in subtropical urban parks. *Urban Forestry & Urban Greening*, 12(3):323–329.

Zhao, L., Lee, X., Smith, R. B., and Oleson, K. (2014). Strong contributions of local background climate to urban heat islands. *Nature*, 511(7508):216–219.

Zhao, L., Oppenheimer, M., Zhu, Q., Baldwin, J. W., Ebi, K. L., Bou-Zeid, E., Guan, K., and Liu, X. (2018). Interactions between urban heat islands and heat waves. *Environmental Research Letters*, 13(3):034003.

Zhou, D., Zhao, S., Zhang, L., and Liu, S. (2016). Remotely sensed assessment of urbanization effects on vegetation phenology in China's 32 major cities. *Remote Sensing of Environment*, 176:272–281.

Zhu, W.-X., Dillard, N. D., and Grimm, N. B. (2004). Urban nitrogen biogeochemistry: status and processes in green retention basins. *Biogeochemistry*, 71(2):177–196.

Zipper, S. C., Schatz, J., Kucharik, C. J., and Loheide, S. P. (2017a). Urban heat island-induced increases in evapotranspirative demand. *Geophysical Research Letters*, 44(2):873–881.

Zipper, S. C., Schatz, J., Singh, A., Kucharik, C. J., Townsend, P. A., and Loheide II, S. P. (2016). Urban heat island impacts on plant phenology: Intra-urban variability and response to land cover. *Environmental Research Letters*, 11(5):054023.

Zipper, S. C., Soylu, M. E., Kucharik, C. J., and Loheide II, S. P. (2017b). Quantifying indirect groundwater-mediated effects of urbanization on agroecosystem productivity using MODFLOW-AgroIBIS (MAGI), a complete critical zone model. *Ecological Modelling*, 359:201–219.

Zoppou, C. (2001). Review of urban storm water models. *Environmental Modelling & Software*, 16(3):195–231.